Prevalence of Earth-size planets orbiting Sun-like stars

Erik A. Petigura[a,b,1], Andrew W. Howard[b], and Geoffrey W. Marcy[a]

[a]Astronomy Department, University of California, Berkeley, CA 94720; and [b]Institute for Astronomy, University of Hawaii at Manoa, Honolulu, HI 96822

Determining whether Earth-like planets are common or rare looms as a touchstone in the question of life in the universe. We searched for Earth-size planets that cross in front of their host stars by examining the brightness measurements of 42,000 stars from National Aeronautics and Space Administration's *Kepler* mission. We found 603 planets, including 10 that are Earth size ($1-2\ R_\oplus$) and receive comparable levels of stellar energy to that of Earth ($0.25-4\ F_\oplus$). We account for *Kepler's* imperfect detectability of such planets by injecting synthetic planet–caused dimmings into the *Kepler* brightness measurements and recording the fraction detected. We find that $11 \pm 4\%$ of Sun-like stars harbor an Earth-size planet receiving between one and four times the stellar intensity as Earth. We also find that the occurrence of Earth-size planets is constant with increasing orbital period (P), within equal intervals of $\log P$ up to $\sim$200 d. Extrapolating, one finds $5.7^{+1.7}_{-2.2}\%$ of Sun-like stars harbor an Earth-size planet with orbital periods of 200–400 d.

extrasolar planets | astrobiology

The National Aeronautics and Space Administration's (NASA's) *Kepler* mission was launched in 2009 to search for planets that transit (cross in front of) their host stars (1–4). The resulting dimming of the host stars is detectable by measuring their brightness, and *Kepler* monitored the brightness of 150,000 stars every 30 min for 4 y. To date, this exoplanet survey has detected more than 3,000 planet candidates (4).

The most easily detectable planets in the *Kepler* survey are those that are relatively large and orbit close to their host stars, especially those stars having lower intrinsic brightness fluctuations (noise). These large, close-in worlds dominate the list of known exoplanets. However, the *Kepler* brightness measurements can be analyzed and debiased to reveal the diversity of planets, including smaller ones, in our Milky Way Galaxy (5–7). These previous studies showed that small planets approaching Earth size are the most common, but only for planets orbiting close to their host stars. Here, we extend the planet survey to *Kepler's* most important domain: Earth-size planets orbiting far enough from Sun-like stars to receive a similar intensity of light energy as Earth.

Planet Survey

We performed an independent search of *Kepler* photometry for transiting planets with the goal of measuring the underlying occurrence distribution of planets as a function of orbital period, P, and planet radius, R_P. We restricted our survey to a set of Sun-like stars (GK type) that are the most amenable to the detection of Earth-size planets. We define GK-type stars as those with surface temperatures $T_{eff} = 4{,}100–6{,}100$ K and gravities $\log g = 4.0–4.9$ ($\log g$ is the base 10 logarithm of a star's surface gravity measured in cm s^{-2}) (8). Our search for planets was further restricted to the brightest Sun-like stars observed by *Kepler* ($Kp = 10–15$ mag). These 42,557 stars (Best42k) have the lowest photometric noise, making them amenable to the detection of Earth-size planets. When a planet crosses in front of its star, it causes a fractional dimming that is proportional to the fraction of the stellar disk blocked, $\delta F = (R_P/R_*)^2$, where R_* is the radius of the star. As viewed by a distant observer, the Earth dims the Sun by $\sim$100 parts per million (ppm) lasting 12 h every 365 d.

We searched for transiting planets in *Kepler* brightness measurements using our custom-built TERRA software package described in previous works (6, 9) and in *SI Appendix*. In brief, TERRA conditions *Kepler* photometry in the time domain, removing outliers, long timescale variability (>10 d), and systematic errors common to a large number of stars. TERRA then searches for transit signals by evaluating the signal-to-noise ratio (SNR) of prospective transits over a finely spaced 3D grid of orbital period, P, time of transit, t_0, and transit duration, ΔT. This grid-based search extends over the orbital period range of 0.5–400 d.

TERRA produced a list of "threshold crossing events" (TCEs) that meet the key criterion of a photometric dimming SNR ratio SNR > 12. Unfortunately, an unwieldy 16,227 TCEs met this criterion, many of which are inconsistent with the periodic dimming profile from a true transiting planet. Further vetting was performed by automatically assessing which light curves were consistent with theoretical models of transiting planets (10). We also visually inspected each TCE light curve, retaining only those exhibiting a consistent, periodic, box-shaped dimming, and rejecting those caused by single epoch outliers, correlated noise, and other data anomalies. The vetting process was applied homogeneously to all TCEs and is described in further detail in *SI Appendix*.

To assess our vetting accuracy, we evaluated the 235 *Kepler* objects of interest (KOIs) among Best42k stars having $P > 50$ d, which had been found by the *Kepler* Project and identified as planet candidates in the official Exoplanet Archive (exoplanetarchive.ipac.caltech.edu; accessed 19 September 2013). Among them, we found four whose light curves are not consistent with being planets. These four KOIs (364.01, 2,224.02, 2,311.01, and 2,474.01) have long periods and small radii (*SI Appendix*). This exercise suggests that our vetting process is robust and that careful scrutiny of the light curves of small planets in long period orbits is useful to identify false positives.

Significance

A major question is whether planets suitable for biochemistry are common or rare in the universe. Small rocky planets with liquid water enjoy key ingredients for biology. We used the National Aeronautics and Space Administration *Kepler* telescope to survey 42,000 Sun-like stars for periodic dimmings that occur when a planet crosses in front of its host star. We found 603 planets, 10 of which are Earth size and orbit in the habitable zone, where conditions permit surface liquid water. We measured the detectability of these planets by injecting synthetic planet-caused dimmings into *Kepler* brightness measurements. We find that 22% of Sun-like stars harbor Earth-size planets orbiting in their habitable zones. The nearest such planet may be within 12 light-years.

ASTRONOMY

Vetting of our TCEs produced a list of 836 eKOIs, which are analogous to KOIs produced by the *Kepler* Project. Each light curve is consistent with an astrophysical transit but could be due to an eclipsing binary (EB), either in the background or gravitationally bound, instead of a transiting planet. If an EB resides within the software aperture of a *Kepler* target star (within ~10 arcsec), the dimming of the EB can masquerade as a planet transit when diluted by the bright target star. We rejected as likely EBs any eKOIs with these characteristics: radii larger than 20 $R_\oplus$, observed secondary eclipse, or astrometric motion of the target star in and out of transit (*SI Appendix*). This rejection of EBs left 603 eKOIs in our catalog.

Kepler photometry can be used to measure R_P/R_* with high precision, but the extraction of planet radii is compromised by poorly known radii of the host stars (11). To determine R_* and T_{eff}, we acquired high-resolution spectra of 274 eKOIs using the HIRES spectrometer on the 10-m Keck I telescope. Notably, we obtained spectra of all 62 eKOIs that have $P > 100$ d. For these stars, the ~35% errors in R_* were reduced to ~10% by matching spectra to standards.

To measure planet occurrence, one must not only detect planets but also assess what fraction of planets were missed. Missed planets are of two types: those whose orbital planes are so tilted as to avoid dimming the star and those whose transits were not detected in the photometry by TERRA. Both effects can be quantified to establish a statistical correction factor. The first correction can be computed as the geometrical probability that an orbital plane is viewed edge-on enough (from Earth) that the planet transits the star. This probability is $P_T = R_*/a$, where a is the semimajor axis of the orbit.

The second correction is computed by the injection and recovery of synthetic (mock) planet-caused dimmings into real *Kepler* photometry. We injected 40,000 transit-like synthetic dimmings having randomly selected planetary and orbital properties into the actual photometry of our Best42k star sample, with stars selected at random. We measured survey completeness, $C(P, R_P)$, in small bins of (P, R_P), determining the fraction of injected synthetic planets that were discovered by TERRA (*SI Appendix*). Fig. 1 shows the 603 detected planets and the survey completeness, C, color-coded as a function of P and R_P.

The survey completeness for small planets is a complicated function of P and R_P. It decreases with increasing P and decreasing R_P as expected due to fewer transits and less dimming, respectively. It is dangerous to replace this injection and recovery assessment with noise models to determine C. Such models are not sensitive to the absolute normalization of C and only provide relative completeness. Models also may not capture the complexities of a multistage transit-finding pipeline that is challenged by correlated, nonstationary, and non-Gaussian noise. Measuring the occurrence of small planets with long periods requires injection and recovery of synthetic transits to determine the absolute detectability of the small signals buried in noise.

Planet Occurrence

We define planet occurrence, f, to be the fraction of stars having a planet within a specified range of orbital period, size, and perhaps other criteria. We report planet occurrence as a function of planet size and orbital period, $f(P, R_P)$ and as a function of planet size and the stellar light intensity (flux) incident on the planet, $f(F_P, R_P)$.

Planet Occurrence and Orbital Period. We computed $f(P, R_P)$ in a 6 × 4 grid of P and R_P shown in Fig. 2. We start by first counting the number of detected planets, n_{cell}, in each P-R_P cell. Then we computed $f(P, R_P)$ by making statistical corrections for planets missed because of nontransiting orbital inclinations and because of the completeness factor, C. The first correction augments each detected transiting planet by $1/P_T = a/R_*$, where P_T is the geometric transit probability, to account for planets missed in inclined orbits. Accounting for the completeness, C, the occurrence in a cell is $f(P, R_P) = 1/n_* \sum_i a_i/(R_{*,i} C_i)$, where $n_* = 42,557$ stars, and the sum is over all detected planets within that cell. Uncertainties in the statistical corrections for a/R_* and for completeness may cause errors in the final occurrence rates of ~10%. Such errors will be smaller than the Poisson uncertainties in the occurrence of Earth-size planets in long period orbits.

Fig. 2 shows the occurrence of planets, $f(P, R_P)$, within the P-R_P plane. Each cell is color-coded to indicate the final planet occurrence: the fraction of stars having a planet with radius and orbital period corresponding to that cell (after correction for both completeness factors). For example, 7.7 ± 1.3% of Sun-like stars have a planet with periods between 25 and 50 d and sizes between 1 and 2 $R_\oplus$.
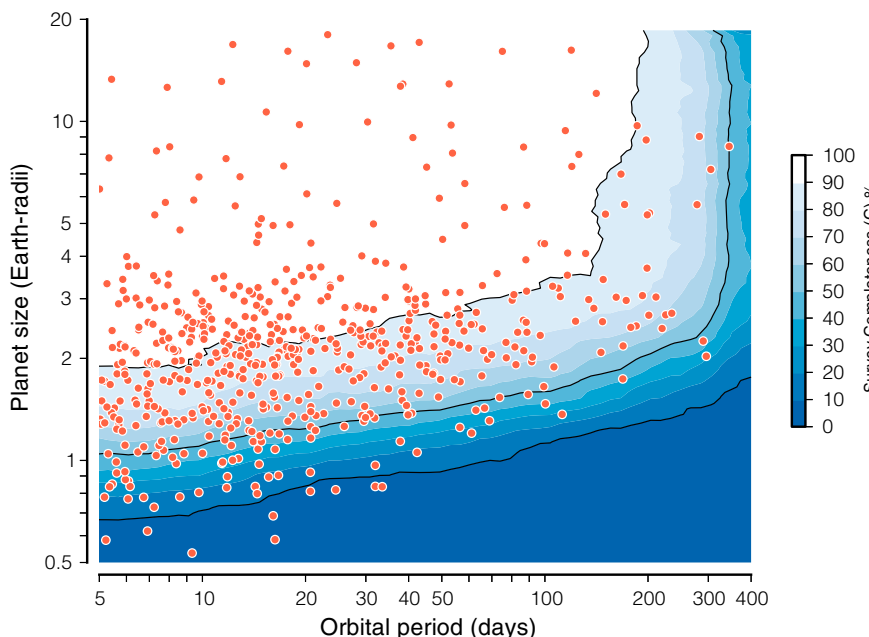
Fig. 1. 2D domain of orbital period and planet size, on a logarithmic scale. Red circles show the 603 detected planets in our survey of 42,557 bright Sun-like stars (*Kp* = 10–15 mag, GK spectral type). The color scale shows survey completeness measured by injection and recovery of synthetic planets into real photometry. Dark regions represent (*P*, *R_P*) with low completeness, *C*, where significant corrections for missed planets must be made to compute occurrence. The most common planets detected have orbital *P* < 20 d and *R_P* ≈ 1 – 3 *R_⊕* (at middle left of graph). However, their detectability is favored by orbital tilt and detection completeness, *C*, that favors detection of such close-in, large planets.
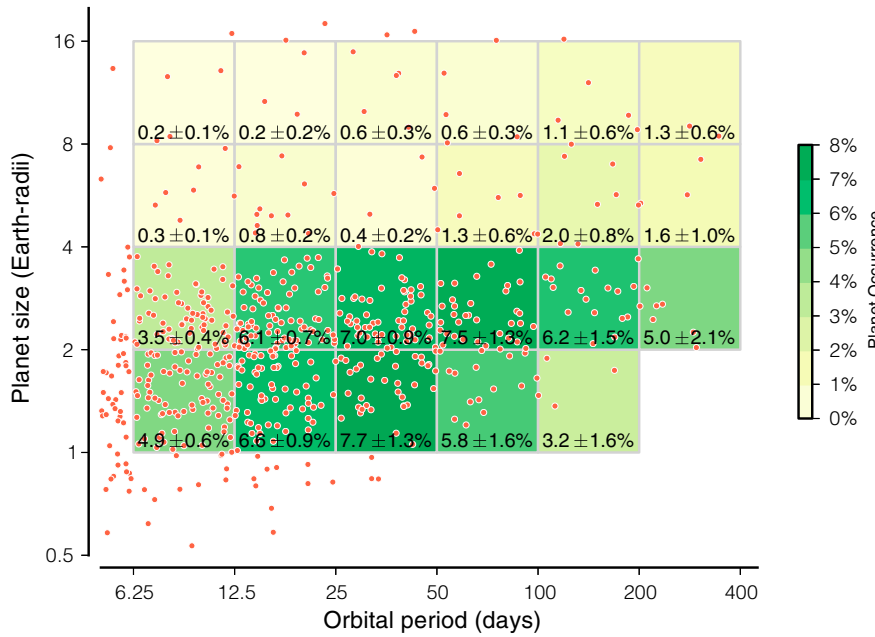
Fig. 2. Planet occurrence, $f(P,R_P)$, as a function of orbital period and planet radius for $P = 6.25$–400 d and $R_P = 0.5$–16 $R_\oplus$. As in Fig. 1, detected planets are shown as red circles. Each cell spans a factor of 2 in orbital period and planet size. Planet occurrence in a cell is given by $f(P,R_P) = 1/n_\star \sum_i a_i/(R_{\star,i} C_i)$, where the sum is over all detected planets within each cell. Here, a_i/R_i is the number of nontransiting planets (for each detected planet) due to large tilt of the orbital plane, $C_i = C(P_i, R_{P,i})$ is the detection completeness factor, and $n_\star = 42{,}557$ stars in the Best42k sample. Cells are colored according to planet occurrence within the cell. We quote planet occurrence within each cell. We do not color cells where the completeness is less than 25%. Among the small planets, 1–2 and 2–4 $R_\oplus$, planet occurrence is constant (within a factor of 2 level) over the entire range of orbital period. This uniformity supports mild extrapolation into the $P = 200$–400 d, $R_P = 1 - 2$ $R_\oplus$ domain.

We compute the distribution of planet sizes, including all orbital periods $P = 5$–100 d, by summing $f(P,R_P)$ over all periods. The resulting planet size distribution is shown in Fig. 3A. Planets with orbital periods of 5–100 d have a characteristic shape to their size distribution (Fig. 3A). Jupiter-sized planets (11 $R_\oplus$) are rare, but the occurrence of planets rises steadily with decreasing size down to about 2 $R_\oplus$. The distribution is nearly flat (equal numbers of planets per log R_P interval) for 1–2 $R_\oplus$ planets. We find that $26 \pm 3\%$ of Sun-like stars harbor an Earth-size planet ($1 - 2$ $R_\oplus$) with $P = 5$–100 d, compared with $1.6 \pm 0.4\%$ occurrence of Jupiter-size planets ($8 - 16$ $R_\oplus$).

We also computed the distribution of orbital periods, including all planet sizes, by summing each period interval of $f(P,R_P)$ over all planet radii. As shown in Fig. 3B, the occurrence of planets larger than Earth rises from $8.9 \pm 0.7\%$ in the $P = 6.25$–12.5 d domain to $13.7 \pm 1.2\%$ in the $P = 12.5$–25 d interval and

is consistent with constant for larger periods. This rise and plateau feature was observed for $\gtrsim 2$ $R_\oplus$ planets in earlier work (5, 12).

Two effects lead to minor corrections to our occurrence estimates. First, some planets in multitransiting systems are missed by TERRA. Second, a small number of eKOIs are false detections. These two effects are small, and they provide corrections to our occurrence statistics with opposite signs. To illustrate their impact, we consider the small and long period ($P > 50$ d) planets that are the focus of this study.

TERRA detects the highest SNR transiting planet per system, so additional transiting planets that cause lower SNR transits are not included in our occurrence measurement. Using the *Kepler* Project catalog (Exoplanet Archive), we counted the number of planets within the same cells in P and R_P as Fig. 2, noting those that did not yield the highest SNR in the system. Inclusion of
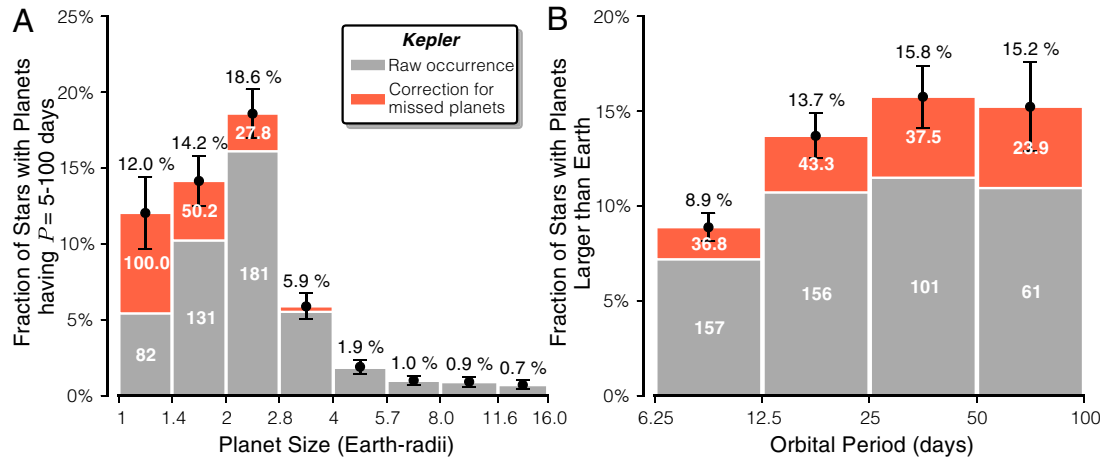
Fig. 3. The measured distributions of planet sizes (A) and orbital periods (B) for $R_P > 1$ $R_\oplus$ and $P = 5$–100 d. Heights of the bars represent the fraction of Sun-like stars harboring a planet within a given P or R_P domain. The gray portion of the bars show planet occurrence without correction for survey completeness, i.e., for $C = 1$. The red region shows the correction to account for missed planets, $1/C$. Bars are annotated to reflect the number of planets detected (gray bars) and missed (red bars). The occurrence of planets of different sizes rises by a factor of 10 from Jupiter-size to Earth-sized planets. The occurrence of planets with different orbital periods is constant, within 15%, between 12.5 and 100 d. Due to the small number of detected planets with $R_P = 1 - 2$ $R_\oplus$ and $P > 100$ d (four detected planets), we do not include $P > 100$ d in these marginalized distributions.

these second and third transiting planets boosts the total number of planets per cell (and hence the occurrence) by 21–28% over the $P = 50$–400 d, $R_P = 1$–4 $R_\oplus$ domain (*SI Appendix*).

Even with our careful vetting of eKOIs, the light curves of some false-positive scenarios are indistinguishable from planets. Fressin et al. (7) simulated the contamination of a previous KOI (4) sample by false positives that were not removed by the *Kepler* Project vetting process. They determined that the largest source of false positives for Earth-size planets are physically bound stars with a transiting Neptune-size planet, with an overall false-positive rate of 8.8–12.3%. As we have shown (Fig. 2), the occurrence of Neptune-size planets is nearly constant as a function of orbital period, in $\log P$ intervals. Thus, this false-positive rate is also nearly constant in period. Therefore, we adopt a 10% false-positive rate for planets having $P = 50$–400 d and $R_P = 1$–2 $R_\oplus$. Planet occurrence, shown in Figs. 2 and 3, has not been adjusted to account for false positives or planet multiplicity. The quoted errors reflect only binomial counting uncertainties. Note that for Earth-size planets in the 50–100 and 100–200 d period bins, planet occurrence is $5.8 \pm 1.8\%$ and $3.2 \pm 1.6\%$, respectively. Corrections due to false positives or planet multiplicity are smaller than fractional uncertainties due to small number statistics.

Planet Occurrence and Stellar Light Intensity. The amount of light energy a planet receives from its host star depends on the luminosity of the star (L_*) and the planet-star separation (a). Stellar light flux, F_P, is given by $F_P = L_*/4\pi a^2$. The intensity of sunlight on Earth is $F_\oplus = 1.36$ kW m^{-2}. We compute L_* using $L_* = 4\pi R_*^2 \sigma T_{\text{eff}}^4$, where $\sigma = 5.670 \times 10^{-8}$ Wm^{-2}K^{-4} is the Stefan-Boltzmann constant. The dominant uncertainty in F_P is due to R_*. Using spectroscopic stellar parameters, we determine F_P to 25% accuracy and to 80% accuracy using photometric parameters. We obtained spectra for all 62 stars hosting planets with $P > 100$ d, allowing more accurate light intensity measurements.

Fig. 4 shows the 2D domain of stellar light flux incident on our 603 detected planets, along with planet size. The planets in our sample receive a wide range of flux from their host stars, ranging from 0.5 to 700 $F_\oplus$. We highlight the 10 small ($R_P = 1$–2 $R_\oplus$) planets that receive stellar flux comparable to Earth: $F_P = 0.25$–4 $F_\oplus$.

Because only two 1–2 $R_\oplus$ planets have $F_P < 1$ $F_\oplus$, we measure planet occurrence in the domain, 1–2 $R_\oplus$ and 1–4 $F_\oplus$. Correcting for survey completeness, we find that $11 \pm 4\%$ of Sun-like stars have a $R_P = 1$–2 $R_\oplus$ planet that receives between one and four times the incident flux as the Earth (*SI Appendix*).

Interpretation

Earth-Size Planets with Year-Long Orbital Periods.
Detections of Earth-size planets having orbital periods of $P = 200$–400 d are expected to be rare in this survey. Low survey completeness ($C \approx 10\%$) and low transit probability ($P_T = 0.5\%$) imply that only a few such planets would be expected, even if they are intrinsically common. Indeed, we did not detect any such planets with TERRA, although the radii of three planets (KIC-4478142, KIC-8644545, and KIC-10593626) have 1σ confidence intervals that extend into the $P = 200$–400 d, $R_P = 1$–2 $R_\oplus$ domain. We can place an upper limit on their occurrence: $f < 12\%$ with 95% confidence using binomial statistics. We would have detected one or two such planets if their occurrence was higher than 12%.

However, one may estimate the occurrence of 1–2 $R_\oplus$ planets with periods of 200–400 d by a modest extrapolation of planet occurrence with P. Fig. 5 shows the fraction of stars with 1–2 $R_\oplus$ planets, whose orbital period is less than a maximum period, P, on the horizontal axis. This cumulative period distribution shows that 20.4% of Sun-like stars harbor a 1–2 $R_\oplus$ planet with an orbital period, $P < 50$ d. Similarly, 26.2% of Sun-like stars harbor a 1–2 $R_\oplus$ planet with a period less than 100 d. The linear increase in cumulative occurrence implies constant planet occurrence per $\log P$ interval. Extrapolating the cumulative period distribution predicts $5.7^{+1.7}_{-2.2}\%$ occurrence of Earth-size (1–2 $R_\oplus$) planets with orbital periods of ~1 y ($P = 200$–400 d). The details of our extrapolation technique are explained in *SI Appendix*. Extrapolation based on detected planets with $P < 200$ d predicts that $5.7^{+1.7}_{-2.2}\%$ of Sun-like stars have an Earth-size planet on an Earth-like orbit ($P = 200$–400 d).

Naturally, such an extrapolation carries less weight than a direct measurement. However, the loss of *Kepler's* second reaction wheel in May 2013 ended observations shortly after the completion of the nominal 3.5-y mission. We cannot count on any additional *Kepler* data to improve the low completeness to Earth
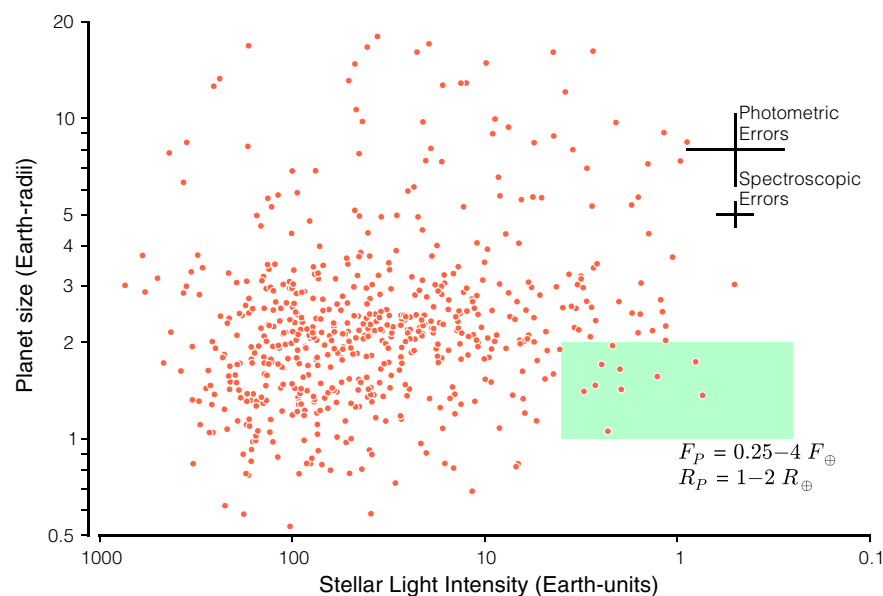
Fig. 4. The detected planets (dots) in a 2D domain similar to Figs. 1 and 2. Here, the 2D domain has orbital period replaced by stellar light intensity, incident flux, hitting the planet. The highlighted region shows the 10 Earth-size planets that receive an incident stellar flux comparable to the Earth: flux = 0.25–4.0 times the flux received by the Earth from the Sun. Our uncertainties on stellar flux and planet radii are indicated at the top right.

Petigura et al.
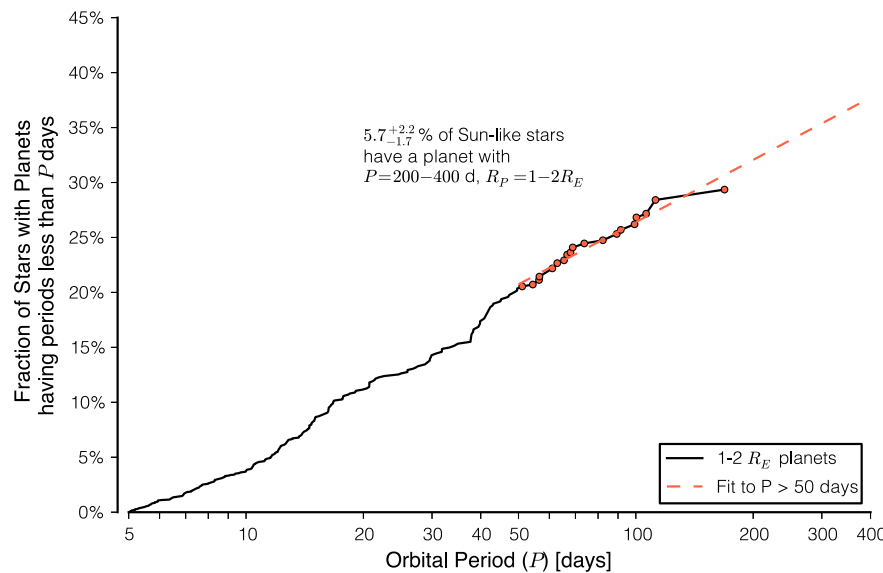
Fig. 5. The fraction of stars having nearly Earth-size planets ($1 - 2$ $R_\oplus$) with any orbital period up to a maximum period, P, on the horizontal axis. Only planets of nearly Earth size ($1 - 2$ $R_\oplus$) are included. This cumulative distribution reaches 20.2% at $P = 50$ d, meaning 20.4% of Sun-like stars harbor a 1–2 $R_\oplus$ planet with an orbital period, $P < 50$ d. Similarly, 26.2% of Sun-like stars harbor a 1–2 $R_\oplus$ planet with a period of $P < 100$ d. The linear increase in this cumulative quantity corresponds to planet occurrence that is constant in equal intervals of $\log P$. One may perform a modest extrapolation into the $P = 200$–400 d range, equivalent to assuming constant occurrence per $\log P$ interval, using all planets with $P > 50$ d. Such an extrapolation predicts that $5.7^{+1.7}_{-2.2}$% of Sun-like stars have a planet with size 1–2 $R_\oplus$, with an orbital period between $P = 200$ and 400 d.

analog planets beyond what is reported here. Indeed, low survey sensitivity to Earth analogs was the primary reason behind a 4-y extension to the *Kepler* mission. Modest extrapolation is required to understand the prevalence of Earth-size planets with Earth-like orbits around Sun-like stars.

We offer empirical and theoretical justification for extrapolation out to 400 d. As shown in Fig. 2, the prevalence of small planets as a function of $\log P$ is remarkably uniform. To test the reliability of our extrapolation into a region of low completeness, we used the same technique to estimate occurrence in more complete regions of phase space and compared the results with our measured occurrence values.

Again, assuming uniform occurrence per $\log P$ interval, extrapolating the occurrence of 2–4 $R_\oplus$ planets from 50 to 200 d orbits out to 400 d predicts $6.4^{+0.5}_{-1.2}$% occurrence of planets in the domain of $R_P = 2 - 4$ $R_\oplus$ and $P = 200$–400 d. The extrapolation is consistent with the measured value of 5.0 ± 2.1% to within 1σ uncertainty. Futhermore, extrapolation based on 1–2 $R_\oplus$ planets with $P = 12.5$–50 d predicts $6.5^{+0.9}_{-1.7}$% occurrence within the $P = 50$–100 d bin. Again, the measured value of 5.8 ± 1.6% agrees to better than 1σ.

Although planet size is governed by nonlinear processes such as runaway gas accretion (13), which favors certain planet sizes over others, no such nonlinear processes occur as a function of orbital period in the range of 200–400 d. Extrapolation out to orbital periods of 200–400 d, although dangerous, seems unlikely to be unrealistic by more than a factor of 2.

Earth-Size Planets in the Habitable Zone. Although the details of planetary habitability are debated and depend on planet-specific properties as well as the stochastic nature of planet formation (14), the habitable zone (HZ) is traditionally defined as the set of planetary orbits that permit liquid water on the surface. The precise inner and outer edges of the HZ depend on details of the model (15–18). For solar analog stars, Zsom et al. (17) estimated that the inner edge of the HZ could reside as close as 0.38 astronomical unit (AU) for planets having either a reduced greenhouse effect due to low humidity or a high reflectivity. One AU is the average distance between the Earth and Sun and is

equal to 1.50×10^{11} m. Pierrehumbert and Gaidos (18) estimated that the outer edge of the HZ may extend up to 10 AU for planets that are kept warm by efficient greenhouse warming with an H_2 atmosphere.

A planet's ability to retain surface liquid water depends, in large part, on the energy received from its host star. We consider a planet to reside in the HZ if it is bathed in a similar level of starlight as Earth. One may adopt $F_P = 0.25$–4 $F_\oplus$ as a simple definition of the HZ, which corresponds to orbital separations of 0.5–2.0 AU for solar analog stars. This definition is more conservative than the range of published HZ boundaries that extend from 0.38 to 10 AU (17, 18). This HZ includes Venus (0.7 AU) and Mars (1.5 AU), which do not currently have surface liquid water. However, Venus may have had liquid water in its past, and there is strong geochemical and geomorphological evidence of liquid water earlier in Mars' history (14).

Previously, we showed that 11 ± 4% of stars harbor a planet having an $R_P = 1 - 2$ $R_\oplus$ and $F_P = 1 - 4$ $F_\oplus$. Using the definition of F_P and Kepler's third law, F_P is proportional to $P^{-4/3}$. Therefore, uniform occurrence in $\log P$ translates to uniform occurrence in $\log F_P$. We find that the occurrence of 1–2 $R_\oplus$ planets is constant per $\log F_P$ interval for $F_P = 100 - 1$ $F_\oplus$. If one was to adopt $F_P = 0.25 - 4$ $F_\oplus$ as the HZ and extrapolate from the $F_P = 1 - 4$ $F_\oplus$

Table 1. Occurrence of small planets in the habitable zone

HZ definition	a_{inner}	a_{outer}	$F_{P,inner}$	$F_{P,outer}$	f_{HZ} (%)
Simple	0.5	2	4	0.25	22
Kasting (1993)	0.95	1.37	1.11	0.53	5.8
Kopparapu et al. (2013)	0.99	1.70	1.02	0.35	8.6
Zsom et al. (2013)	0.38		6.92		26*
Pierrehumbert and Gaidos (2011)		10		0.01	~50†

*Zsom et al. (17) studied the inner edge of the habitable zone. Here we adopt an outer edge of 2 AU from the Simple model.
†Pierrehumbert and Gaidos (18) studied the outer edge of the habitable zone. Here we adopt an inner edge of 0.5 AU from the Simple model. Extrapolation out to 10 AU is severely underconstrained. This estimate is highly uncertain and is included for completeness.

domain, then the occurrence of Earth-size planets in the HZ is $22 \pm 8\%$ for Sun-like stars.

One may adopt alternative definitions of both the properties of Earth-size planets and the domain of the HZ. We showed previously that the occurrence of planets is approximately constant as a function of both R_P (for $R_P < 2.8 \, R_\oplus$) and P (in logarithmic intervals). Thus, the occurrence of planets in this domain is proportional to logarithmic area in the R_P–F_P parameter space being considered. For example, the occurrence of planets of size 1.0–1.4 $R_\oplus$ in orbits that receive 0.25–1.0 $F_\oplus$ in stellar flux is 22%/4 = 5.5%. We offer a number of estimates for the prevalence of Earth-size planets in the HZ based on different published definitions of the HZ in Table 1.

Cooler, M dwarf stars also have a high occurrence of Earth-size planets. Based on the *Kepler* planet catalog, Dressing et al. (19) found that $15^{+15}_{-6}\%$ of early M dwarfs have an Earth-size planet $(0.5 - 1.4 \, R_\oplus)$ in the HZ using a conservative definition of 0.5–1.1 $F_\oplus$ (15) and three times that value when the HZ is expanded to 0.25–1.5 $F_\oplus$ (20). This result is consistent with a Doppler survey that found that $41^{+54}_{-13}\%$ of nearby M dwarfs have planets with masses 1–10 Earth masses $(M_\oplus)$ in the HZ (21). Thus, Earth-size planets appear to be common in the HZs of a range of stellar types.

Conclusions

Using *Kepler* photometry of Sun-like stars (GK-type), we measured the prevalence of planets having different orbital periods and sizes, down to the size of the Earth and out to orbital periods of 1 y. We gathered Keck spectra of all host stars of planets having periods greater than 100 d to accurately determine their radii. The detection of planets with periods longer than 100 d is challenging, and we characterized our sensitivity to such planets by using injection and recovery of synthetic planets in the photometry. After correcting for orbital tilt and detection completeness, we find that $26 \pm 3\%$ of Sun-like stars have an Earth-size $(1 - 2 \, R_\oplus)$ planet with $P = 5$–100 d. We also find that $11 \pm 4\%$ of Sun-like stars harbor an Earth-size planet that receives nearly Earth levels of stellar energy $(F_P = 1 - 4 \, F_\oplus)$.

We showed that small planets far outnumber large ones. Only $1.6 \pm 0.4\%$ of Sun-like stars harbor a Jupiter-size $(8 - 16 \, R_\oplus)$ planet with $P = 5$–100 d compared with a $23 \pm 3\%$ occurrence of Earth-size planets. This pattern supports the core accretion scenario in which planets form by the accumulation of solids first and gas later in the protoplanetary disk (13, 22–24). The details of this family of models are hotly debated, including the movement of material within the disk, the timescale for planet formation, and the amount of gas accretion in small planets. Our measurement of a constant occurrence of 1–2.8 $R_\oplus$ planets per log$P$ interval establishes an important observational constraint for these models.

The occurrence of Earth-size planets is constant with decreasing stellar light intensity from 100 $F_\oplus$ down to 1 $F_\oplus$. If one was to assume that this pattern continues down to 0.25 $F_\oplus$, then the occurrence of planets having flux levels of 1–0.25 $F_\oplus$ is also $11 \pm 4\%$.

Earth-size planets are common in the *Kepler* field. If the stars in the *Kepler* field are representative of stars in the solar neighborhood, then Earth-size planets are common around nearby Sun-like stars. If one were to adopt a 22% occurrence rate of Earth-size planets in habitable zones of Sun-like stars, then the nearest such planet is expected to orbit a star that is less than 12 light-years from Earth and can be seen by the unaided eye. Future instrumentation to image and take spectra of these Earths need only observe a few dozen nearby stars to detect a sample of Earth-size planets residing in the HZs of their host stars.

1. Borucki WJ, et al. (2010) Kepler planet-detection mission: Introduction and first results. *Science* 327(5968):977–980.
2. Koch DG, et al. (2010) Kepler mission design, realized photometric performance, and early science. *Astrophys J Lett* 713(2):L79–L86.
3. Borucki WJ, et al. (2011) Characteristics of planetary candidates observed by Kepler. II. Analysis of the first four months of data. *Astrophys J* 736(1):19–40.
4. Batalha NM, et al. (2013) Planetary candidates observed by Kepler. III. Analysis of the first 16 months of data. *Astrophys J* 204(2):24–44.
5. Howard AW, et al. (2012) Planet occurrence within 0.25 AU of solar-type stars from Kepler. *Astrophys J* 201(2):15–39.
6. Petigura EA, Marcy GW, Howard AW (2013) A plateau in the planet population below twice the size of Earth. *Astrophys J* 770(1):69–89.
7. Fressin F, et al. (2013) The false positive rate of Kepler and the occurrence of planets. *Astrophys J* 766(2):81–100.
8. Pinsonneault MH, et al. (2012) A revised effective temperature scale for the Kepler input catalog. *Astrophys J* 199(2):30–51.
9. Petigura EA, Marcy GW (2012) Identification and removal of noise modes in Kepler photometry. *Publ Astron Soc Pac* 124(920):1073–1082.
10. Mandel K, Agol E (2002) Analytic light curves for planetary transit searches. *Astrophys J Lett* 580(2):L171–L175.
11. Brown TM, Latham DW, Everett ME, Esquerdo GA (2011) Kepler input catalog: Photometric calibration and stellar classification. *Astron J* 142(4):112–129.
12. Youdin AN (2011) The exoplanet census: A general method applied to Kepler. *Astrophys J* 742(1):38–50.
13. Ida S, Lin DNC, Nagasawa M (2013) Toward a deterministic model of planetary formation. VII. Eccentricity distribution of gas giants. *Astrophys J* 775(1):42–64.
14. Seager S (2013) Exoplanet habitability. *Science* 340(6132):577–581.
15. Kasting JF, Whitmire DP, Reynolds RT (1993) Habitable zones around main sequence stars. *Icarus* 101(1):108–128.
16. Kopparapu RK, et al. (2013) Habitable zones around main-sequence stars: New estimates. *Astrophys J* 765(2):131–146.
17. Zsom A, Seager S, de Wit J, Stamenkovic V Towards the minimum inner edge distance of the habitable zone *Astrophys J.*, in press.
18. Pierrehumbert R, Gaidos E (2011) Hydrogen greenhouse planets beyond the habitable zone. *Astrophys J Lett* 734(1):L13–L17.
19. Dressing CD, Charbonneau D (2013) The occurrence rate of small planets around small stars. *Astrophys J* 767(1):95–114.
20. Kopparapu RK (2013) A revised estimate of the occurrence rate of terrestrial planets in the habitable zones around Kepler M-dwarfs. *Astrophys J Lett* 767(1):L8–L12.
21. Bonfils X, et al. (2013) The HARPS search for southern extra-solar planets. XXXI. The M-dwarf sample. *Astron Astrophys* 549:A109.
22. Levy EH, Lunine JI, eds (1993) *Growth of Planets from Planetesimals* (University of Arizona Press, Tucson, AZ), pp 1061–1088.
23. Pollack JB, et al. (1996) Formation of the giant planets by concurrent accretion of solids and gas. *Icarus* 124(1):62–85.
24. Mordasini C, et al. (2012) Characterization of exoplanets from their formation. II. The planetary mass-radius relationship. *Astron Astrophys* 547:A112.

Supporting Information (SI)

In this supplement to "Prevalence of Earth-size planets orbiting Sun-like stars" by Petigura et al., we elaborate on the technical details of our analysis. In Section S1, we define our sample of 42,557 Sun-like stars that are amenable to the detection of small planets — the "Best42k" stellar sample. In Section S2, we describe the algorithmic components of TERRA, our custom pipeline that we used to find transiting planets within *Kepler* photometry. Section S3 describes "data validation," how we prune the large number of "Threshold Crossing Events" into a list of 836 eKOIs, analogous to KOIs from the *Kepler* Project. Section S4 shows four KOIs in the current online Exoplanet Archive (*1*) that failed the data validation step. Section S5 describes the procedure by which we remove astrophysical false positives from our list of eKOIs. Section S6 describes how we refine our initial estimate of planet radii using using spectra of the eKOIs coupled with MCMC-based light curve fitting. Section S7 contains a description of the fundamental component of this study: measuring the completeness of our planet search by injecting synthetic transit light curves, caused by planets of all sizes and orbital periods, directly into the *Kepler* photometry, and analyzing the photometry with our pipeline to determine the fraction of planets detected. In Section S8 we provide details describing our calculation of planet occurrence and discuss the effects of multiplanet systems and false positives.

S1   The Best42k Stellar Sample

We restrict our planet search to Sun-like stars with well-determined photometric properties and low photometric noise. We select stars having revised *Kepler* Input Catalog (KIC) parameters. Effective temperatures are based on the Pinsonneault et al. (*2*) revisions to the KIC effective temperatures. Surface gravities are based on fits to Yonsei-Yale stellar evolution mod-

els (*3*) assuming [Fe/H] = -0.2. Further details regarding isochrone fitting can be found in Batalha et al. (*4*); Burke et al., submitted; and Rowe et al., in prep. These revised stellar parameters are tabulated on the Exoplanet Archive with the `prov_prim` flag set to "Pinsonneault." Out of the 188,329 stars observed at some point during Q1–Q15, we selected stars that:

1. Have revised KIC stellar properties. (155,046 stars),

2. Kp = 10–15 mag (98,471 stars),

3. T_{eff} = 4100–6100 K (63,915 stars), and

4. $\log g$ = 4.0–4.9 (cgs) (42,557 stars).

Figure S1 shows the position of the 155,046 stars with revised stellar properties along with the "solar subset" corresponding to G and K dwarfs. Figure S2 shows the distribution of brightness and noise level of the Best42k stellar sample.
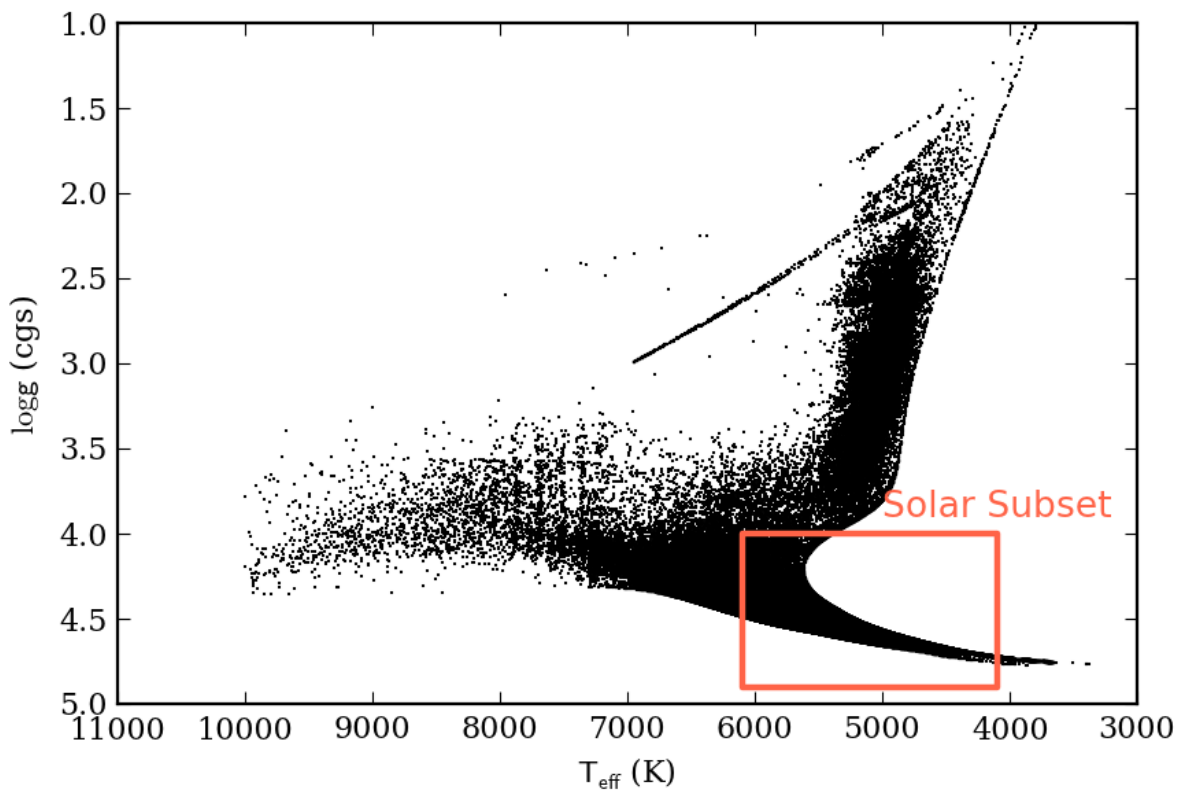
Figure S1: Distribution of 155,046 stars with revised photometric stellar parameters. The Best42k sample of 42000 stars is made up of Solar-type stars with T_{eff} = 4100–6100 K, $\log g$ = 4.0–4.9 (cgs), and Kepmag = 10-15 (brighter half of targets).
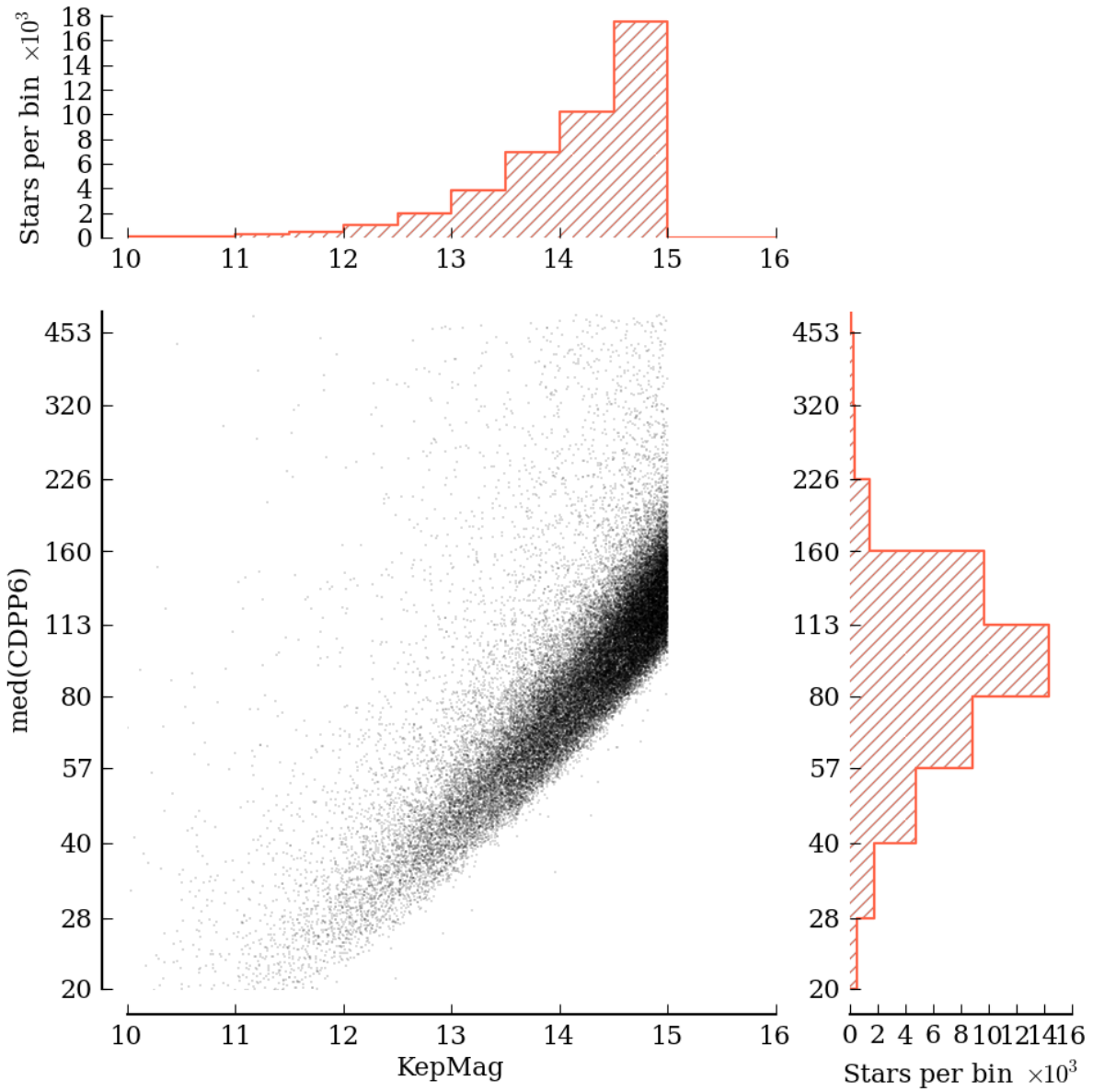
Figure S2: Distribution of photometric noise (median quarterly 6 hour CDPP) and brightness *Kp* for the 42,557 stars in the Best42k stellar sample.

S2 Planet Search Photometric Pipeline

We search for planet candidates in the Best42k stellar sample using the `TERRA` pipeline described in detail in Petigura & Marcy (2012) and in Petigura, Marcy, and Howard (2013; P13, hereafter) (*5, 6*). We review the major components of `TERRA` below, noting the changes since P13.

S2.1 Time-domain pre-processing of raw *Kepler* Photometry

`TERRA` begins by conditioning the photometry in the time-domain. `TERRA` first searches for single cadence outliers, mostly due to cosmic rays. `TERRA` also searches for abrupt drops in the raw photometry known as Sudden Pixel Sensitivity Drops (SPSDs) discussed by Stumpe et al. (*7*). SPSDs are particularly challenging since they mimic transit ingress, and aggressive attempts to remove them run the risk of removing real transits. `TERRA` removes the largest SPSDs, but they remain a source of non-astrophysical false positives that we remove during manual triage (Section S3.2).

TERRA also removes trends longer than ∼10 days. In P13, this high-pass filtering was implemented by fitting a spline to the raw photometry with the knots of the spline separated by 10 days. But in this work we employ high-pass filtering using Gaussian Process regression (*8*), which gives finer control over the timescales removed. We adopt a squared exponential kernel with a 5-day correlation length. After this high-pass filter, `TERRA` identifies systematic noise modes via principle components analysis on large number of stars.

S2.2 Grid-based transit search

We search for periodic box-shaped dimmings by evaluating the signal-to-noise ratio (SNR) of a putative transit over a finely-spaced grid of period, P; epoch, t_0; and transit duration, ΔT. In P13, we searched over a period range, P = 5–50 days, and over transit durations ranging from 1.5–8.8 hr. But in this work, we extend our search in orbital period to P = 0.5–400 days.

Table S1.   TERRA Grid Search Parameters

P_1 days	P_2 days	Trial Transit Duration (ΔT) long cadence measurements
5.0	7.7	[3, 4, 5, 7, 9, 11]
7.7	12.0	[4, 5, 7, 9, 13]
12.0	18.6	[4, 5, 7, 9, 13, 15]
18.6	28.9	[5, 7, 9, 12, 16, 17]
28.9	44.7	[6, 8, 11, 14, 19, 20]
44.7	69.3	[7, 9, 12, 16, 22, 23]
69.3	107.4	[8, 11, 14, 19, 25, 26]
107.4	166.5	[9, 12, 16, 21, 28, 31]
166.5	258.1	[10, 13, 18, 24, 31, 35]
258.1	400.0	[12, 16, 21, 28, 38, 41]

Since we search over nearly three decades in orbital period, and because transit duration is proportional to $P^{1/3}$, we let the range of trial transit durations vary with period. We break our period range into 10 equal logarithmic intervals. Then, using photometrically determined parameters for each star, namely $M_\star$ and $R_\star$, we compute an approximate, expected transit duration ($\Delta T_{\rm circ}$) for the simple case of circular orbits with impact parameter, $b = 1$. However, we actually search over $\Delta T = 0.5$–1.5 $\Delta T_{\rm circ}$ to account for a range of impact parameters and orbital eccentricities and for mis-characterized $M_\star$ and $R_\star$. As an example, Table S1 shows our trial ΔT for a star with solar mass and radius.

S3 Data Validation

If TERRA detects a $(P, t_0, \Delta T)$ with SNR > 12, we flag the light curve for additional scrutiny. While the grid-based component of TERRA is well-matched to exoplanet transits, there are other phenomena that can produce SNR > 12 events and contaminate our planet sample. We distinguish between two classes of contaminates: "astrophysical false positives" such as diluted eclipsing binaries (EBs), and "non-astrophysical false positives" such as noise that can mimic a transit. We establish a series of quality control measures called "Data Validation" (DV), designed to remove formally strong dimmings (i.e. SNR > 12) found by the blind photometric pipeline that are not consistent with an astrophysical transit. DV consists of two steps:

1. *Machine triage*: Select potential transits by automated cuts.

2. *Manual triage*: Manually remove light curves that are inconsistent with a Keplerian transit.

Manual triage is accomplished by inspection of DV summary plots which contain numerous useful diagnostics necessary to warrant planet status. The diagnostics permit a multi-faceted evaluation of the integrity (as a potential planet candidate) of a given dimming identified by the photometric pipeline. Figure S3 shows an sample DV report, this for KIC-5709725 that passed examination.

The product of the DV quality control is a list of "eKOIs," for which most instrumental events identified preliminarily and erroneously by the photometric pipeline have been rejected. The resulting planet candidates are analogous to the KOIs *Kepler* Project. Astrophysically plausible causes (i.e. transiting planets and background eclipsing binaries) are retained among our eKOIs. We address astrophysical false positives in Section S5.
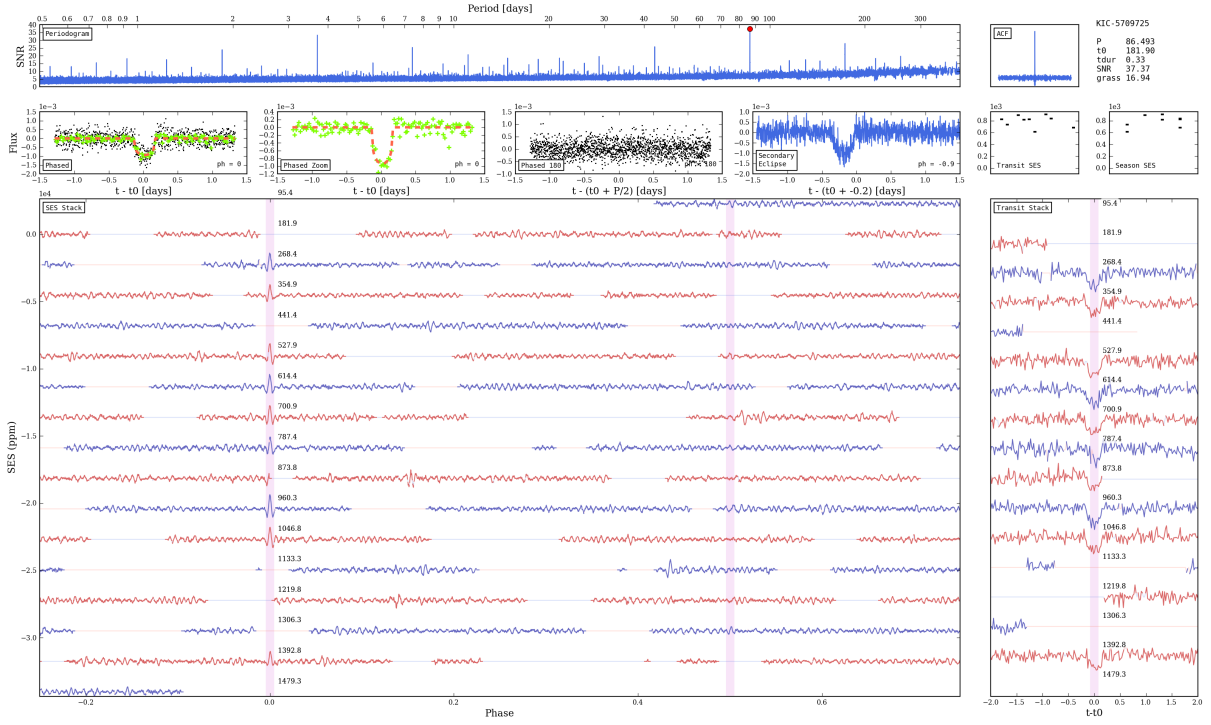
Figure S3: DV summary plots for KIC-5709725. Top row: SNR "periodogram" of box-car photometric search for transiting planets, ranging from 0.5 to 400 days. The red dot shows the P and SNR of the most significant peak in the periodogram at $P = 86.5$ days (also found by the *Kepler* Project as KOI-555.02). Also visible is a second set of peaks corresponding to KOI-555.01 at $P = 3.702$ days. TERRA does not search for more than one planet per system. Moreover, KOI-555.01 would be excluded from our planet sample since $P < 5$ days. The autocorrelation function, "ACF", plot at upper right shows the circular auto-correlation function from the phase folded photometry, used to identify secondary eclipses and correlated noise in the photometry. Second row: at left "Phase" shows the phase–folded photometry, where black points represent detrended photometry near the time of transit, green symbols show median flux over 30 min bins, and the dashed line shows the best-fitting Mandel-Agol transit model (*9*). At second from left, "Phased Zoom" shows a zoomed y-axis to highlight the transit itself. For this TCE, the transit model is a good match to the photometry. At third from left, "Phased 180" shows phase folded photometry 180° in orbital phase from transit center. At fourth from left, "Secondary eclipse" shows how TERRA notches out the putative transit and searches for secondary eclipses. We show the photometry folded on the second most significant dimming. For KIC-5709725, this phase is 0.9° relative to the primary transit, so close in phase that the primary transit is still visible. This transit does not show signs of a secondary eclipse. Transit SES — transit single event statistic as a function of transit number. Conceptually, SES is the depth of the transit in ppm, as described by Petigura and Marcy (*5*). "Season SES" shows the SES statistic grouped according to season. Bottom row: At left, "SES stack" shows SES for the entire light curve, split on the best-fitting transit period and stacked so that transit number increases downward. Compelling transits appear as a sequence of SES peaks at phase = 0°. "Transit stack" shows for TCEs with fewer than 20 transits a plot of the TERRA-calibrated photometry of each transit (transit number increases downward).

S3.1 Machine Triage

Prior to the identification of final eKOIs, we carry out machine triage to identify a set of "Threshold Crossing Events" (TCEs) that can be classified by a human in a reasonable amount of time. TCE status requires a SNR > 12; however, we find that 16227 light curves (out of the 42000 target stars) meet this criterion. Outliers and correlated noise are responsible for the majority of SNR > 12 events. We show set of diagnostic plots for such an outlier in Figure S4. Here, an uncorrected sudden pixel sensitivity dropoff at $t = 365.3$ days, raises the noise floor to SNR~15 for $P \lesssim 100$ days. Its contribution to SNR is averaged down for shorter periods.

We flag such outliers by comparing the most significant period, P_{max}, to nearby periods. We call the ratio of the maximum SNR to the median of the next tallest five peaks between $[P_{\mathrm{max}}/1.4, P_{\mathrm{max}} \times 1.4]$ the `s2n_on_grass` statistic. We require `s2n_on_grass` > 1.2 for TCE status. After that cut, 3438 TCEs remain. We also require $P_{\mathrm{max}} > 5$ d, which leaves 2184 TCEs.

S3.2 Manual Triage

The sample of 2184 TCEs has a significant degree of contamination from non-astrophysical false positives. In P13, we relied on aggressive automatic cuts that removed nearly all of the non-astrophysical false positives (final sample was $\sim 90\%$ pure). However, by comparing our sample to that of Batalha et al. (*4*), we found that these automatic cuts were removing a handful of compelling planet candidates.

In this work, we aim for higher completeness and rely more heavily on visual inspection of light curves. We assess whether a TCE is due to a string of three or more transits or instead caused by outlier(s) such as SPSDs. Figure S5 shows an example of a light curve that passed machine triage, but was removed manually. During manual triage, we do not attempt to distinguish between planets and astrophysical false positives. The end product is a list of 836 eKOIs,
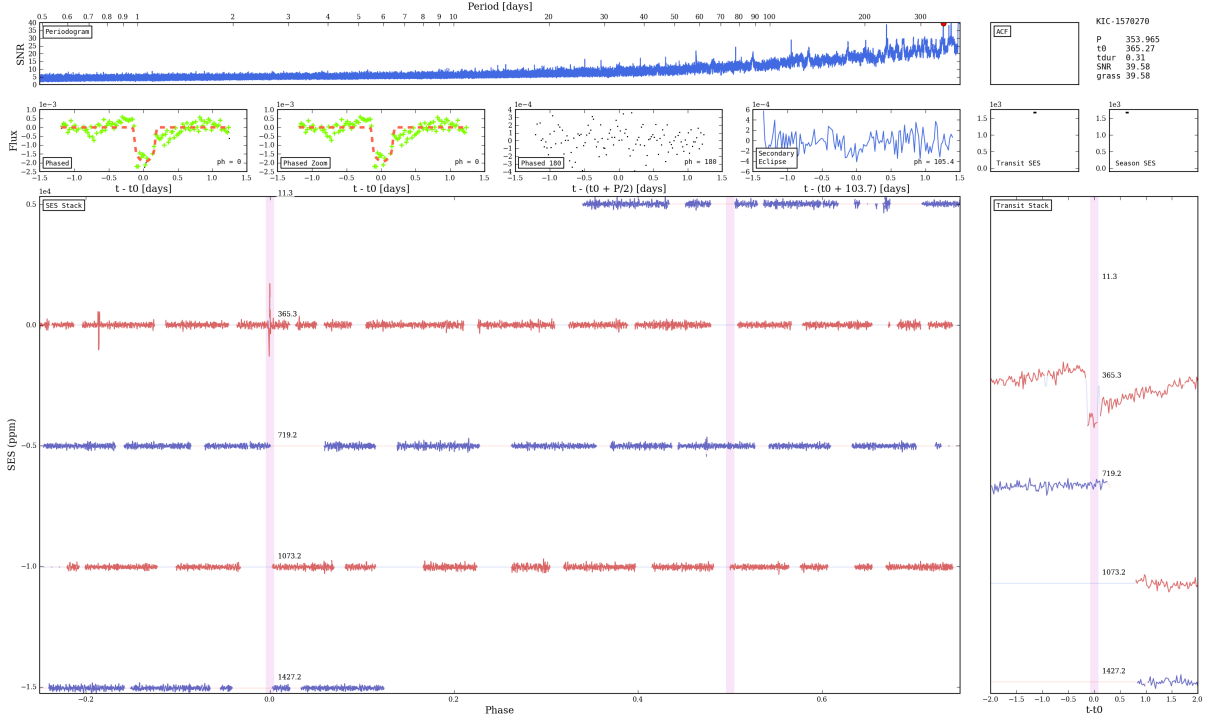
Figure S4: DV summary plots (defined in Figure S3) for KIC-1570270 showing a non-astrophysical false positive removed in the machine triage step. Here, an uncorrected SPSD at $t = 365.3$ days resulted in a SNR~40 event with $P = 353.965$ days, seen in the SNR periodogram. SES stack plot shows this high SNR TCE is due to a single spike in SES due to the SPSD. $P = 353.965$ days is favored over nearby periods because the anomaly aligns with gaps in the photometry. We flag cases like this with our `s2n_on_grass` statistic. We find several nearby peaks with nearly equal SNR. For KIC-1570270, `s2n_on_grass` is less than our threshold of 1.2 and does not pass machine triage.

which are analogous to KOIs produced by the *Kepler* Project in that they are highly likely to be astrophysical in origin but false positives have not been ruled out.

S10
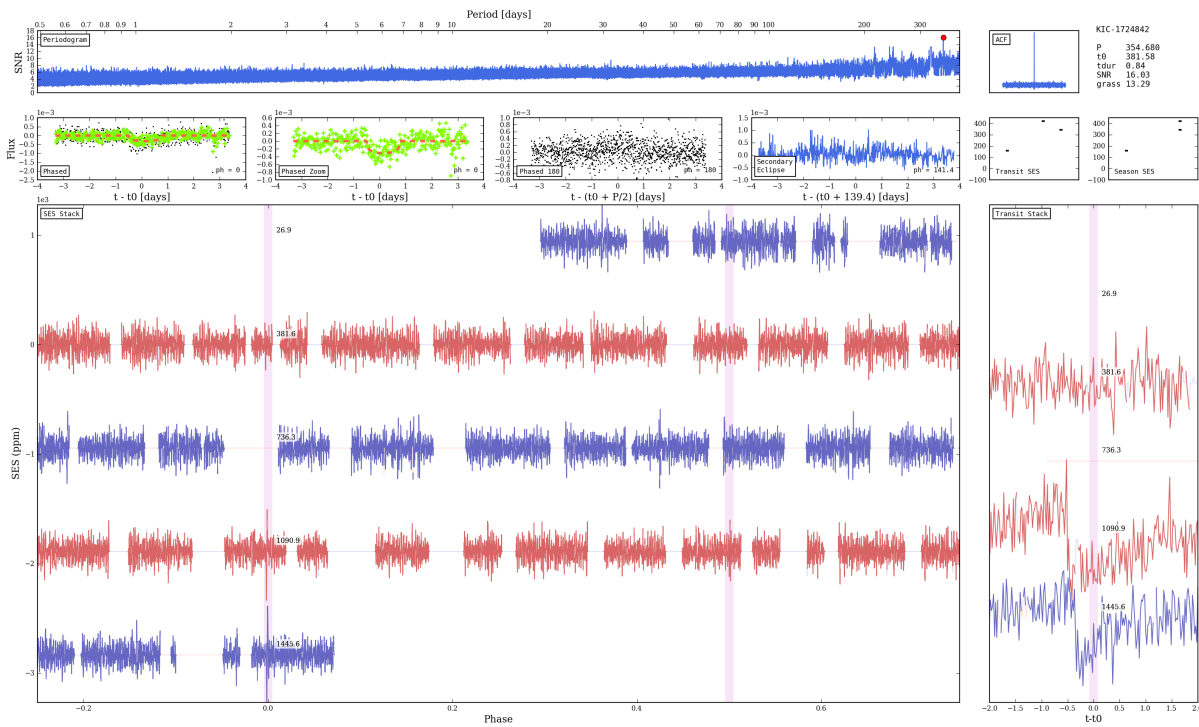
Figure S5: DV summary plots (defined in Figure S3) for the KIC-1724842 TCE at $P = 354.680$ days that we removed during the manual triage. This photometry contains two pixel sensitivity drops spaced by 354.680 days. These two data anomalies combine to produce SNR = 16.035 event, which is substantially higher than the background ("grass" = 13.294) Since `s2n_on_grass` = 1.206 > 1.2, this event passed our `TERRA` software-based triage. However, such data anomalies are easily identified by eye.

S4 KOIs That Fail Data Validation

As a cross-check of our DV quality control methods, we performed the same inspection on 235 KOIs that had been identified by the *Kepler* Project and which appear currently in the online Exoplanet Archive (*1*). These KOIs have periods longer than 50 days, representative of long period transiting planets that enjoy a reduced number transits (compared to short-period planets) during the 4-year lifetime of the *Kepler* mission. We found four KOIs, 2311.01, 2474.01, 364.01, and 2224.01, that are not consistent with an astrophysical transit. We show the raw light curves around the published ephemerides in Figure S6. All four have $R_P \leq 2.04\,R_{\oplus}$, and three have $P \geq 173$ days. Due to the small number of KOIs near the habitable zone, inclusion of these KOIs would bias occurrence measurements upward by a large amount. Vetting all 3000 KOIs in the Exoplanet Archive requires a substaintial effort, and is beyond the scope of this paper. However, these four KOIs are a reminder than detailed, expert, and visual vetting of DV diagnostics existing KOIs is useful.
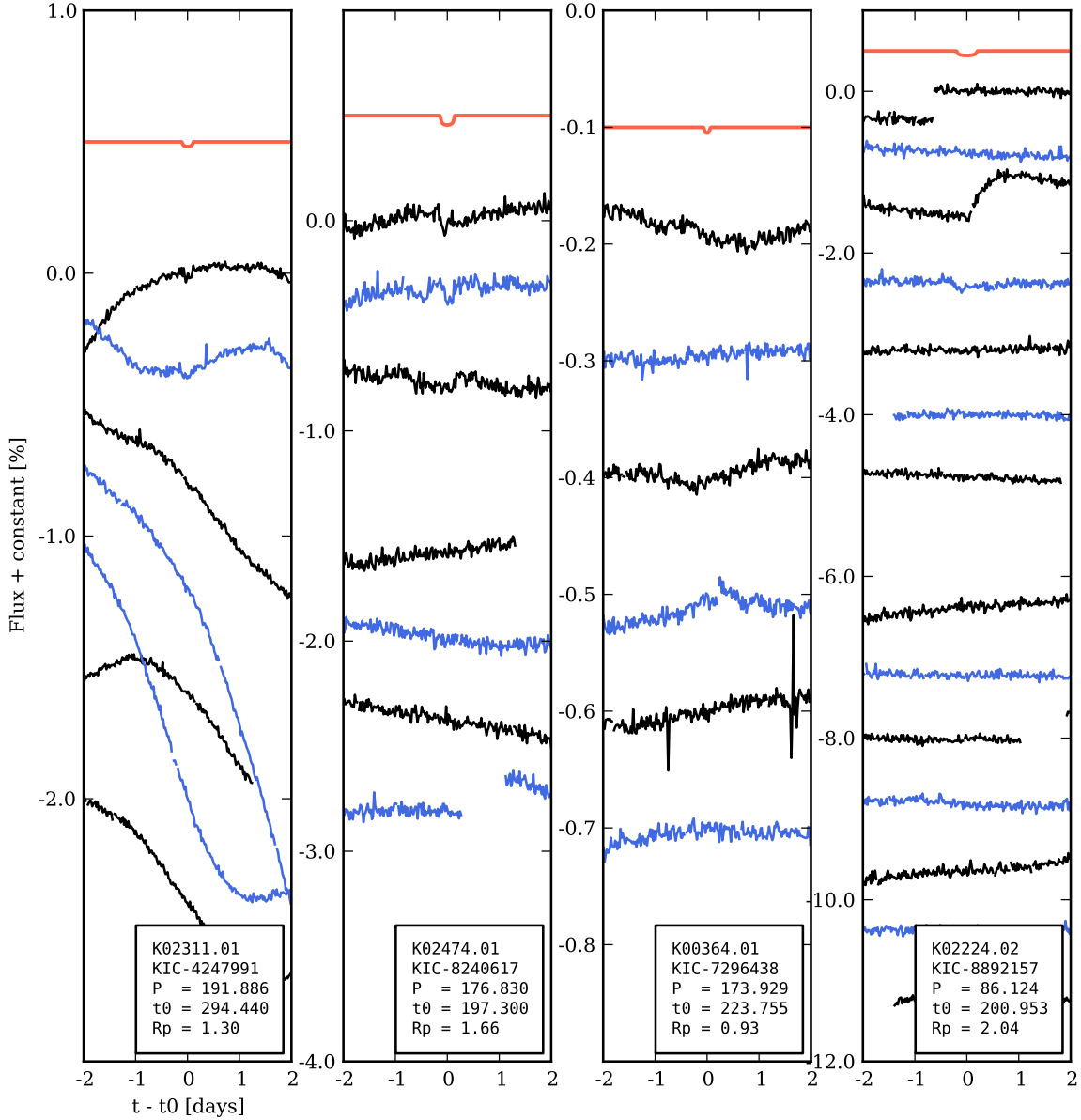
Figure S6: Four small KOIs with long orbital periods that fail our manual vetting. We show 4-day chunks of raw photometry ("SAP_FLUX" in fits table) around the supposed transits. Transit number increases downward. We alternate the use of black and blue lines for clarity. The red lines show a Mandel Agol light curve model synthesized according to the published transit parameters.

S5   Removal of Astrophysical False Positives

We take great care to cleanse our sample of false positives (FPs). Some transits are so deep ($\delta F \gtrsim 10\%$) that they can only be caused by an EB. However, if an EB is close enough to a *Kepler* target star, the dimming of the EB can be diluted to the point where it resembles a planetary transit. For each eKOI, we assess four indicators of EB status. Here, we list the indicators along with the number of eKOIs removed from our planet sample due to each cut:

1. *Radius too large (115).* We consider any transit where the best fit planet radius is larger than 20 $R_\oplus$ to be stellar. Planets are generally smaller than $1.5\ R_{\mathrm{J}} = 16\ R_\oplus$ especially for $P > 5$ days, where planets are less inflated. Our cut at 20 $R_\oplus$ allows some margin of safety to account for mis-characterized stellar radii.

2. *Secondary eclipse (44).* The expected equilibrium temperature for a planet with $P > 5$ days is too small to produce a detectable secondary eclipse. Therefore, the presence of a secondary eclipse indicates the eclipsing body is stellar. We search for secondary eclipses by masking out the primary transit and searching for additional transits at the same period. If an eKOI, such as KIC-8879427 shown in Figure S7, has a secondary eclipse, we designate it an EB.

3. *Variable depth transits (27).* Since *Kepler* photometric apertures are typically two or three pixels (8 or 12 arcsec) on a side, light from neighboring stars can contribute to the overall photometry. A faint EB, when diluted with the target star's light, can produce a dimming that looks like a planetary transit. If the angular separation between the two stars is large enough, the EB will contribute a different amount of light at each *Kepler* orientation. For eKOIs like KIC-2166206 shown in Figure S8, the contribution of a nearby EB results in a season-dependent transit depths. Since the target apertures are defined to include

nearly all ($\gtrsim 90\%$) of the light from the target star, variations between quarters produce a negligible effect on transits associated with the target star, i.e. fractional changes of $\lesssim 1\%$.

4. *Centroid offset (31). Kepler* project DV reports exist for nearly all (609/650) of the eKOIs that survive the previous cuts and are available on the Exoplanet Archive. We inspect the transit astronomy diagnostics (*10*) for significant motion of the transit photocenter in and out of transit. eKOIs with significant motion are designated false positives.

We remove a small number of eKOIs (11) with V-shaped transits. Since planets are so much smaller than their host stars, ingress/egress durations are short compared to the duration of the transit, i.e. planetary transits are box-shaped. Stellar eclipses tend to be V-shaped. Limb-darkening, the 30-minute integration time, and the possibility of grazing incidence blur this distinction. We assessed transit shape visually rather than using more detailed approaches based on light curve fitting and models of Galactic structure (*11, 12*). Only 1.3% of eKOIs are removed in this way and are a small effect compared to other uncertainties in our occurrence measurements.

We also remove five eKOIs with large TTVs. Since TERRA's light curve fitting assumes constant period, fits are biased toward smaller planet radii in the presence of transit timing variations $\gtrsim \Delta T$. If the resulting error is $\gtrsim 25\%$, we remove that eKOI. While these eKOIs are likely planets, our constant period model results in a significant bias in derived planet radii. Given the small number of eKOIs with such large TTVs, our decision to remove them has small effect on our statistical results based off of hundreds of planets.

We compute planet occurrence from the 603 eKOIs that survive the above cuts. We show the distribution of TERRA candidates and FPs on the $P-R_P$ plane in Figure S9. All 836 eKOIs are listed in Table S2. For each eKOI, Table S2 lists KIC identifier, transit ephemeris, FP des-
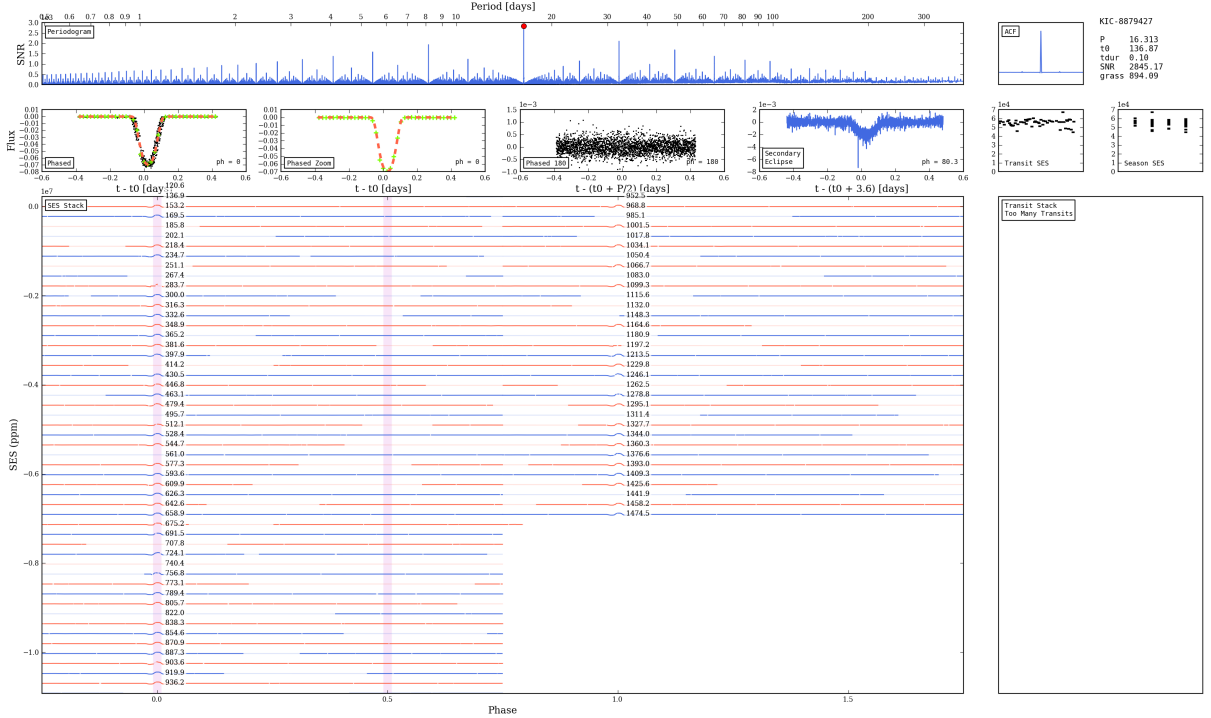
Figure S7: DV summary plots (defined in Figure S3) for eKOI KIC-8879427 (P = 16.313). The "Secondary Eclipse" plot shows the second most significant dimming at P = 16.313, offset from the primary transit in phase by 80.3°. The ratio of the primary to secondary eclipses (δF_{pri} = 0.07; δF_{sec} = 0.002) along with the effective temperature of the primary (T_{eff} = 5995 K) imply the transiting object is 2343 K – too high to be consistent with a planet with P = 16.313 days orbital period.

ignation, Mandel-Agol fit parameters, adopted host star parameters, and size. We also crossed checked our eKOIs against the catalog *Kepler* team KOIs accessed from the NASA Exoplanet Archive (*1*) on 13 September 2013. If the *Kepler* Project KOI number exists for an eKOI, we include it in Table S2.
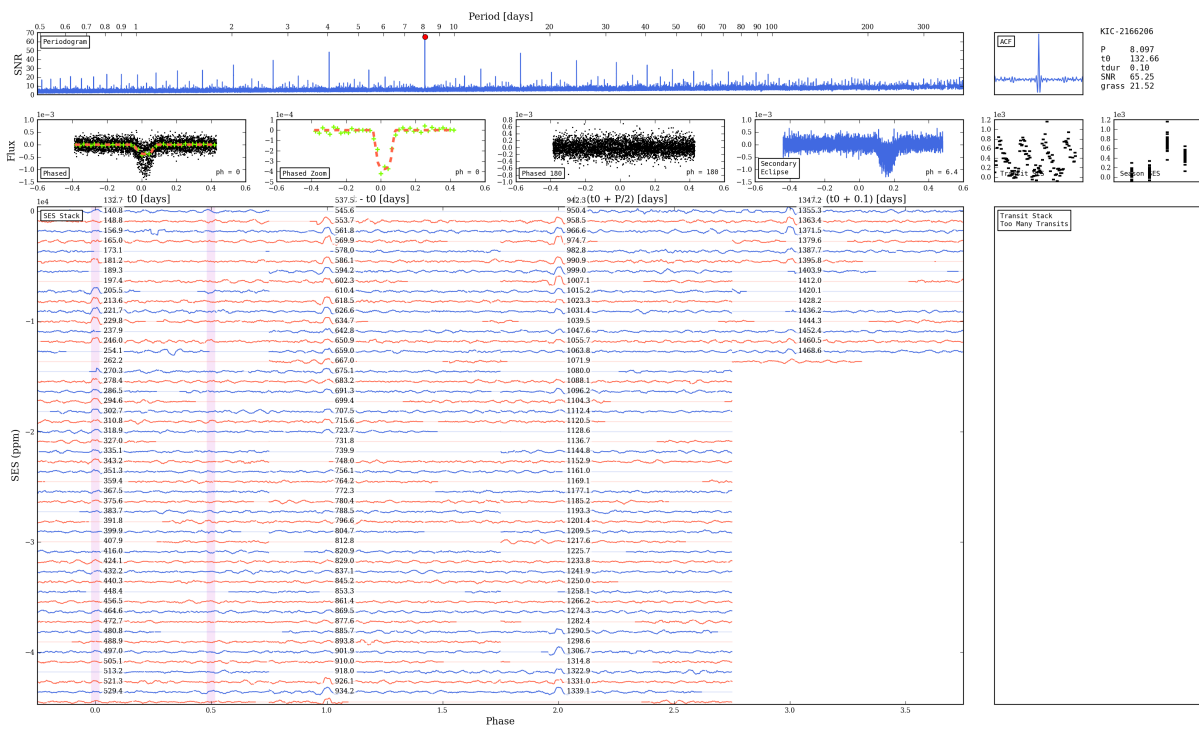
Figure S8: DV summary plots (defined in Figure S3) for eKOI KIC-2166206 with season-dependent transit depths. Season SES plot shows that the transit depths vary significantly for different observing seasons. Since the apparent dimming is a strong function of the orientation of the spacecraft, the dimming is likely not associated with KIC-2166206, but rather an EB displaced from the target by several arc seconds.
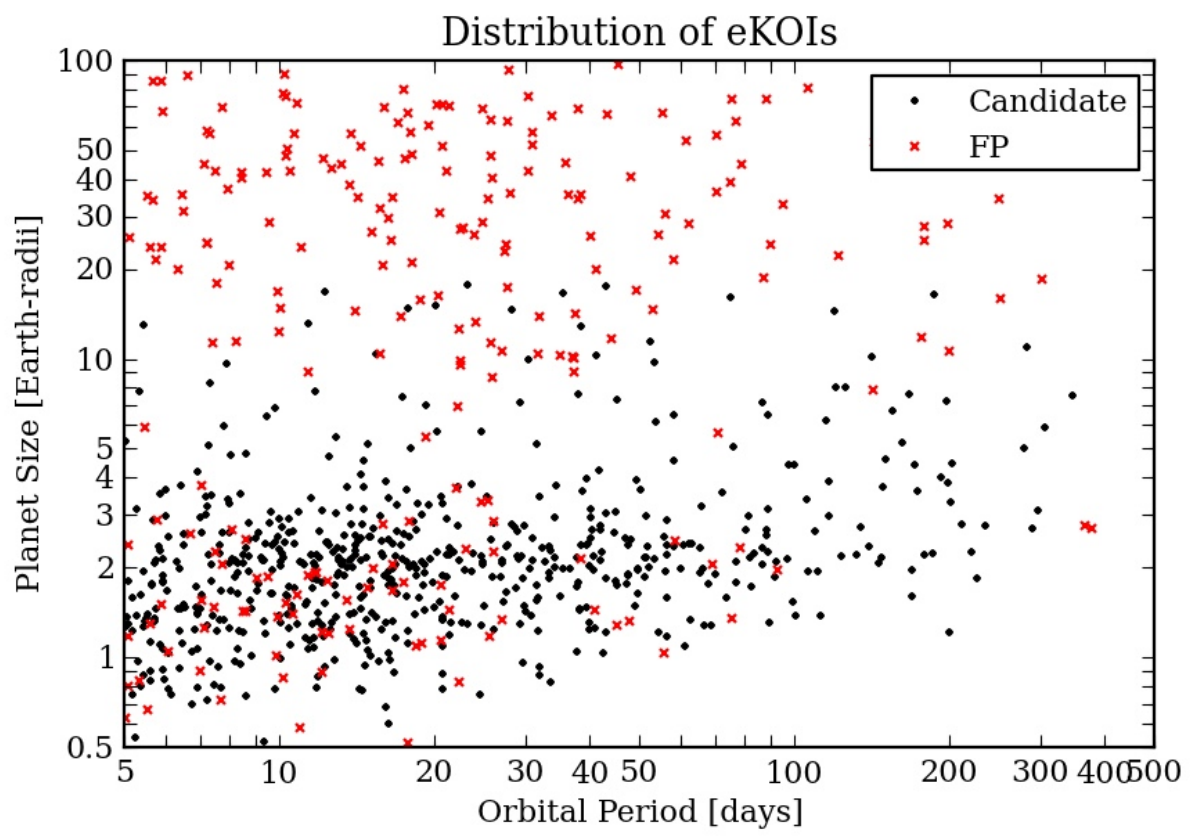
Figure S9: Distribution of TERRA planet candidates as a function of planet size and period. Candidates are labeled as black points; FPs are labeled as red Xs.

S6   Planet Radius Refinement

We fit the phase folded transit photometry of each eKOI with a Mandel-Agol model (*9*). That model has three free parameters: $R_P/R_\star$, the planet to star radius radio, τ, the time for the planet travel a distance $R_\star$ during during transit; and b, the impact parameter. Following P13, we account for the covariance among the three parameters using an MCMC exploration of the parameter posteriors. The error on $R_P/R_\star$ in Table S2 incorporates the covariance with τ and b.

Because photometry alone only provides the $R_P/R_\star$, knowledge of the planet population depends heavily on our characterization of their stellar hosts. We obtained spectra of 274 eKOIs with HIRES on the Keck I telescope using the standard configuration of the California Planet Survey (Marcy et al. 2008). These spectra have resolution of $\sim$50,000 and SNR of $\sim$45/pixel at 5500 Å. We obtained spectra for all 62 eKOIs with $P > 100$ days.

We determine stellar parameters using a routine called `SpecMatch` (Petigura et al., in prep). `SpecMatch` compares a target stellar spectrum to a library of ~ 800 spectra from stars that span the HR diagram (T_{eff} = 3500–7500 K; $\log g$ = 2.0–5.0). Parameters for the library stars are determined from LTE spectral modeling. Once the target spectrum and library spectrum are placed on the same wavelength scale, we compute χ^2, the sum of the squares of the pixel-by-pixel differences in normalized intensity. The weighted mean of the ten spectra with the lowest χ^2 values is taken as the final value for the effective temperature, stellar surface gravity, and metallicity. We estimate `SpecMatch`-derived stellar radii are uncertain to 10% RMS, based on tests of stars having known radii from high resolution spectroscopy and asteroseismology.

S7 Completeness

When measuring planet occurrence, understanding the number of missed planets is as important as the planet catalog itself. We measure TERRA's planet finding efficiency as a function of P and R_P using the injection/recovery framework developed for P13. We briefly review the key aspects of our pipeline completeness study; for more detail, please see P13. We generate 40,000 synthetic light curves according to the following steps:

1. Select a star randomly from the Best42k sample,

2. draw (P,R_P) randomly from log-uniform distributions over 5–400 d and 0.5–16 $R_\oplus$,

3. draw impact parameter and orbital phase randomly from uniform distributions over 0–1,

4. synthesize a Mandel-Agol model (*9*), and

5. inject the model into the "simple aperture photometry" of a random Best42k star.

We process the synthetic photometry with the calibration, grid-based search, and DV components of TERRA. We consider a synthetic light curve successfully recovered if the injected (P, t_0) agree with the recovered (P,t_0) to 0.1 days. Figure S10 shows the distribution of recovered simulations as a function of injected planet size and orbital period.

Pipeline completeness is determined in small bins in (P,R_P)-space by dividing the number of successfully recovered transits by the total number of injected transits on a bin-by-bin basis. This ratio is TERRA's recovery rate of putative planets within the Best42k sample. Pipeline completeness is higher among a more rarefied sample of low noise stars. However, a smaller sample of stars yields fewer planets.

We show survey completeness for a dense grid of P and R_P cells in Figure S11. Completeness falls toward smaller R_P and longer P. Above 2 $R_\oplus$, completeness is greater than

50% even for the longest periods searched (except for the R_P = 2–2.8 $R_\oplus$, P = 283–400 days bin). Completeness falls precipitously toward smaller planet sizes; very few simulated planets smaller than Earth are recovered. Compared to a 1 $R_\oplus$ planet, a 2 $R_\oplus$ planet produces a transit with 4 times the SNR and is much easier to detect. For planets larger than 2 $R_\oplus$, we note a gradual drop in completeness toward longer periods, that steepens at ~300 days. Above ~300 days, the probability that a two or more transits land in data gaps becomes appreciable, and the completeness falls off more rapidly.

Measuring completeness by injection and recovery captures the vagaries in planet search pipeline. Real and synthetic transits are treated the same way, up until the manual triage section. Recall from Section S3.2 that 836 of 2184 TCEs pass machine triage. We perform no such manual inspection of TCEs from the injection and recovery simulations. A potential concern is that a planet may pass machine triage, but is accidentally thrown out in manual triage. Such a planet would be missing from our planet catalog, but not properly accounted in the occurrence measurement by lower completeness. However, because our SNR > 12 threshold for TCE status is high, distinguishing non-astrophysical false positives and eKOIs is easy. Therefore, we consider it unlikely that they are cut during the manual triage stage, and do not expect the lack of manual vetting of the injected TCEs to bias our completeness measurements.
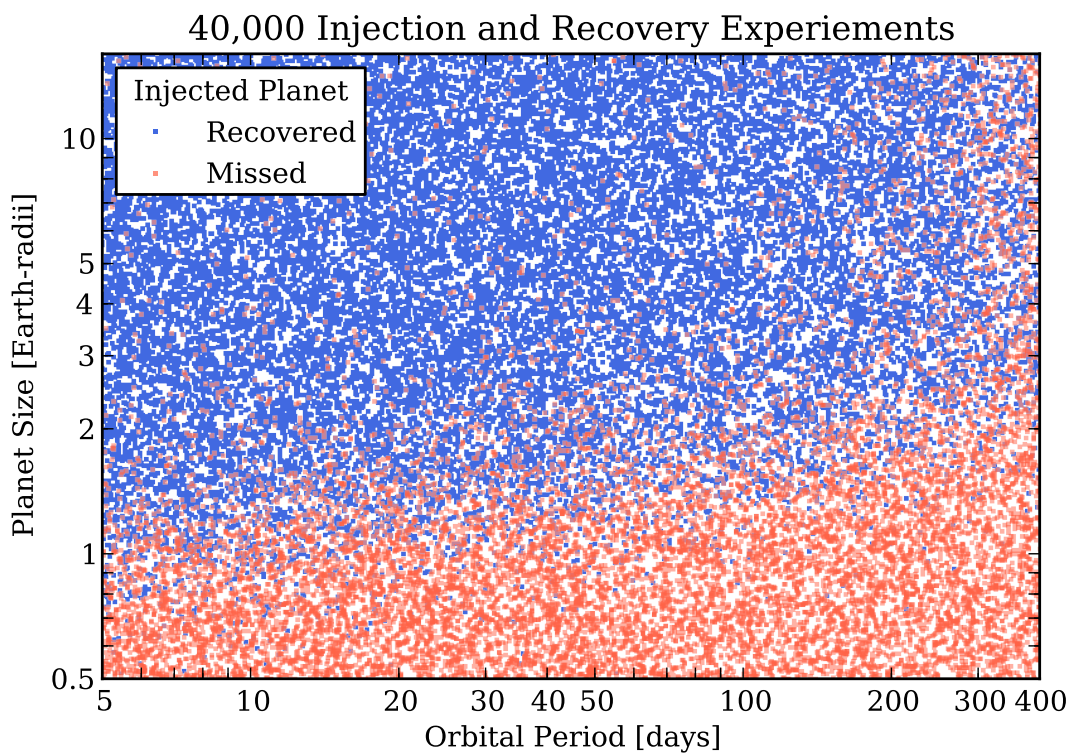
Figure S10: P and R_P of 40,000 injected planets color coded by whether they were recovered by TERRA. Completeness over a small range in P–R_P is computed by dividing the number of successfully recovered transits (blue points) by the total number of injected transits (blue and red points). For planets larger than $2\ R_\oplus$, completeness is $> 50\%$ out to 400 d. Completeness rapidly falls over 1–2 $R_\oplus$ and is $\lesssim 10\%$ for planets smaller than $1\ R_\oplus$.
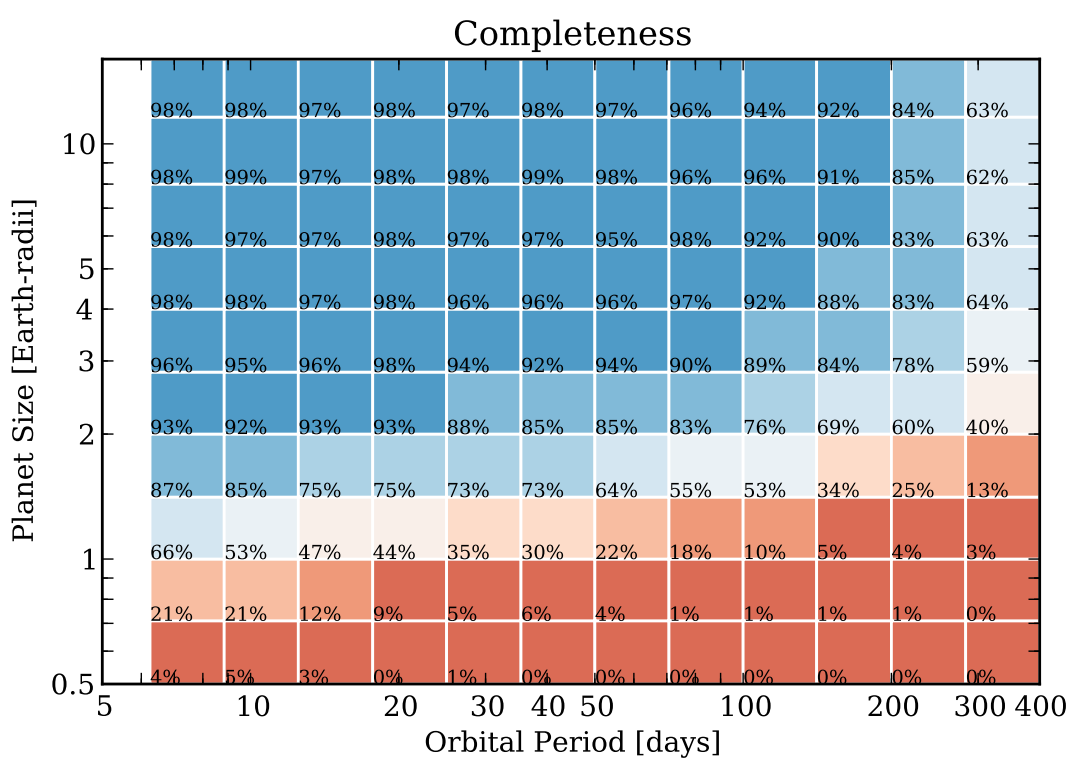
Figure S11: Completeness computed over small bins in P and R_P.

S8   Planet Occurrence

Here, we expand on the key planet occurrence results presented in the main text. We describe our method for extrapolation into the R_P = 1–2 $R_\oplus$, P = 200–400 day domain. We give additional details regarding our measurement of the prevalence of Earth-size planets in the HZ. We also discuss two minor corrections to our occurrence measurements due to planets in multi-planet systems and false positives (FPs).

S8.1   Occurrence of Earth-Size Planets on Year-Long Orbits

In the main text, we reported $5.7^{+1.7}_{-2.2}\%$ occurrence of planets with R_P = 1–2 $R_\oplus$ and P = 200–400 days based on extrapolation from shorter periods. The use of such extrapolation is supported by uniform planet occurrence per $\log P$ interval. Cumulative Planet Occurrence (CPO) is helpful to understand the detailed shape of the planet period distribution. If planet occurrence is constant per $\log P$ interval, CPO is a linear function in $\log P$. The slope of the CPO conveys planet occurrence: the higher the planet occurrence, the steeper the slope of the CPO.

Figure S12 shows CPO for R_P = 2–4 $R_\oplus$ planets. Planet occurrence increases with period from 5 days up to $\sim$ 10 days, and is consistent with uniform for larger periods. This change in the planet period distribution was noted in previous work (*13–15*). We fit a line to the CPO from 50–200 days and extrapolate into the 200–400 day range. The extrapolation predicts $6.4^{+0.5}_{-1.2}\%$ occurrence, which agrees with our measured value of $5.0 \pm 2.1\%$ to 1 σ. We estimate errors on our extrapolation by fitting subsets of the CPO that span half the original period range. We fit 100 subsections ranging from P = 50–100 days up to P = 100–200 days.

We also compare occurrence in the P = 50–100 day, R_P = 1–2 $R_\oplus$ domain based on extrapolation to our measured value. Figure S13 shows the CPO for R_P = 1–2 $R_\oplus$ planets. We fit the CPO from P = 12.5–50 days. This fit predicts an occurrence of $6.5^{+0.9}_{-1.7}\%$ in the 50–100 day range, in good agreement with our measured value of $5.8 \pm 1.6\%$. The uniformity in the oc-
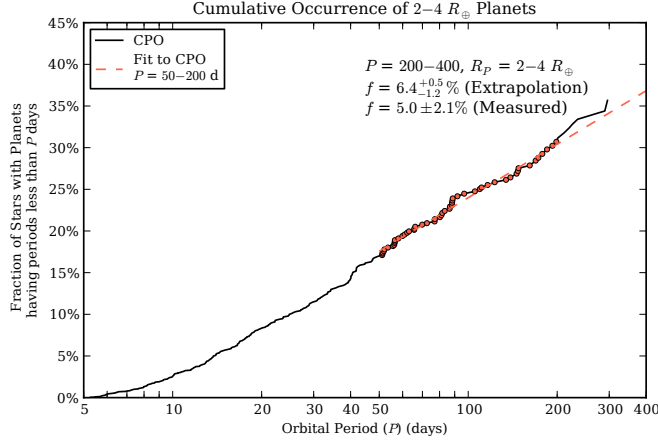
Figure S12: The fraction of stars having 2–4 $R_{\oplus}$ planets with any orbital period up to a maximum period, P, on the horizontal axis. This is the Cumulative Planet Occurrence (CPO). A linear increase in CPO corresponds to planet occurrence that is constant in equal intervals of $\log P$. The CPO steepens from 5 to ~ 10 days, corresponding to increasing planet occurrence in the 5–10 day range. For $P \gtrsim 10$ days, the CPO has a constant slope, reflecting uniform planet occurrence per $\log P$ interval. Planet occurrence in the $R_P = 2$–4 $R_{\oplus}$, $P = 200$–400 day domain is predicted to be $6.4^{+0.5}_{-1.2}\%$ by extrapolation from shorter periods, which is consistent with our measured value of $5.0 \pm 2.1\%$.

currence of small planets as a function of period, lends support to the same kind of modest extrapolation into the $R_P = 1$–2 $R_{\oplus}$, $P = 200$–400 day domain.

S8.2 Planet Occurrence in the Habitable Zone

We consider a planet to reside in the habitable zone if it receives a similar amount of light flux, F_P, from its host star as does the Earth. As described in the main text, we consider the most recent theoretical work on habitability of planets following the seminal work by Kasting (*16–20*).

We adopt an inner edge of the HZ at 0.5 AU for a Sun-like star where a planet would receive four times the light flux that Earth does. This inner edge is slightly more conservative than that found by Zsom et al. (*19*). The outer edge of the HZ less well understood. Kasting found the outer edge to be at 1.7 AU (*16*); Pierrehumbert and Gaidos (*20*) found it could extend to 10 AU
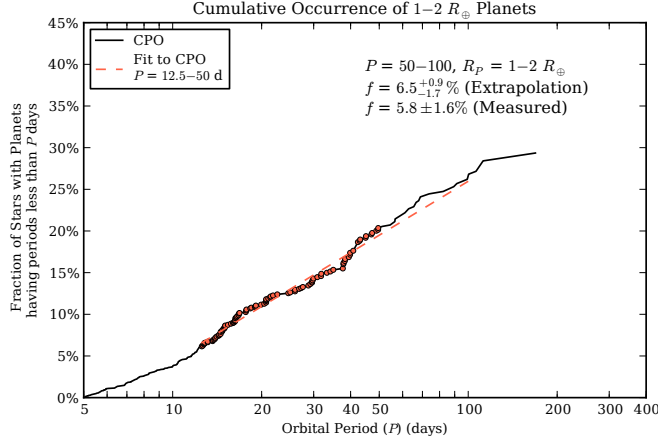
Figure S13: Same as Figure S12, but showing the CPO for 1–2 $R_\oplus$ planets. Planet occurrence in the R_P = 1–2 $R_\oplus$, P = 50–100 day bin is predicted to be $6.5^{+0.9}_{-1.7}\%$ by extrapolation from shorter periods, which is consistent with our measured value of $5.8 \pm 1.6\%$.

for planets with thick H_2 atmospheres. Here, we adopt an intermediate value of 2 AU for solar analogs where the stellar flux is 1/4 that incident on the Earth. This outer edge is consistent with the presence of liquid water on Mars in its past. Mars might still have liquid water today, if it were more massive. Thus following the theory of planetary habitability, we adopt a habitable zone for stars in general based on stellar flux between 4x and 1/4 the solar flux falling on the Earth: F_P = 0.25–4 $F_\oplus$.

The stellar light flux hitting a planet, F_P, depends linearly on stellar luminosity, $L_\star$, and inversely as the square of the distance between the planet and the star. Stellar luminosity, $L_\star$, is given by:

$$L_\star = 4\pi R_\star^2 \sigma T_{\text{eff}}^4,$$

where $\sigma = 5.670 \times 10^{-8}$ W m^{-2} K^{-4} is the Stefan-Boltzmann constant. In our study, the stellar radii and temperatures, T_{eff}, are computed two ways. We obtained high SNR spectra with high spectral resolution using the Keck Observatory HIRES spectrometer for all of the 62 stars that host planets with periods over 100 days, approaching the HZ. For those 62 stars,

we performed a `SpecMatch` analysis (*6*) to determine T_{eff} and the surface gravity, $\log g$, and metalicity, [Fe/H]. These stellar values were matched to stellar evolution models (Yonsei-Yale) to yield the radii and masses of the stars. The resulting values of stellar radii are uncertain by 10%, as determined by calibrations with nearby stars having parallaxes and hence having more accurately determined stellar radii. The values of T_{eff} are accurate to within 2%. Thus, summing the fractional errors in quadrature, the resulting stellar luminosities for the 62 stars (having $P > 100$ days) are measured but carry uncertainties of 25%. For those stars without Keck spectra, we adopted photometric stellar radius and mass, for which the stellar radii are in error by 35% and the T_{eff} values are uncertain by 4%, giving errors in luminosity of 80%. We estimated the star-planet separation (a) using P, $M_{\star}$, and Kepler's third law. The stellar light flux falling on a planet is now easily calculated from $F_P \propto L_{\star}/a^2$. In what follows, we quote the flux falling on a planet relative to that falling on the Earth.

We find 10 planets having radii 1–2 $R_{\oplus}$ that fall within the stellar incident flux domain of the habitable zone, 0.25–4 $F_{\oplus}$. As a reference, we plot their phase folded light curves in Figure S15 along with the KIC identifier, period, radius, and stellar light flux. To compute the prevalence of such planets within the HZ, we apply the usual geometric correction for orbital tilts too large to cause transits, augmenting the counting of each transiting planet by $a/R_{\star}$ total planets. We compute F_P for each synthetic planet in our completeness measurement study. Figure S16 shows stellar flux level and radii of the 10 habitable zone planets, having size 1–2 $R_{\oplus}$, along with the synthetic HZ planets from our completeness study. Because the number of synthetic trials is small for $F_P < 1$ $F_{\oplus}$, we compute occurrence using the 8 planets with $F_P = 1$–4 $F_{\oplus}$. We find $11 \pm 4\%$ of Sun-like stars have a $R_P = 1$–2 $R_{\oplus}$ planet that receives $F_P = 1$–4 $F_{\oplus}$ light energy from their host star.

We account for the entire HZ (extending out to 0.25 $F_{\oplus}$) by extrapolating occurrence in F_P, assuming constant planet occurrence per $\log P$ interval. Figure S14 shows the CPO as a
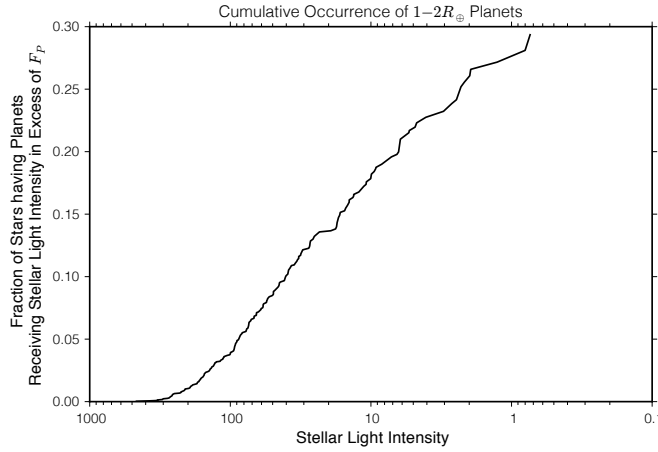
Figure S14: Same as Figure S12, but showing the CPO for 1–2 $R_\oplus$ planets as a function of decreasing flux. Planet occurrence is constant over a wide range of incident flux values, $F_P = 100$–4 $F_\oplus$, which supports extrapolation to the outer edge of our adopted HZ, $F_P = 0.25$ $F_\oplus$.

function of F_P. Planet occurrence is constant from ~ 100 $F_\oplus$ down to ~ 4 $F_\oplus$, beyond which, small number fluctuations are significant. Assuming the occurrence of planets is constant in $\log F_P$ implies that the same number of 1–2 $R_\oplus$ planets have incident fluxes of 1–0.25 $F_\oplus$ as have fluxes of 1–4 $F_\oplus$ where we computed directly the occurrence of planets to be 11%. Thus, $22 \pm 8\%$ of Sun-like stars have a $R_P = 1$–2 $R_\oplus$ planet within our adopted habitable zone with fluxes of 0.25-4.0 $F_\oplus$.
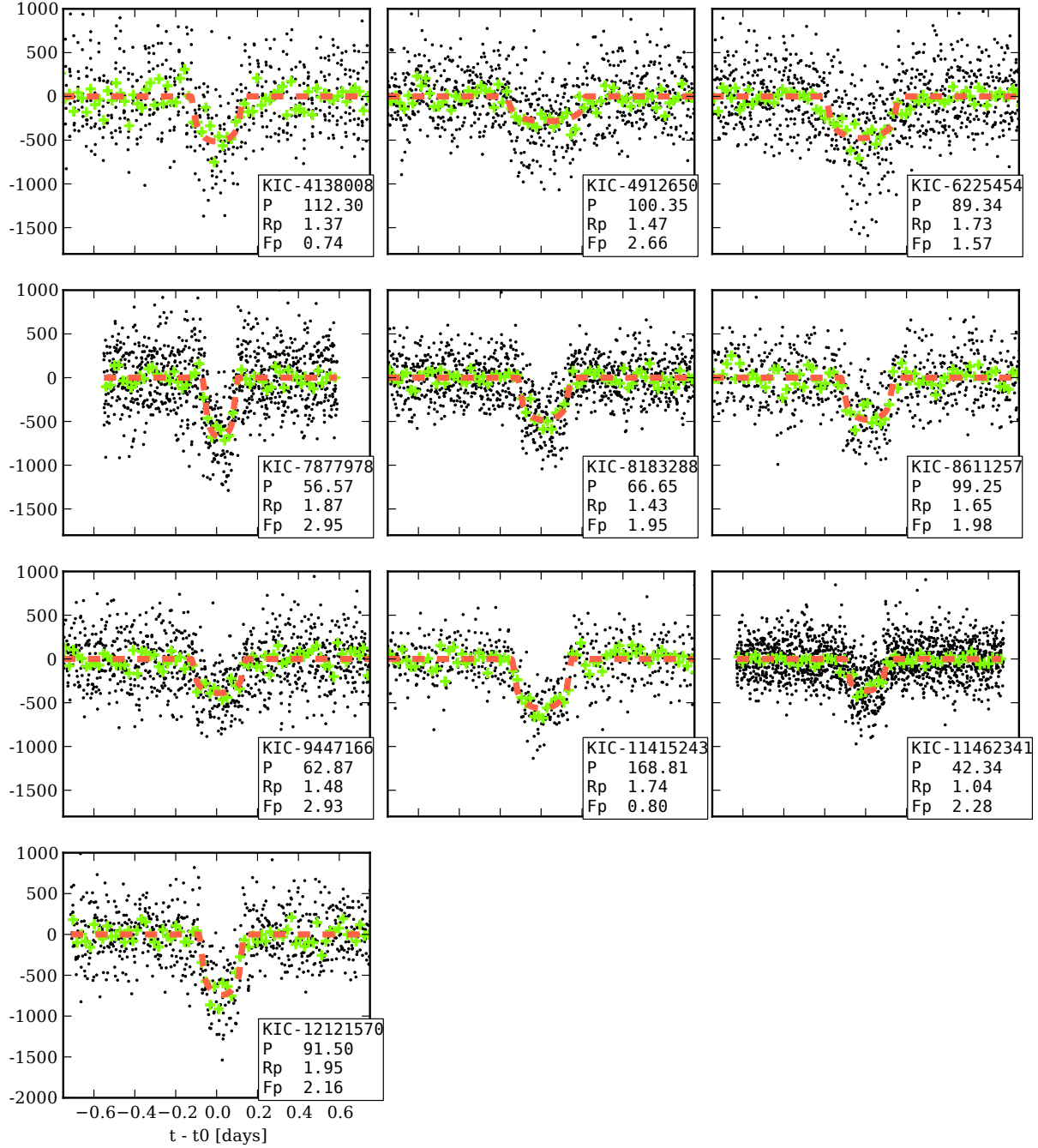
Figure S15: Phase folded photometry for ten Earth-size HZ candidates. Black point shows show TERRA-calibrated photometry folded on the best fit ephemeris listed in Table S2. The green symbols show the median flux value in 30-minute bins. The red dashed lines shows the best-fit Mandel-Agol model. We have annotated each plot with the KIC identifier, period, planet size (Earth-radii), incident flux level (relative to Earth). All measurements of planet size and incident flux are based on spectra taken with the Keck 10 m telescope. Spectra for KIC-6225454, KIC-7877978, KIC-9447166, and KIC-11462341 were obtained during peer-review and were added in proof (see Table S3).
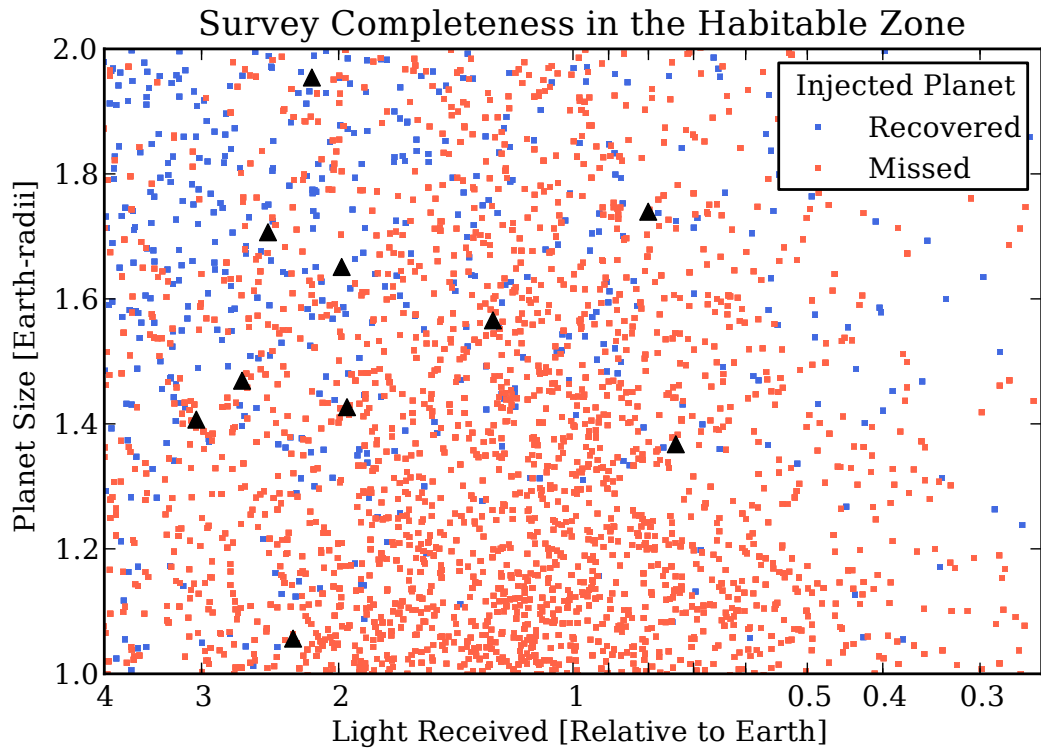
Figure S16: Ten small ($R_P = 1$–$2\ R_\oplus$) planets (black triangles) fall within our adopted habitable zone of $F_P = 1/4$–$4\ F_\oplus$. We also plot the injected planets over this same domain. Survey completeness C is computed locally for each planet by dividing the number of injected planets that were recovered by the total number of injected planets in a small box centered on the real planet.

S8.3 Occurrence Including Planets in Multi-planet Systems

For systems harboring more than one planet, TERRA only detects the planet with highest SNR, i.e. the most significant planet. The actual rate of planet occurrence is higher than we report when the missed planets in these multi-transiting systems is included. (Note that this correction only applies to multi-transiting system and not all multi-planet systems.) We estimate the size of this effect using the Q12 sample of KOIs from the *Kepler* project, which includes stars with multiple planets. We selected the 1190 "candidates" with well-determined periods ($\sigma(P) <$ 0.1 days) that orbit stars in the Best42k. In order to make a fair comparison between our planet sample and the Q12 sample, we computed the SNR of each of the 1190 candidates using TERRA. We excluded 82 KOIs with SNR < 12, i.e. candidates that would have been deemed sub-significant by TERRA.

For each planet in a multi-transiting system, we rank order each candidate by its "Relative SNR" defined as:

$$\text{Relative SNR} = \delta F \sqrt{\frac{\Delta T}{P}}.$$

Figure S17 shows the distribution of Q12 candidates in the Best42k as points on the P–R_P plane. We highlight points corresponding to the most significant planet. We assess the boost in planet counts due to multi-transiting systems for different domains in P and R_P. For $P > 50$ days and $R_P < 4\ R_\oplus$, this multi-boost factor ranges from 21 to 28%, neglecting bins with fewer than 8 detected planets that suffer from small number fluctuations. Had we included additional planets, our occurrence measurements would rise by $\sim 25\%$, which is comparable to or slightly smaller than the fractional occurrence error for small planets in long-period orbits.

S8.4 Correction due to False Positives

As discussed earlier, the sample of eKOIs is polluted by astrophysical false positives. Like the *Kepler* team, we do our best to identify and remove transits that are clearly due to eclipsing
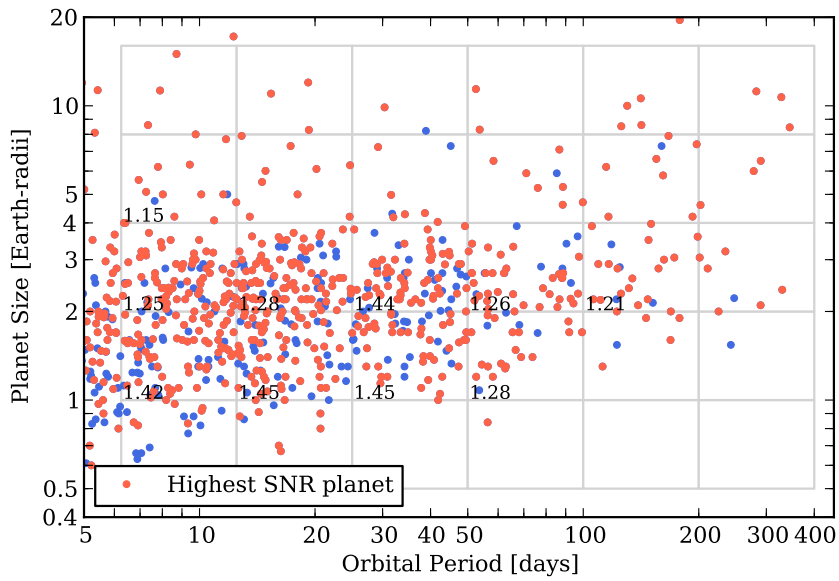
Figure S17: – Distribution of P and R_P for *Kepler* team candidates from the Q12 catalog. We include planets with TERRA SNR > 12 and well-determined orbital periods ($\sigma(P) < 0.1$ days) that around "Best42k" stars. Planets that are either single or are the most significant planet in a multi-planet system are shown in red. Blue points correspond to additional planets in multi planet systems. For each cell with 10 or more planets, we compute the boost in planet counts due to multiplanet systems, the total number of planets divide by the number of most significant planets. For planets smaller than 4 $R_\oplus$ and P 50 days, the boost ranges from 21–28%. Thus, including multis, we expect $\sim 25\%$ higher occurrence.

binaries, but cannot remove all eclipsing binary configurations. Thus, our sample, as well as those produced by the Kepler team, still contain a false positive component.

Fressin et al. (2013) addressed the contamination of the February 2012 *Kepler* Project sample of KOIs (*4*) by FPs that were not removed by the *Kepler* Project vetting process. FPs include background eclipsing binaries, physically associated eclipsing binaries (hierarchical triples), and physically associated stars, which themselves have a transiting planet. We consider the last scenario to be a FP because even though the transiting object is a planet, the radius is at least 1.4 times larger (1.4 corresponds stars of equal brightness). Fressin et al. (2013) added FPs to the Batalha et al (2012) sample of KOIs according to models of galactic structure, stellar binarity, and assumptions about the distributions of planets. Simulated FPs that would exhibit a detectable secondary eclipse or a significant centroid offset were removed, assuming the Kepler Project vetting process catches these FPs.

Fressin et al. (2013) found an overall FP rate of $8.8 \pm 1.9\%$ for 1.25–2.0 $R_\oplus$ planets and $12.3 \pm 3.0\%$ for 0.8–1.25 $R_\oplus$ planets. Again, note that this fractional occurrence correction is small compared to our reported errors for small planets in long-period orbits. Stars with bound companions with transiting planets are the dominant fraction of FPs for small planets (76% for 1.25–2.0 $R_\oplus$ planets and 66% for 0.8–1.25 $R_\oplus$ planets). FPs of this type are very difficult to identify. A Sun-like star with V = 14.7 mag (typical for our sample) is 1 kpc away. The binary star separation distribution peaks at 50 AU (*21*) or 0.05 arcsec assuming a face-on orbit. Detecting companions separated by 0.05 arcsec is near the limits of current ground-based AO. Even if a companion was detected, we still wouldn't know which star harbored the transiting planet.

We adopt a 10% FP rate for planets having P = 50–400 days and R_P = 1–2 $R_\oplus$. Adopting a false positive rate that is constant with period is justified because the occurrence of Neptune-sized planets is approximately constant with period, as shown in the main text. In the context of

the occurrence of Earth-size planets with $P = 200$–400 days ($5.7^{+1.7}_{-2.2}\%$) and Earth-size planets in the HZ ($22 \pm 8\%$), FPs contribute 10% fractional uncertainty and are secondary compared to statistical uncertainty.

References

1. Akeson RL, et al. (2013) The NASA Exoplanet Archive: Data and Tools for Exoplanet Research. PASP 125:989–999.

2. Pinsonneault MH, et al. (2012) A Revised Effective Temperature Scale for the Kepler Input Catalog. ApJS 199:30.

3. Yi S, et al. (2001) Toward Better Age Estimates for Stellar Populations: The Y^2 Isochrones for Solar Mixture. ApJS 136:417–437.

4. Batalha NM, et al. (2013) Planetary Candidates Observed by Kepler. III. Analysis of the First 16 Months of Data. ApJS 204:24.

5. Petigura EA, Marcy GW (2012) Identification and Removal of Noise Modes in Kepler Photometry. PASP 124:1073–1082.

6. Petigura EA, Marcy GW, Howard AW (2013) A Plateau in the Planet Population below Twice the Size of Earth. ApJ 770:69.

7. Stumpe MC, et al. (2012) Kepler Presearch Data Conditioning I - Architecture and Algorithms for Error Correction in Kepler Light Curves. PASP 124:985–999.

8. Rasmussen CE, Williams CKI (2006) *Gaussian Processes for Machine Learning* (MIT Press).

9. Mandel K, Agol E (2002) Analytic Light Curves for Planetary Transit Searches. ApJ 580:L171–L175.

10. Bryson ST, et al. (2013) Identification of Background False Positives from Kepler Data. PASP 125:889–923.

11. Torres G, et al. (2011) Modeling Kepler Transit Light Curves as False Positives: Rejection of Blend Scenarios for Kepler-9, and Validation of Kepler-9 d, A Super-earth-size Planet in a Multiple System. ApJ 727:24.

12. Morton TD (2012) An Efficient Automated Validation Procedure for Exoplanet Transit Candidates. ApJ 761:6.

13. Youdin AN (2011) The Exoplanet Census: A General Method Applied to Kepler. ApJ 742:38.

14. Howard AW, et al. (2012) Planet Occurrence within 0.25 AU of Solar-type Stars from Kepler. ApJS 201:15.

15. Dong S, Zhu Z (2012) Fast Rise of "Neptune-Size" Planets (4-8 R_Earth) from P˜10 to ˜250 days – Statistics of Kepler Planet Candidates Up to ˜0.75 AU. *ArXiv e-prints*.

16. Kasting JF, Whitmire DP, Reynolds RT (1993) Habitable Zones around Main Sequence Stars. Icarus 101:108–128.

17. Seager S (2013) Exoplanet Habitability. *Science* 340:577–581.

18. Kopparapu RK, et al. (2013) Habitable Zones around Main-sequence Stars: New Estimates. ApJ 765:131.

19. Zsom A, Seager S, de Wit J, Stamenkovic V (2013) Towards the Minimum Inner Edge Distance of the Habitable Zone. *arXiv:1304.3714*.

20. Pierrehumbert R, Gaidos E (2011) Hydrogen Greenhouse Planets Beyond the Habitable Zone. ApJ 734:L13.

21. Raghavan D, et al. (2010) A Survey of Stellar Families: Multiplicity of Solar-type Stars. ApJS 190:1–42.

22. Brown TM, Latham DW, Everett ME, Esquerdo GA (2011) Kepler Input Catalog: Photometric Calibration and Stellar Classification. AJ 142:112.

KIC	KOI	P days	t_0 days	Disp.	p %	$\sigma(p)$	T_{eff} K	$\log g$ cgs	$R_\star$ $R_\odot$	$\sigma(R_\star)$	Prov.	R_P $R_\oplus$	$\sigma(R_P)$	F_P $F_\oplus$
1026032		8.460	133.78	R	40.6	0.09	6044	4.5	0.95	0.29	P	42.12	12.64	159.7
1026957	958.01	21.762	144.77	P	3.1	0.42	4861	4.6	0.72	0.07	SM	2.46	0.41	13.4
1571511	362.01	14.023	135.52	SE	12.8	0.00	6055	4.4	1.04	0.31	P	14.46	4.34	98.7
1718189	993.01	21.854	144.32	P	1.7	0.10	5827	4.5	0.88	0.26	P	1.65	0.50	34.6
1849702	2538.01	39.833	155.62	P	1.7	0.37	5023	4.6	0.73	0.07	SM	1.37	0.33	7.1
1872821	2351.01	10.274	134.64	P	1.8	0.11	5706	4.6	0.85	0.25	P	1.69	0.52	82.7
2141783	2201.01	116.521	144.14	P	2.5	0.37	6063	4.2	1.53	0.15	SM	4.09	0.74	10.9
2164169	1029.01	32.312	133.88	P	2.3	0.07	5975	4.5	0.96	0.29	P	2.39	0.72	26.5
2166206	1028.01	8.097	132.66	VD	1.8	0.09	6014	4.2	1.41	0.42	P	2.75	0.83	364.7
2304320	2033.01	16.541	133.94	P	1.8	0.09	5061	4.6	0.75	0.07	SM	1.43	0.16	24.6
2305255		24.567	155.97	P	2.1	0.05	5980	4.5	0.98	0.29	P	2.21	0.66	40.3
2306740		10.307	138.75	R	54.7	0.13	5932	4.2	1.26	0.38	P	75.44	22.63	208.0
2309719	1020.01	54.357	164.06	R	16.0	0.40	6159	4.3	1.34	0.13	SM	23.41	2.41	25.6
2438264	440.01	15.907	146.12	P	2.8	0.12	5070	4.6	0.77	0.08	SM	2.35	0.25	26.0
2441495	166.01	12.493	138.46	P	2.4	0.05	5208	4.6	0.77	0.08	SM	2.05	0.21	41.8
2444412	103.01	14.911	141.34	P	2.8	0.14	5554	4.5	0.92	0.09	SM	2.79	0.31	55.2
2449431	2009.01	86.752	170.29	P	2.1	0.16	5578	4.4	0.94	0.09	SM	2.11	0.27	5.9
2557816	488.01	9.379	138.93	P	2.6	0.15	5770	4.5	0.91	0.27	P	2.56	0.78	114.4
2571238	84.01	9.287	135.99	P	2.4	0.03	5523	4.5	0.89	0.09	SM	2.31	0.23	96.9
2576692		87.877	194.10	R	74.9	5.10	5801	4.5	0.87	0.26	P	71.11	21.88	5.3
2580872		15.927	145.55	R	71.9	0.70	5434	4.5	0.88	0.26	P	68.76	20.64	44.7
2695110	400.01	44.189	165.80	VD	9.4	0.88	6089	4.4	1.03	0.31	P	10.60	3.33	21.4
2715135	1024.01	5.748	133.31	P	2.4	0.11	4302	4.7	0.56	0.17	P	1.50	0.45	35.1
2716979		8.832	137.72	P	0.8	0.05	6098	4.3	1.22	0.37	P	1.05	0.32	257.8
2837111	1110.01	8.735	135.09	P	1.6	0.07	5948	4.5	0.93	0.28	P	1.59	0.48	139.3
2854698	986.01	8.187	138.05	P	2.2	0.10	5475	4.5	0.91	0.09	SM	2.15	0.24	107.9
2985767	2032.01	14.080	139.97	P	1.2	0.06	5530	4.5	0.86	0.26	P	1.14	0.35	52.9
2987027	197.01	17.276	133.84	P	9.2	0.10	4945	4.6	0.74	0.07	SM	7.39	0.74	20.2
2990873	2335.01	16.224	136.01	P	1.5	0.12	5555	4.5	0.93	0.09	SM	1.54	0.20	50.4
3002478	2380.01	6.357	135.48	P	1.5	0.08	5951	4.5	0.92	0.28	P	1.51	0.46	209.7
3003991		7.245	131.86	R	27.9	0.22	5532	4.6	0.80	0.24	P	24.35	7.31	107.9
3098194		30.477	136.97	R	71.4	1.67	5484	4.4	0.96	0.29	P	74.64	22.46	23.3
3098197	3362.01	30.477	136.97	R	41.9	0.69	5962	4.5	0.92	0.28	P	42.08	12.64	26.1
3102024		13.783	139.48	R	67.3	0.36	5353	4.6	0.77	0.23	P	56.71	17.02	39.1
3102384	273.01	10.574	132.78	P	1.6	0.04	5672	4.4	1.12	0.11	SM	1.94	0.20	125.9
3109930	1112.01	37.811	158.36	P	2.0	0.08	6099	4.5	1.01	0.30	P	2.19	0.66	25.2
3116412	1115.01	12.992	136.33	P	1.5	0.07	5760	4.2	1.31	0.13	SM	2.09	0.23	139.7
3120308	3380.01	10.266	136.50	C	1.5	0.13	5706	4.5	0.93	0.28	P	1.54	0.48	102.4
3120320		10.266	136.50	R	48.0	2.27	5903	4.5	0.93	0.28	P	48.78	14.81	111.7
3120904	3277.01	42.915	139.87	P	1.2	0.08	6152	4.3	1.23	0.12	SM	1.58	0.19	30.5
3128552	2055.01	8.679	133.04	P	2.1	0.10	5748	4.6	0.86	0.26	P	1.97	0.60	108.3
3128793	1786.01	24.679	137.78	P	8.3	0.07	4669	4.7	0.64	0.19	P	5.73	1.72	8.3
3217264	401.01	29.199	156.24	P	4.1	0.05	5363	4.5	0.89	0.09	SM	4.01	0.40	17.7
3218908	1108.01	18.925	149.49	P	2.4	0.13	5546	4.6	0.81	0.24	P	2.08	0.64	30.5
3219037	3395.01	10.005	136.78	P	1.0	0.09	5948	4.5	0.97	0.29	P	1.05	0.33	130.5
3223433	4548.01	61.079	132.53	P	1.4	0.33	5518	4.6	0.80	0.24	P	1.20	0.46	6.2
3230753	2928.01	17.734	143.92	P	1.4	0.08	5250	4.6	0.78	0.23	P	1.15	0.35	27.1
3230787		17.734	143.92	R	59.4	1.75	5905	4.4	1.00	0.30	P	64.98	19.59	63.3
3231341	1102.01	12.334	137.58	P	2.0	0.12	6005	4.2	1.38	0.14	SM	3.08	0.36	194.1
3236705	3343.01	83.264	194.26	P	2.3	0.32	5965	4.5	0.94	0.28	P	2.39	0.79	7.1
3239671	2066.01	147.976	263.08	P	3.4	0.33	5573	4.4	0.91	0.09	SM	3.42	0.47	2.7
3323289		33.693	158.87	R	67.2	0.03	5401	4.4	0.89	0.27	P	65.36	19.61	16.8

KIC	KOI	P days	t_0 days	Disp.	p %	$\sigma(p)$	T_{eff} K	$\log g$ cgs	$R_\star$ $R_\odot$	$\sigma(R_\star)$	Prov.	R_P $R_\oplus$	$\sigma(R_P)$	F_P $F_\oplus$
3323887	377.01	19.273	143.96	TTV	8.0	1.60	5780	4.4	1.06	0.11	SM	9.32	2.07	56.7
3326377	1830.02	198.711	156.52	P	4.3	0.19	5180	4.6	0.79	0.08	SM	3.69	0.40	1.1
3337425	1114.01	7.048	132.72	P	1.5	0.08	5721	4.4	1.03	0.31	P	1.69	0.51	210.5
3342467	3278.01	88.181	209.16	P	3.0	0.27	5414	4.6	0.77	0.23	P	2.56	0.80	3.4
3342592	402.01	17.177	136.19	SE	13.6	0.05	6004	4.5	0.94	0.28	P	13.90	4.17	59.2
3353050	384.01	5.080	133.80	P	1.4	0.04	6156	4.4	1.14	0.11	SM	1.73	0.18	465.0
3433668	3415.01	15.022	143.71	P	1.0	0.09	5823	4.2	1.37	0.14	SM	1.47	0.20	136.8
3442055	1218.01	29.619	133.70	P	1.6	0.06	5624	4.4	1.01	0.10	SM	1.80	0.19	27.2
3446746	385.01	13.145	135.41	P	1.9	0.12	5412	4.5	0.91	0.09	SM	1.85	0.22	57.9
3448130	2043.01	78.546	144.08	C	2.2	0.16	6005	4.5	0.94	0.28	P	2.28	0.70	7.8
3531558	118.01	24.994	138.66	P	1.5	0.07	5807	4.3	1.14	0.11	SM	1.85	0.20	46.0
3534118	3641.01	178.420	218.19	R	20.3	3.12	6079	4.3	1.15	0.11	SM	25.41	4.66	4.0
3539231	4626.01	91.954	183.13	P	1.7	0.16	5971	4.3	1.11	0.33	P	2.02	0.64	8.9
3541946	624.01	17.790	146.86	P	2.7	0.05	5576	4.5	0.90	0.09	SM	2.65	0.27	41.2
3547760	4535.01	9.848	136.80	V	1.2	0.09	5339	4.6	0.80	0.24	P	1.05	0.33	65.4
3548044	2194.02	67.968	163.57	P	1.7	0.12	5725	4.3	1.04	0.10	SM	1.99	0.24	10.8
3559935	492.01	29.913	134.86	P	2.7	0.07	5465	4.4	0.95	0.28	P	2.81	0.85	23.0
3632089	3308.01	31.777	136.82	P	1.5	0.08	5683	4.4	1.02	0.31	P	1.64	0.50	27.7
3642741	242.01	7.258	138.36	P	5.7	0.11	5546	4.5	0.86	0.26	P	5.30	1.59	127.8
3655332	1179.01	15.066	140.67	R	23.5	1.24	5818	4.4	0.98	0.30	P	25.25	7.69	73.1
3657176	2903.01	17.417	141.09	C	1.7	0.10	5887	4.5	0.97	0.29	P	1.84	0.56	59.9
3728701	2536.01	51.131	137.17	P	1.9	0.19	6054	4.4	1.12	0.33	P	2.28	0.72	20.4
3732035	3966.01	138.946	153.91	P	2.3	0.22	6014	4.4	1.11	0.11	SM	2.81	0.38	5.2
3745690	442.01	13.541	144.59	P	2.0	0.13	5768	4.4	0.99	0.10	SM	2.16	0.26	81.5
3747817	4103.01	184.778	217.35	P	2.9	0.27	5275	4.6	0.78	0.08	SM	2.49	0.34	1.2
3749134	1212.01	11.301	134.94	P	1.6	0.15	5916	4.4	0.98	0.29	P	1.66	0.52	111.1
3756264	3108.01	7.363	136.87	P	2.0	0.18	5853	4.5	0.89	0.27	P	1.93	0.60	153.2
3757588		24.090	154.27	SE	13.1	0.49	5386	4.4	0.89	0.27	P	12.79	3.87	26.2
3761319		16.249	143.94	P	1.8	0.11	5758	4.4	0.95	0.29	P	1.91	0.58	60.4
3833007	443.01	16.218	147.59	P	2.6	0.10	5891	4.5	0.90	0.27	P	2.52	0.76	55.8
3835670	149.01	14.557	145.10	P	2.9	0.08	5724	4.1	1.59	0.16	SM	4.98	0.52	152.5
3847138	444.01	11.723	142.16	P	2.0	0.07	5551	4.4	0.93	0.09	SM	2.06	0.22	80.6
3848966	3389.01	29.766	155.58	P	1.4	0.11	6025	4.5	0.97	0.29	P	1.44	0.45	31.0
3852655	3002.01	11.629	132.82	P	0.9	0.06	5716	4.3	1.16	0.12	SM	1.15	0.14	129.2
3858917	3294.01	25.950	180.86	SE	9.8	0.13	5565	4.6	0.81	0.24	P	8.61	2.59	20.4
3858949	995.01	25.952	154.89	SE	2.8	0.03	5341	4.6	0.75	0.23	P	2.28	0.68	15.7
3858988	3388.01	25.953	154.85	SE	2.5	0.03	5738	4.3	1.06	0.32	P	2.86	0.86	39.7
3859079	1199.01	53.529	147.86	P	3.1	0.23	4767	4.6	0.66	0.20	P	2.23	0.69	3.4
3938073		31.024	158.87	R	45.5	0.04	6007	4.3	1.16	0.35	P	57.63	17.29	42.2
3939150	1215.01	17.324	142.12	P	1.4	0.11	6034	4.3	1.34	0.13	SM	2.12	0.27	111.9
3942670	392.01	33.420	137.85	P	1.5	0.03	5989	4.3	1.29	0.13	SM	2.10	0.22	41.8
3962872	4539.01	25.954	148.82	P	1.1	0.04	6055	4.4	1.05	0.32	P	1.26	0.38	44.7
3966801	494.01	25.696	137.40	P	3.4	0.22	5055	4.7	0.69	0.21	P	2.56	0.79	11.3
3969687	2904.01	16.358	141.26	P	1.0	0.09	6049	4.1	1.60	0.16	SM	1.77	0.24	162.7
3970233	604.01	8.255	133.15	SE	12.4	0.00	5354	4.5	0.84	0.25	P	11.41	3.42	94.2
4035640	1881.01	28.267	140.93	P	3.1	0.07	5257	4.5	0.82	0.25	P	2.83	0.85	16.7
4043190	1220.01	6.401	136.89	P	1.1	0.06	5296	3.8	2.50	0.25	SM	3.01	0.34	737.3
4043443	231.01	119.839	161.88	P	10.4	1.40	4604	4.7	0.65	0.06	SM	7.37	1.23	1.0
4049901	2295.01	16.291	132.10	P	0.6	0.04	5430	4.5	0.83	0.08	SM	0.58	0.07	38.9
4075064		61.423	161.24	R	69.0	3.93	4945	4.7	0.67	0.20	P	50.13	15.31	3.1
4076976		9.761	133.68	P	1.0	0.04	4960	4.6	0.71	0.21	P	0.80	0.24	43.4
4077526	1336.01	10.218	136.89	P	2.1	0.12	6082	4.4	1.09	0.33	P	2.46	0.75	168.3

KIC	KOI	P days	t_0 days	Disp.	p %	$\sigma(p)$	$T_{\rm eff}$ K	$\log g$ cgs	$R_\star$ $R_\odot$	$\sigma(R_\star)$	Prov.	R_P $R_\oplus$	$\sigma(R_P)$	F_P $F_\oplus$
4077901	2239.01	12.110	140.73	C	1.0	0.07	5516	4.5	0.83	0.25	P	0.92	0.28	58.7
4138008	4742.01	112.303	230.45	P	2.2	0.28	4402	4.7	0.57	0.06	SM	1.37	0.22	0.7
4165473	550.01	13.023	139.46	P	2.2	0.09	5627	4.5	0.98	0.10	SM	2.39	0.26	74.5
4172013	2386.01	16.270	145.12	P	2.0	0.15	5877	4.5	0.89	0.27	P	1.94	0.60	54.3
4178389	185.01	23.211	134.39	P	18.2	0.67	5927	4.5	0.91	0.27	P	18.02	5.45	36.0
4242147	1934.01	28.783	132.33	P	2.7	0.10	4569	4.7	0.59	0.18	P	1.76	0.53	5.3
4247092	403.01	21.056	150.11	P	2.8	0.15	6160	4.4	1.13	0.11	SM	3.48	0.40	69.0
4249725	222.01	6.313	132.66	P	3.3	0.07	4533	4.7	0.59	0.18	P	2.11	0.63	39.7
4252322	396.01	14.591	137.09	P	3.2	0.09	5922	4.2	1.34	0.40	P	4.62	1.39	145.2
4254466	2134.01	42.300	168.80	P	2.2	0.08	5718	4.4	0.97	0.29	P	2.30	0.70	17.2
4262581	2122.01	37.646	161.47	P	1.9	0.14	5778	4.5	0.88	0.27	P	1.79	0.55	16.7
4263529	3358.01	10.104	132.92	P	3.0	0.11	5520	4.5	0.84	0.25	P	2.74	0.83	77.9
4270253	551.01	11.637	132.31	P	2.2	0.11	5841	4.5	0.88	0.26	P	2.11	0.64	81.6
4276716	1619.01	20.665	132.02	P	1.0	0.12	4882	4.6	0.71	0.07	SM	0.81	0.12	14.5
4281895		9.544	137.78	R	27.1	0.09	5608	4.4	0.97	0.29	P	28.67	8.60	118.7
4352168		10.644	134.94	R	63.2	0.18	5374	4.5	0.81	0.24	P	55.84	16.75	62.3
4376644	397.01	27.677	146.14	V	15.0	1.39	6059	4.5	0.96	0.29	P	15.77	4.95	33.9
4454934	2245.01	33.470	140.16	P	1.8	0.11	5900	4.3	1.12	0.34	P	2.18	0.67	34.0
4474462	4452.01	12.858	141.85	P	1.0	0.10	6050	4.2	1.40	0.42	P	1.58	0.50	197.3
4478142		219.909	329.43	P	2.5	0.34	5699	4.5	0.89	0.27	P	2.45	0.80	1.6
4544907	2024.01	46.878	137.66	P	2.3	0.08	5839	4.4	1.04	0.31	P	2.57	0.78	18.2
4551663	2576.01	12.077	140.48	C	1.4	0.18	5376	4.5	0.87	0.26	P	1.34	0.43	61.3
4552729	2691.01	97.447	204.83	P	6.2	0.99	4704	4.6	0.65	0.19	P	4.37	1.49	1.4
4563268	627.01	7.752	137.42	P	1.8	0.06	5999	4.2	1.45	0.14	SM	2.85	0.30	366.6
4633570	446.01	16.709	141.34	P	2.6	0.07	4629	4.7	0.63	0.19	P	1.77	0.53	13.3
4639868	1326.01	53.099	136.01	TTV	14.5	1.75	5467	4.4	0.95	0.09	SM	15.04	2.35	10.9
4644604	628.01	14.486	131.55	P	2.0	0.06	5783	4.3	1.05	0.11	SM	2.31	0.24	88.5
4644952	1805.01	6.941	137.56	P	2.7	0.13	5529	4.5	0.88	0.09	SM	2.56	0.29	139.6
4676964	3069.01	43.103	140.13	P	1.7	0.17	5637	4.4	1.02	0.31	P	1.91	0.60	17.8
4679314		7.697	133.27	VD	0.8	0.03	5747	4.6	0.86	0.26	P	0.74	0.22	127.1
4753988		7.304	135.03	R	52.5	1.85	6039	4.5	0.95	0.28	P	54.38	16.43	193.0
4773155		25.705	156.64	R	65.3	0.13	5606	4.5	0.89	0.27	P	63.31	18.99	26.3
4813563	1959.01	36.516	151.29	P	2.7	0.10	4869	4.6	0.69	0.21	P	2.03	0.61	6.6
4815520	367.01	31.578	145.65	P	4.2	0.08	5688	4.4	1.08	0.11	SM	4.98	0.51	28.6
4820550	3823.01	202.121	292.04	P	5.7	0.65	5796	4.5	0.87	0.26	P	5.37	1.72	1.7
4827723	632.01	7.239	135.03	P	1.5	0.02	5398	4.5	0.87	0.09	SM	1.44	0.15	114.5
4833421	232.01	12.466	134.00	P	4.6	0.12	6063	4.4	1.12	0.11	SM	5.63	0.58	133.6
4841374	633.01	161.472	170.62	P	2.7	0.18	5758	4.4	1.03	0.10	SM	3.03	0.37	3.3
4847534	499.01	9.669	135.86	P	1.9	0.07	5214	4.5	0.80	0.24	P	1.68	0.51	63.1
4847832		30.960	139.44	R	60.5	0.12	5186	4.5	0.79	0.24	P	52.29	15.69	13.1
4857058	3061.01	7.329	132.10	P	1.3	0.11	5062	4.6	0.75	0.22	P	1.03	0.32	73.8
4860678	1602.01	9.977	137.25	P	1.5	0.13	5813	4.5	0.87	0.26	P	1.44	0.45	96.9
4860932	1600.01	12.366	137.89	VD	1.8	0.08	6059	4.5	0.96	0.29	P	1.85	0.56	98.9
4912650		100.348	152.82	P	1.7	0.19	5180	4.5	0.80	0.08	SM	1.47	0.22	2.7
4932442	1665.01	6.934	137.07	P	1.0	0.07	5869	4.2	1.43	0.14	SM	1.63	0.20	377.9
4948730		23.029	139.87	SE	2.2	0.18	5876	4.4	0.98	0.29	P	2.38	0.74	42.4
4949751	404.01	31.805	154.58	V	9.9	0.45	5956	4.5	0.92	0.28	P	9.94	3.01	24.5
4951877	501.01	24.796	145.53	P	2.2	0.07	5750	4.5	0.90	0.27	P	2.14	0.65	30.3
4989057	1923.01	7.234	137.70	P	2.0	0.13	5416	4.5	0.88	0.09	SM	1.92	0.23	116.8
5003117	405.01	37.610	153.11	SE	14.8	0.04	5576	4.5	0.88	0.26	P	14.24	4.27	15.3
5025294		5.463	134.29	SE	7.3	2.53	5978	4.5	0.95	0.28	P	7.50	3.45	277.5
5035972	406.01	49.266	141.93	SE	14.7	0.34	5848	4.4	1.04	0.31	P	16.68	5.02	17.0

KIC	KOI	P days	t_0 days	Disp.	p %	$\sigma(p)$	$T_{\rm eff}$ K	$\log g$ cgs	$R_\star$ $R_\odot$	$\sigma(R_\star)$	Prov.	R_P $R_\oplus$	$\sigma(R_P)$	F_P $F_\oplus$
5042210	2462.01	12.146	131.57	P	0.8	0.02	5995	4.3	1.33	0.13	SM	1.11	0.12	172.7
5088591	1801.01	14.532	140.73	P	3.5	0.11	5331	4.5	0.86	0.26	P	3.24	0.98	45.8
5091614		21.142	138.40	R	40.3	0.14	6077	4.5	0.97	0.29	P	42.47	12.74	49.5
5095082	4320.01	20.658	145.63	P	0.9	0.07	5520	4.4	0.96	0.29	P	0.92	0.29	39.6
5096590	3093.01	29.610	137.34	P	1.0	0.07	5818	4.3	1.17	0.12	SM	1.31	0.16	38.5
5098444	637.01	26.949	151.03	SE	13.8	0.09	4918	4.6	0.70	0.21	P	10.57	3.17	10.5
5103942	1668.01	10.102	131.82	P	2.2	0.16	6090	4.5	0.97	0.29	P	2.28	0.70	133.3
5113822	638.01	23.640	149.00	P	3.1	0.35	5685	4.4	0.97	0.10	SM	3.24	0.49	35.6
5121511	640.01	30.997	160.79	P	2.4	0.06	5216	4.5	0.84	0.08	SM	2.18	0.22	13.9
5128673	2698.01	87.974	168.29	P	3.0	0.20	5845	4.3	1.20	0.12	SM	3.91	0.47	9.7
5131180	641.01	14.852	133.43	C	3.0	0.15	4240	4.7	0.55	0.17	P	1.78	0.54	9.1
5193077	3492.01	22.296	146.43	C	0.9	0.05	5785	4.5	0.87	0.26	P	0.85	0.26	32.2
5199426		78.603	144.00	R	35.8	3.87	5946	4.4	0.99	0.30	P	38.86	12.39	8.7
5213404	3468.01	20.706	139.95	P	1.2	0.12	5793	4.4	0.98	0.29	P	1.26	0.40	46.8
5217586	1592.01	26.069	143.12	P	2.5	0.03	5614	4.4	1.02	0.31	P	2.83	0.85	34.9
5254230		7.036	137.95	SE	4.2	1.39	5369	4.5	0.89	0.27	P	4.04	1.81	131.6
5266937		5.917	132.90	R	62.5	0.04	5655	4.4	0.99	0.30	P	67.70	20.31	241.5
5272233	2711.01	9.024	133.56	P	1.4	0.08	5823	4.3	1.16	0.12	SM	1.72	0.20	186.6
5282051	502.01	5.910	135.68	C	1.4	0.05	5546	4.4	1.02	0.30	P	1.53	0.46	240.6
5299459	1576.01	10.416	132.64	P	2.6	0.04	5489	4.4	0.99	0.10	SM	2.84	0.29	94.9
5301750	1589.01	8.726	138.77	P	2.0	0.07	6094	4.4	1.11	0.11	SM	2.38	0.25	212.2
5303346	3275.01	37.325	143.04	SE	11.5	0.21	5297	4.6	0.79	0.24	P	9.90	2.97	10.5
5308537	4409.01	14.265	143.22	P	0.8	0.07	5896	4.4	0.98	0.29	P	0.84	0.26	80.2
5340644	503.01	8.222	131.84	P	3.5	0.16	4272	4.7	0.56	0.17	P	2.13	0.65	21.0
5351250	408.01	7.382	136.17	P	3.5	0.11	5554	4.5	0.89	0.09	SM	3.39	0.36	131.9
5360082	3768.01	11.354	133.27	SE	12.7	0.07	4723	4.6	0.65	0.20	P	9.00	2.70	25.4
5374403	2556.01	40.837	152.84	P	1.4	0.08	5523	4.5	0.91	0.09	SM	1.38	0.16	14.3
5375194	1825.01	13.523	142.18	P	2.3	0.06	5337	4.6	0.81	0.08	SM	2.05	0.21	42.7
5393558		10.217	137.25	R	62.5	0.61	5888	4.2	1.30	0.39	P	88.98	26.71	219.5
5431027	4558.01	8.823	136.89	P	1.1	0.11	5596	4.3	1.08	0.33	P	1.32	0.42	164.3
5438757	1601.01	10.351	133.72	P	1.5	0.04	5727	4.6	0.85	0.26	P	1.41	0.43	83.7
5443604	2713.01	21.391	141.30	VD	2.2	0.33	4896	4.7	0.66	0.20	P	1.58	0.53	12.0
5444548	409.01	13.249	139.77	P	2.4	0.12	5796	4.4	1.12	0.11	SM	2.95	0.33	102.9
5446285	142.01	10.922	134.76	TTV	0.1	0.36	5423	4.5	0.90	0.09	SM	0.05	0.36	70.1
5461440	504.01	40.606	158.67	P	2.4	0.19	5579	4.6	0.81	0.24	P	2.11	0.66	11.4
5474613	1599.01	20.409	140.11	P	1.6	0.08	5762	4.5	0.92	0.28	P	1.57	0.48	41.3
5478055	411.01	15.852	142.52	VD	2.2	0.07	5982	4.3	1.16	0.35	P	2.84	0.86	101.9
5480640	2707.01	58.033	138.77	P	2.7	0.15	5610	4.6	0.82	0.25	P	2.41	0.74	7.4
5481148	2701.01	22.024	135.19	C	3.8	0.13	5836	4.5	0.92	0.27	P	3.75	1.13	37.9
5520547	2990.01	11.200	137.52	P	1.4	0.08	6055	4.5	0.95	0.29	P	1.48	0.45	111.3
5526527	1838.01	16.737	143.14	P	3.1	0.09	4565	4.7	0.61	0.18	P	2.09	0.63	12.1
5526717	1677.01	52.069	178.16	P	2.2	0.16	5717	4.6	0.85	0.25	P	2.06	0.64	9.6
5530882	1680.01	5.083	132.94	C	0.9	0.06	5709	4.6	0.85	0.25	P	0.81	0.25	212.3
5535280		74.987	146.12	R	41.0	4.19	5950	4.5	0.92	0.28	P	40.99	12.99	7.8
5546277	3797.01	7.500	137.40	SE	2.4	0.05	5809	4.5	0.87	0.26	P	2.29	0.69	141.6
5546761	2160.01	17.671	131.57	P	1.6	0.09	5807	4.5	0.87	0.26	P	1.53	0.47	45.0
5553624		25.762	150.56	R	52.8	0.94	5545	4.5	0.84	0.25	P	48.14	14.47	22.2
5562784	608.01	25.337	142.24	VD	5.1	0.05	4502	4.7	0.60	0.18	P	3.33	1.00	6.4
5563300	3309.01	71.053	134.76	V	7.3	0.98	5272	4.5	0.83	0.25	P	6.66	2.18	5.0
5640085	448.01	10.139	137.91	P	3.3	0.19	4616	4.6	0.66	0.07	SM	2.36	0.28	26.9
5652010		14.641	140.32	P	1.0	0.10	5399	4.4	0.90	0.27	P	0.97	0.31	52.4
5686174	610.01	14.282	137.99	P	3.2	0.27	4207	4.7	0.55	0.16	P	1.91	0.59	9.2

KIC	KOI	P days	t_0 days	Disp.	p %	$\sigma(p)$	T_{eff} K	$\log g$ cgs	$R_\star$ $R_\odot$	$\sigma(R_\star)$	Prov.	R_P $R_\oplus$	$\sigma(R_P)$	F_P $F_\oplus$
5700330		53.220	181.70	P	7.4	0.04	5883	4.3	1.21	0.36	P	9.76	2.93	20.9
5702939	3000.01	18.398	144.94	C	1.1	0.04	5606	4.4	0.99	0.10	SM	1.18	0.13	52.0
5706966	1908.01	12.551	137.27	P	2.1	0.12	4350	4.7	0.57	0.17	P	1.28	0.39	13.3
5709725	555.02	86.493	181.90	P	2.9	0.21	5246	4.5	0.83	0.08	SM	2.59	0.32	3.5
5728139	206.01	5.334	131.98	P	6.3	0.05	6043	4.3	1.14	0.34	P	7.81	2.34	434.7
5731312		7.946	135.11	R	48.1	0.82	4938	4.6	0.71	0.21	P	37.10	11.15	55.2
5735762	148.02	9.674	135.01	P	2.8	0.03	5189	4.5	0.84	0.08	SM	2.53	0.26	64.4
5738496	556.01	9.502	137.66	SE	1.9	0.09	5921	4.5	0.91	0.27	P	1.92	0.58	118.0
5768816	3288.01	47.987	160.67	P	2.4	0.06	5613	4.4	0.96	0.29	P	2.51	0.75	13.6
5770074	1928.01	63.040	169.11	P	2.4	0.13	5804	4.4	1.06	0.11	SM	2.73	0.31	11.6
5771719	190.01	12.265	139.30	P	10.9	0.05	5538	4.1	1.42	0.42	P	16.86	5.06	168.3
5774349	557.01	15.656	139.48	P	3.5	0.11	5147	4.5	0.78	0.23	P	2.94	0.89	30.6
5780930	3412.01	16.753	131.59	P	1.7	0.07	4683	4.6	0.64	0.19	P	1.20	0.36	14.3
5781192		9.460	138.34	R	69.2	0.81	5539	4.6	0.80	0.24	P	60.63	18.20	76.5
5786676	650.01	11.955	142.87	P	2.6	0.10	5064	4.6	0.76	0.08	SM	2.18	0.23	37.2
5791986	413.01	15.229	146.10	P	3.1	0.09	5439	4.6	0.81	0.24	P	2.74	0.83	39.4
5794570	2675.01	5.448	132.49	P	2.3	0.16	5693	4.5	0.95	0.10	SM	2.42	0.29	235.4
5796675	652.01	16.081	134.52	P	5.4	0.10	5305	4.5	0.83	0.08	SM	4.93	0.50	34.4
5807769	2614.01	7.990	132.27	P	1.3	0.09	5948	4.5	0.92	0.27	P	1.31	0.40	152.9
5812960	507.01	18.492	136.52	P	3.7	0.10	5290	4.5	0.84	0.25	P	3.37	1.02	31.2
5819801	4686.01	11.831	138.25	P	0.6	0.04	5522	4.1	1.44	0.43	P	0.90	0.27	179.5
5866099	1055.01	36.977	133.64	SE	6.3	0.37	5571	4.1	1.39	0.42	P	9.58	2.93	37.9
5872150	414.01	20.355	134.64	SE	14.3	0.02	6041	4.4	1.05	0.31	P	16.28	4.88	60.8
5903749	3029.01	18.976	134.84	P	1.8	0.12	5421	4.4	0.92	0.28	P	1.82	0.56	38.7
5906426	2377.01	13.903	143.53	P	1.8	0.18	5229	4.5	0.81	0.24	P	1.56	0.49	41.0
5940165	2031.01	9.304	140.36	P	3.8	0.54	4452	4.7	0.59	0.18	P	2.44	0.81	22.7
5941160	654.01	8.595	137.25	P	1.7	0.08	5662	4.5	0.93	0.09	SM	1.74	0.19	126.5
5953297	2733.01	5.620	132.94	P	1.3	0.04	4809	4.6	0.67	0.20	P	0.92	0.28	73.2
5959719	2498.01	6.738	133.31	P	0.9	0.11	5153	4.6	0.78	0.08	SM	0.78	0.12	92.0
5959753	226.01	8.309	138.11	P	2.6	0.07	5241	4.6	0.73	0.22	P	2.09	0.63	63.8
5966322	303.01	60.928	173.38	P	2.5	0.06	5560	4.4	0.93	0.09	SM	2.52	0.26	9.1
5972334	191.01	15.359	132.39	P	10.9	0.07	5417	4.5	0.90	0.09	SM	10.66	1.07	46.4
5978361	558.01	9.178	136.39	P	2.6	0.13	5505	4.6	0.80	0.24	P	2.23	0.68	78.1
5992270	1855.01	58.430	168.31	C	5.7	1.55	4386	4.7	0.58	0.17	P	3.61	1.46	1.8
6029130		12.592	134.74	R	74.6	10.82	5289	4.6	0.74	0.22	P	60.37	20.12	38.9
6034945	1683.01	9.115	133.98	P	1.7	0.10	5919	4.4	1.01	0.30	P	1.85	0.57	156.6
6037187	1061.01	41.806	142.81	P	2.1	0.13	5899	4.5	0.97	0.29	P	2.22	0.68	18.9
6037581	1916.02	9.600	136.58	P	1.6	0.08	5865	4.4	1.12	0.11	SM	1.94	0.22	163.0
6046540	200.01	7.341	134.35	P	8.2	0.05	5940	4.5	0.91	0.27	P	8.18	2.46	169.7
6058816	3500.01	73.750	188.54	P	1.4	0.09	6093	4.5	0.99	0.30	P	1.53	0.47	9.9
6072593	3070.01	5.076	133.90	C	1.0	0.10	5914	4.3	1.12	0.34	P	1.23	0.39	423.2
6119141	2343.01	29.073	136.97	P	1.9	0.10	5781	4.4	1.06	0.32	P	2.20	0.67	34.7
6124512	2627.01	8.384	134.41	P	0.9	0.06	5469	4.4	0.95	0.28	P	0.98	0.30	125.8
6131659		17.528	144.57	R	57.0	0.10	5088	4.6	0.76	0.23	P	46.91	14.07	24.0
6137704	3605.01	178.274	255.32	R	28.5	2.79	5195	4.5	0.80	0.24	P	24.76	7.81	1.3
6142862	2336.01	5.335	133.43	C	1.4	0.11	4423	4.7	0.58	0.18	P	0.87	0.27	45.6
6146418		22.446	149.15	SE	7.5	0.09	6077	4.3	1.20	0.36	P	9.79	2.94	70.7
6146838		27.467	143.67	R	23.6	0.04	5600	4.4	0.94	0.28	P	24.23	7.27	27.0
6147573		25.837	137.36	R	40.4	0.73	5695	4.5	0.91	0.27	P	40.31	12.12	28.8
6152974	216.01	20.172	141.22	P	7.1	0.35	5187	4.5	0.79	0.24	P	6.11	1.86	23.3
6184894		7.203	135.21	P	3.8	0.10	5485	4.5	0.85	0.26	P	3.51	1.06	122.8
6185476	227.01	17.706	135.97	TTV	0.9	0.15	5491	4.4	1.28	0.13	SM	1.29	0.24	70.3

KIC	KOI	P days	t_0 days	Disp.	p %	$\sigma(p)$	$T_{\rm eff}$ K	$\log g$ cgs	$R_\star$ $R_\odot$	$\sigma(R_\star)$	Prov.	R_P $R_\oplus$	$\sigma(R_P)$	F_P $F_\oplus$
6185711	169.01	11.702	139.42	VD	2.0	0.05	5814	4.5	0.88	0.26	P	1.95	0.59	79.0
6209677	1750.01	7.769	138.05	P	1.3	0.06	5799	4.5	0.94	0.28	P	1.38	0.42	159.1
6225454		89.338	218.54	P	2.4	0.58	4549	4.7	0.61	0.18	P	1.57	0.61	1.3
6266741	508.01	7.930	137.81	P	2.6	0.09	5614	4.3	1.15	0.34	P	3.29	0.99	213.7
6267535	660.01	6.080	134.13	P	1.6	0.09	5317	3.9	2.10	0.21	SM	3.74	0.43	598.8
6289650	415.01	166.790	245.14	P	6.4	0.33	5663	4.4	1.01	0.10	SM	6.99	0.79	2.9
6305192	219.01	8.025	132.47	P	5.3	0.08	6006	4.2	1.45	0.15	SM	8.42	0.85	352.7
6307062		75.377	167.11	R	88.5	6.03	5416	4.6	0.77	0.23	P	74.67	22.97	4.2
6307063		376.891	317.87	SE	3.3	1.29	5872	4.4	1.11	0.11	SM	4.01	1.62	1.2
6307083	2050.01	75.378	167.11	SE	1.7	0.09	5047	4.6	0.74	0.22	P	1.38	0.42	3.2
6342333	2065.01	80.232	162.39	P	3.1	0.40	5655	4.5	0.88	0.26	P	2.97	0.97	5.7
6346809	2775.01	17.578	137.72	P	2.1	0.14	5681	4.4	0.94	0.28	P	2.16	0.67	51.2
6347299	661.01	14.401	131.80	P	1.8	0.05	5789	4.4	1.10	0.11	SM	2.19	0.23	90.4
6351097	2618.01	12.491	136.33	C	1.3	0.11	5771	4.5	0.95	0.28	P	1.30	0.41	84.6
6356692	2948.01	11.391	141.57	P	0.6	0.04	5561	4.2	1.39	0.14	SM	0.98	0.12	160.1
6359798	1121.01	14.154	140.69	R	36.4	0.37	5855	4.4	1.07	0.11	SM	42.44	4.27	89.7
6364582	3456.01	30.861	200.05	P	1.2	0.02	6012	4.4	1.09	0.33	P	1.37	0.41	37.6
6383821	1238.01	27.072	139.11	P	2.2	0.10	5611	4.5	0.86	0.26	P	2.05	0.62	23.0
6421188		16.434	136.29	R	20.0	0.05	5948	4.3	1.14	0.34	P	24.80	7.44	91.7
6428794	4054.01	169.135	201.82	P	2.5	0.28	5172	4.5	0.81	0.08	SM	2.18	0.33	1.3
6432345	2757.01	234.639	172.62	P	2.8	0.27	5421	4.5	0.89	0.09	SM	2.72	0.38	1.2
6442340	664.01	13.137	143.96	P	1.5	0.08	5717	4.4	1.07	0.11	SM	1.74	0.20	93.5
6449552		20.149	135.82	R	69.7	0.05	5524	4.4	0.92	0.28	P	69.89	20.97	37.7
6468138	1826.01	134.250	182.74	P	2.7	0.17	5807	4.4	1.03	0.10	SM	2.98	0.35	4.2
6468938		7.217	135.45	R	40.1	1.17	6068	4.2	1.30	0.39	P	57.03	17.19	374.4
6471021	372.01	125.630	253.34	P	7.9	0.11	5614	4.4	0.93	0.09	SM	7.99	0.81	3.5
6500206	2451.01	13.375	142.40	P	2.2	0.19	5315	4.5	0.86	0.26	P	2.02	0.63	50.6
6501635	560.01	23.675	131.92	P	2.8	0.10	5277	4.6	0.74	0.22	P	2.28	0.69	16.4
6504534		28.162	143.73	P	19.5	0.23	4909	4.6	0.70	0.21	P	14.90	4.47	9.8
6508221	416.01	18.208	149.43	P	3.6	0.02	5085	4.6	0.74	0.07	SM	2.91	0.29	21.8
6521045	41.01	12.816	135.78	P	1.3	0.02	5889	4.3	1.20	0.12	SM	1.77	0.18	129.0
6522750		17.446	135.74	R	78.4	1.15	5802	4.5	0.94	0.28	P	80.07	24.05	53.5
6523351	3117.01	6.067	136.13	P	0.8	0.09	5544	4.5	0.90	0.09	SM	0.77	0.12	168.5
6525209	3479.01	75.132	200.78	P	18.7	0.09	5421	4.6	0.79	0.24	P	16.10	4.83	4.4
6541920	157.03	31.995	154.17	P	3.4	0.08	5801	4.4	1.06	0.11	SM	3.87	0.40	28.8
6584273	3287.01	51.110	143.79	P	2.0	0.20	5979	4.5	0.93	0.28	P	1.98	0.63	13.4
6587002	612.02	47.428	169.13	P	2.7	0.12	5124	4.5	0.80	0.08	SM	2.36	0.26	7.0
6594972		10.819	132.98	R	81.9	1.43	5957	4.4	1.01	0.30	P	89.89	27.01	125.9
6607357	2838.01	7.700	134.39	P	0.9	0.10	5731	4.3	1.15	0.12	SM	1.07	0.16	217.5
6613006	1223.01	7.389	133.94	SE	11.7	0.02	5858	4.5	0.89	0.27	P	11.36	3.41	152.8
6634112		9.942	133.86	V	18.8	0.34	5253	4.5	0.82	0.25	P	16.90	5.08	66.9
6634133	2262.01	9.942	133.86	VD	1.7	0.09	5123	4.5	0.77	0.23	P	1.41	0.43	54.2
6665223	1232.01	119.414	232.62	P	17.3	2.12	5317	4.5	0.86	0.09	SM	16.22	2.57	2.7
6665512	2005.01	6.921	135.64	P	2.2	0.12	4559	4.7	0.61	0.18	P	1.45	0.44	38.9
6665695	561.01	5.379	131.96	P	2.0	0.10	5072	4.6	0.76	0.08	SM	1.67	0.19	112.9
6685609	665.01	5.868	135.13	P	2.0	0.09	5923	4.2	1.45	0.15	SM	3.17	0.35	500.2
6692833	1244.01	10.805	134.09	C	1.6	0.16	6075	4.5	0.96	0.29	P	1.71	0.54	119.6
6694186		5.554	135.17	R	34.3	0.50	5458	4.4	0.94	0.28	P	35.13	10.54	212.9
6705137	2609.01	5.597	131.88	C	1.3	0.12	5799	4.5	0.88	0.26	P	1.24	0.39	213.3
6707835	666.01	22.248	151.88	P	2.3	0.08	5615	4.4	0.99	0.10	SM	2.45	0.26	37.0
6751874	2282.01	6.892	132.47	P	1.5	0.16	6054	4.5	0.96	0.29	P	1.57	0.50	213.4
6752002	4184.01	6.080	136.89	P	1.1	0.15	4936	4.6	0.71	0.21	P	0.87	0.28	78.9

KIC	KOI	P days	t_0 days	Disp.	p %	$\sigma(p)$	$T_{\rm eff}$ K	$\log g$ cgs	$R_\star$ $R_\odot$	$\sigma(R_\star)$	Prov.	R_P $R_\oplus$	$\sigma(R_P)$	F_P $F_\oplus$
6761777	4571.01	47.312	146.33	P	1.7	0.11	6005	4.4	1.00	0.30	P	1.81	0.55	17.6
6762829	1740.01	18.795	138.66	SE	15.2	0.00	5898	4.5	0.95	0.29	P	15.77	4.73	52.6
6786037	564.01	21.057	150.84	P	2.3	0.10	5951	4.5	0.92	0.28	P	2.29	0.69	42.7
6803202	177.01	21.061	143.59	P	1.6	0.07	5711	4.4	1.04	0.10	SM	1.84	0.20	48.3
6838050	512.01	6.510	133.86	P	2.3	0.13	5488	4.4	0.96	0.29	P	2.43	0.74	181.9
6841577		15.537	140.28	R	45.8	0.05	5741	4.5	0.92	0.27	P	45.67	13.70	57.9
6842682	2649.01	7.561	135.64	P	1.4	0.10	5820	4.5	0.88	0.26	P	1.29	0.40	141.3
6846911	2477.01	14.026	135.19	P	2.0	0.18	5911	4.4	1.09	0.33	P	2.36	0.74	102.7
6850504	70.01	10.854	138.62	P	3.5	0.05	5506	4.5	0.90	0.09	SM	3.44	0.35	77.5
6851425	163.01	11.120	139.75	P	2.3	0.04	5079	4.6	0.73	0.07	SM	1.81	0.18	41.1
6864893	2375.01	40.880	163.41	SE	1.8	0.14	5441	4.6	0.78	0.23	P	1.49	0.46	9.7
6871071	2220.02	5.028	134.11	P	1.3	0.08	6023	4.5	0.97	0.29	P	1.32	0.41	329.6
6879865	417.01	19.193	138.60	P	10.1	2.64	5867	4.5	0.89	0.27	P	9.78	3.89	43.1
6922203	2578.01	13.331	133.76	P	2.3	0.22	5992	4.4	1.06	0.32	P	2.66	0.83	107.0
6924203	1370.01	6.883	135.27	P	2.0	0.12	5704	4.6	0.84	0.25	P	1.80	0.55	140.2
6934986	2294.01	131.488	177.49	P	2.7	0.72	5755	4.2	1.39	0.14	SM	4.08	1.16	6.6
6936977		36.473	159.77	R	41.3	0.41	5468	4.6	0.79	0.24	P	35.43	10.63	11.6
6947164	3531.01	70.584	190.48	R	53.3	2.39	5976	4.5	0.93	0.28	P	53.78	16.31	8.7
6960445	669.01	5.074	136.05	VD	2.4	0.03	5633	4.5	0.91	0.27	P	2.39	0.72	241.1
6960913	1361.01	59.878	151.19	P	3.5	0.22	4338	4.7	0.57	0.06	SM	2.14	0.26	1.6
6964159	3129.01	25.503	139.36	C	1.3	0.12	5806	4.5	0.87	0.26	P	1.27	0.40	27.7
7019524	2877.01	5.309	134.27	P	1.0	0.11	5883	4.5	0.93	0.28	P	1.05	0.33	268.9
7046804	205.01	11.720	142.18	P	9.3	0.10	5210	4.6	0.77	0.23	P	7.77	2.33	44.9
7047207	2494.01	19.119	138.44	P	1.4	0.07	5999	4.5	0.97	0.29	P	1.50	0.46	55.4
7047299		35.882	165.55	R	43.8	2.50	5885	4.5	0.90	0.27	P	42.81	13.07	19.2
7090524	2920.01	6.740	132.29	P	1.1	0.12	5707	4.5	0.90	0.27	P	1.10	0.35	166.3
7091432	3353.01	11.555	134.13	P	1.7	0.19	5140	4.5	0.77	0.23	P	1.42	0.46	45.4
7098355	454.01	29.007	141.57	P	2.8	0.40	5258	4.6	0.77	0.23	P	2.32	0.77	13.8
7101828	455.01	47.878	145.35	VD	2.2	0.10	4257	4.7	0.55	0.17	P	1.34	0.41	2.0
7103919	4310.01	10.777	140.28	P	1.3	0.10	5483	4.4	0.96	0.29	P	1.35	0.42	93.1
7105574		20.726	143.20	R	49.8	0.25	6031	4.5	0.94	0.28	P	51.33	15.40	47.4
7107802	2420.01	10.417	137.46	P	1.4	0.14	5813	4.5	0.88	0.26	P	1.30	0.41	92.0
7115785	672.02	41.749	153.85	P	2.9	0.04	5543	4.5	0.90	0.09	SM	2.87	0.29	12.9
7124026	2275.01	15.744	145.61	P	1.1	0.03	6088	4.5	0.97	0.29	P	1.20	0.36	74.3
7133294	4473.01	13.648	132.23	P	0.8	0.08	5791	4.1	1.45	0.43	P	1.31	0.41	171.9
7211221	1379.01	5.621	136.91	P	1.2	0.09	5634	4.4	0.93	0.09	SM	1.24	0.15	224.7
7219906		35.089	153.42	SE	11.3	0.45	5556	4.6	0.81	0.24	P	9.93	3.00	13.6
7269974	456.01	13.700	144.08	P	3.2	0.05	5889	4.5	0.92	0.28	P	3.16	0.95	73.1
7286173	1862.01	56.435	151.41	P	2.3	0.16	5537	4.4	1.06	0.11	SM	2.68	0.33	11.5
7286911	2180.01	11.555	138.21	P	2.0	0.12	5630	4.6	0.83	0.25	P	1.83	0.56	65.3
7289317	2450.01	16.832	140.52	P	1.8	0.19	5784	4.5	0.93	0.28	P	1.79	0.57	55.2
7289577	1974.01	109.441	198.00	P	3.4	0.78	5403	4.5	0.87	0.09	SM	3.22	0.81	3.2
7336754		12.155	133.76	R	41.3	1.68	5798	4.4	0.99	0.30	P	44.79	13.56	98.3
7353970	3574.01	198.445	155.60	R	30.6	0.41	5421	4.5	0.91	0.09	SM	30.35	3.06	1.5
7357531	1368.01	251.068	230.00	V	11.8	1.69	5710	4.3	1.17	0.12	SM	14.96	2.62	2.1
7368664	614.01	12.875	144.28	P	7.0	0.70	5889	4.5	0.90	0.27	P	6.87	2.17	75.5
7376490	3586.01	5.877	136.42	R	19.1	0.11	5802	4.3	1.12	0.34	P	23.40	7.02	332.1
7382313	2392.01	7.427	133.11	P	1.3	0.09	5810	4.4	0.99	0.30	P	1.42	0.44	189.0
7386827	1704.01	10.419	137.74	P	2.4	0.09	5637	4.4	1.03	0.31	P	2.68	0.81	121.7
7428316	2809.01	7.126	137.46	C	1.3	0.15	6077	4.5	0.96	0.29	P	1.36	0.44	209.6
7445445	567.01	10.688	137.87	P	2.5	0.09	5817	4.5	0.89	0.27	P	2.44	0.74	93.4
7446631	2598.01	29.226	143.98	P	1.2	0.08	6018	4.5	1.00	0.30	P	1.36	0.42	33.6

KIC	KOI	P days	t_0 days	Disp.	p %	$\sigma(p)$	$T_{\rm eff}$ K	$\log g$ cgs	$R_\star$ $R_\odot$	$\sigma(R_\star)$	Prov.	R_P $R_\oplus$	$\sigma(R_P)$	F_P $F_\oplus$
7447200	676.01	7.973	131.72	P	5.1	0.02	4503	4.7	0.63	0.06	SM	3.54	0.35	31.5
7455981	3096.01	14.454	135.48	P	0.8	0.04	5642	4.5	0.93	0.28	P	0.80	0.24	63.2
7456001	1517.01	40.069	151.80	P	2.9	0.12	6062	4.4	1.03	0.31	P	3.20	0.97	23.9
7504328	458.01	53.719	154.36	P	6.3	1.10	5832	4.3	1.17	0.35	P	8.06	2.79	19.0
7534267	3147.01	39.440	169.21	P	1.5	0.11	5764	4.6	0.86	0.26	P	1.45	0.45	14.7
7602070	514.01	11.756	140.81	SE	2.2	0.05	5656	4.6	0.83	0.25	P	1.96	0.59	65.3
7624297		18.020	148.66	R	57.7	0.55	5366	4.6	0.76	0.23	P	47.77	14.34	26.3
7626506	150.01	8.409	134.00	P	2.8	0.06	5535	4.4	0.97	0.10	SM	2.94	0.30	136.3
7630229	683.01	278.128	177.53	P	5.0	0.43	5834	4.4	1.04	0.10	SM	5.68	0.75	1.6
7668663	1898.01	6.498	136.01	P	1.3	0.07	5726	4.3	1.15	0.11	SM	1.63	0.19	272.5
7700622	315.01	35.582	153.48	P	2.7	0.08	4780	4.6	0.69	0.07	SM	2.02	0.21	6.2
7742408		33.498	163.76	P	1.1	0.05	4802	4.6	0.67	0.20	P	0.84	0.25	6.7
7743464		55.249	164.98	R	61.7	2.72	6013	4.5	0.94	0.28	P	63.42	19.23	12.7
7747425	1952.01	8.010	135.33	P	1.5	0.07	5998	4.4	1.01	0.30	P	1.71	0.52	192.8
7750419	1708.01	32.774	151.45	P	2.3	0.22	5890	4.5	0.90	0.27	P	2.22	0.70	21.8
7768451	1527.01	192.669	162.88	P	3.2	0.30	5405	4.5	0.88	0.09	SM	3.06	0.42	1.5
7779077	1842.01	16.842	137.99	P	2.6	0.07	5526	4.4	0.95	0.29	P	2.65	0.80	51.6
7802136	1449.01	10.980	137.15	R	22.1	0.12	6010	4.5	0.98	0.30	P	23.72	7.12	120.3
7812179	515.01	17.794	134.03	SE	3.4	0.24	5467	4.6	0.79	0.24	P	2.94	0.91	30.2
7813039	3787.01	141.734	167.39	V	4.0	0.74	5611	4.5	0.94	0.09	SM	4.07	0.86	2.9
7826659	2686.01	211.032	279.14	P	4.1	0.21	4662	4.6	0.67	0.07	SM	3.03	0.34	0.5
7830637	1454.01	121.599	211.47	R	21.1	0.18	6076	4.5	0.96	0.29	P	22.21	6.66	4.8
7833305	4528.01	8.312	139.66	P	0.8	0.09	5437	4.0	1.53	0.46	P	1.31	0.42	304.5
7840044	516.01	13.542	144.02	VD	1.5	0.24	5891	4.4	1.01	0.30	P	1.61	0.55	92.6
7841925	1499.01	14.164	140.58	P	2.6	0.12	5437	4.4	0.92	0.28	P	2.63	0.80	58.4
7866914	3971.01	366.020	182.66	SE	4.0	1.15	6082	4.5	0.99	0.30	P	4.38	1.81	1.2
7870032	1818.01	16.877	138.64	P	2.8	0.16	5497	4.5	0.88	0.09	SM	2.64	0.30	40.8
7877978	2760.01	56.573	146.59	P	2.5	0.35	4588	4.7	0.62	0.19	P	1.71	0.56	2.5
7906671	3018.01	45.117	157.01	VD	1.7	0.12	5559	4.4	1.00	0.30	P	1.87	0.58	15.7
7906739	2165.01	7.014	136.93	VD	0.9	0.04	5951	4.5	0.93	0.28	P	0.93	0.28	189.1
7906882	686.01	52.514	171.68	P	11.7	0.14	5589	4.4	1.01	0.10	SM	12.90	1.30	12.5
7918652	2984.01	11.455	136.33	P	0.8	0.08	6116	4.4	1.15	0.11	SM	0.99	0.14	154.6
7938499		7.227	143.40	P	1.2	0.04	4387	4.7	0.58	0.17	P	0.73	0.22	29.1
7941200	92.01	65.705	137.44	P	2.5	0.14	5800	4.3	1.23	0.12	SM	3.28	0.38	14.5
7949593	4759.01	17.768	146.61	P	1.1	0.09	6027	4.4	1.08	0.32	P	1.31	0.41	76.9
7971389		13.175	136.46	R	39.2	0.89	6077	4.4	1.03	0.31	P	43.98	13.23	106.7
7975727	418.01	22.418	150.39	SE	10.2	0.13	5352	4.5	0.88	0.26	P	9.76	2.93	27.1
7977197	459.01	19.446	150.66	P	3.3	0.32	5833	4.4	0.98	0.29	P	3.51	1.11	51.3
7987749		17.031	145.55	R	41.0	0.45	5574	4.1	1.37	0.41	P	61.03	18.32	104.0
7989422	2151.01	7.478	133.41	VD	0.9	0.05	6012	4.2	1.35	0.41	P	1.33	0.41	374.8
8008067		15.771	137.60	P	2.1	0.07	5594	4.4	1.10	0.11	SM	2.52	0.27	69.1
8008206	569.01	20.729	143.98	P	2.5	0.24	5174	4.5	0.78	0.23	P	2.10	0.66	21.2
8009496	1869.01	38.477	150.58	VD	2.1	0.06	6097	4.5	0.97	0.29	P	2.17	0.66	22.6
8009500		38.476	150.58	R	38.5	0.09	5329	4.5	0.85	0.25	P	35.61	10.68	12.2
8017703	518.01	13.982	140.03	P	2.9	0.04	4917	4.6	0.69	0.07	SM	2.20	0.22	24.3
8022244	519.01	11.903	142.63	P	2.5	0.13	6027	4.5	0.95	0.28	P	2.58	0.78	99.5
8022489	2674.01	197.511	272.38	P	5.3	0.09	5756	4.2	1.52	0.15	SM	8.81	0.89	4.4
8023317		16.579	146.73	R	20.2	0.29	5862	4.1	1.59	0.48	P	34.85	10.47	161.4
8041216	237.01	8.508	134.78	P	2.3	0.08	5767	4.4	1.08	0.11	SM	2.74	0.29	167.7
8043638	460.01	17.588	140.89	P	3.4	0.06	5520	4.4	0.98	0.30	P	3.66	1.10	52.1
8044608	3523.01	106.176	234.62	R	55.2	2.76	6095	4.3	1.27	0.38	P	76.57	23.29	10.0
8074805	2670.01	170.866	186.05	P	3.7	0.35	5987	4.2	1.41	0.14	SM	5.69	0.78	5.6

KIC	KOI	P days	t_0 days	Disp.	p %	$\sigma(p)$	$T_{\rm eff}$ K	$\log g$ cgs	$R_\star$ $R_\odot$	$\sigma(R_\star)$	Prov.	R_P $R_\oplus$	$\sigma(R_P)$	F_P $F_\oplus$
8087812	4343.01	27.211	132.37	P	1.0	0.09	6014	4.2	1.40	0.42	P	1.49	0.47	71.0
8095441	2743.01	11.874	140.24	P	1.4	0.14	5530	4.5	0.88	0.09	SM	1.35	0.19	68.0
8099138	2338.01	66.184	141.63	P	2.1	0.24	5899	4.5	0.90	0.27	P	2.11	0.68	8.7
8107225	235.01	5.633	133.82	P	2.3	0.08	5127	4.6	0.70	0.21	P	1.80	0.54	93.8
8107380	162.01	14.006	142.22	P	2.4	0.03	5795	4.3	1.17	0.12	SM	3.10	0.31	103.3
8121328	3486.01	19.072	145.63	P	1.2	0.08	5430	4.0	1.53	0.46	P	1.99	0.61	100.8
8127586	1752.01	16.610	147.57	C	1.8	0.08	6043	4.4	1.05	0.32	P	2.04	0.62	80.5
8127607	1919.01	16.609	147.61	VD	2.2	0.23	5225	4.6	0.75	0.22	P	1.79	0.57	26.7
8142787	4005.01	178.146	210.10	P	2.6	0.24	5431	4.5	0.88	0.09	SM	2.47	0.34	1.7
8142942	1985.01	5.756	133.90	P	2.8	0.24	4931	4.6	0.72	0.07	SM	2.20	0.29	83.7
8160953	1858.01	116.331	173.71	P	3.9	0.15	5354	4.5	0.83	0.08	SM	3.52	0.38	2.6
8168187	2209.01	18.302	142.89	P	1.4	0.14	5744	4.5	0.86	0.26	P	1.35	0.42	40.5
8183288	3255.01	66.650	171.19	P	2.1	0.13	4550	4.7	0.64	0.06	SM	1.43	0.17	2.0
8193178	572.01	10.640	137.21	P	2.1	0.09	6166	4.4	1.14	0.11	SM	2.61	0.28	174.4
8197343	1746.01	11.791	134.56	P	1.9	0.14	5965	4.5	0.93	0.28	P	1.89	0.59	93.6
8210721		22.673	138.15	R	23.9	0.23	5584	4.3	1.05	0.32	P	27.39	8.22	43.5
8218379	1920.01	16.571	133.90	P	2.4	0.07	5488	4.6	0.79	0.24	P	2.03	0.61	34.0
8219673	419.01	20.132	149.13	P	14.5	0.35	5986	4.5	0.93	0.28	P	14.80	4.45	47.2
8223328	1767.01	35.516	165.94	P	11.4	0.17	5719	4.2	1.34	0.40	P	16.70	5.02	40.7
8226050	1910.01	34.270	147.02	P	2.4	0.09	5299	4.5	0.84	0.25	P	2.21	0.67	13.7
8233802	3302.01	69.379	154.19	VD	2.3	0.26	5803	4.5	0.88	0.27	P	2.19	0.70	7.5
8242434	1726.01	44.963	144.57	P	2.6	0.07	4684	4.6	0.68	0.07	SM	1.90	0.20	4.1
8247770	2569.01	8.282	136.25	P	1.0	0.12	5650	4.4	1.03	0.31	P	1.15	0.37	167.1
8260234	2085.01	5.715	132.12	P	1.5	0.07	5237	4.5	0.81	0.24	P	1.32	0.40	136.2
8260902	2144.01	38.671	157.63	P	2.2	0.08	5420	4.0	1.54	0.46	P	3.72	1.12	39.5
8265218	522.01	12.830	144.28	P	3.3	0.22	5897	4.5	0.90	0.27	P	3.27	1.00	76.4
8280511		10.435	134.82	P	1.6	0.11	5489	4.5	0.88	0.09	SM	1.58	0.19	82.3
8301878	3301.01	20.711	140.89	P	1.2	0.12	5613	4.5	0.91	0.27	P	1.16	0.37	36.8
8313667	1145.01	30.587	132.29	P	1.9	0.05	5943	4.4	1.10	0.11	SM	2.32	0.24	36.4
8321314	2293.01	15.034	144.98	P	1.7	0.14	5451	4.4	0.93	0.28	P	1.76	0.55	55.0
8323753	175.01	6.714	134.31	VD	1.9	0.06	6075	4.3	1.27	0.38	P	2.63	0.79	395.8
8326342	2680.01	14.408	142.03	P	5.1	1.17	5474	4.6	0.79	0.24	P	4.39	1.66	40.4
8332986	1137.01	302.374	309.16	V	15.8	3.62	5330	4.5	0.83	0.08	SM	14.26	3.57	0.8
8344004	573.01	5.996	136.54	P	2.4	0.07	6010	4.3	1.12	0.34	P	2.99	0.90	354.1
8349399	4763.01	56.449	170.58	P	1.0	0.13	5980	4.4	1.10	0.33	P	1.25	0.41	17.0
8349582	122.01	11.523	131.98	P	2.3	0.06	5695	4.3	1.26	0.13	SM	3.21	0.33	140.9
8352537	420.01	6.010	132.02	P	5.3	0.18	4860	4.6	0.69	0.21	P	3.99	1.21	71.9
8355239	574.01	20.135	151.23	P	3.0	0.13	5217	4.6	0.72	0.22	P	2.33	0.71	19.0
8358008		10.065	135.25	SE	16.2	0.06	5260	4.5	0.83	0.25	P	14.65	4.40	66.9
8358012	2929.01	10.065	135.25	P	1.7	0.20	5387	4.6	0.76	0.23	P	1.40	0.45	58.5
8364115		7.736	137.99	SE	2.0	0.02	5953	4.5	0.93	0.28	P	2.06	0.62	164.4
8364119		7.736	137.99	R	75.2	3.52	5661	4.6	0.83	0.25	P	68.40	20.77	114.6
8374580	615.01	176.240	192.51	V	10.3	1.26	5565	4.2	1.39	0.14	SM	15.52	2.46	4.1
8378922		43.263	150.39	R	79.1	2.22	5676	4.4	1.03	0.31	P	89.15	26.86	18.6
8409295	3404.01	82.299	211.96	P	1.8	0.32	6049	4.5	0.95	0.29	P	1.92	0.66	7.7
8429668	4449.01	5.008	134.68	C	0.8	0.08	5306	4.6	0.75	0.22	P	0.62	0.20	136.8
8453211	236.01	5.777	131.53	VD	2.8	1.41	5578	4.3	1.05	0.31	P	3.21	1.88	268.6
8460600	1730.01	6.352	134.21	SE	23.6	0.11	5163	4.5	0.77	0.23	P	19.88	5.96	101.0
8474898	576.01	199.441	240.87	V	8.8	1.18	5650	4.3	1.26	0.13	SM	12.11	2.02	3.1
8481129	2402.01	16.302	133.78	P	1.5	0.10	4763	4.6	0.66	0.20	P	1.08	0.33	16.5
8491277	234.01	9.614	132.19	P	2.6	0.09	5940	4.4	1.09	0.33	P	3.10	0.94	172.3
8509781		70.334	198.96	R	21.1	2.17	6074	4.2	1.37	0.41	P	31.58	10.01	19.9

KIC	KOI	P days	t_0 days	Disp.	p %	$\sigma(p)$	$T_{\rm eff}$ K	$\log g$ cgs	$R_\star$ $R_\odot$	$\sigma(R_\star)$	Prov.	R_P $R_\oplus$	$\sigma(R_P)$	F_P $F_\oplus$
8543278		7.549	135.03	SE	23.9	1.88	5159	4.6	0.71	0.21	P	18.48	5.73	65.4
8547429	2658.01	11.660	140.65	P	1.2	0.09	6009	4.5	0.94	0.28	P	1.19	0.37	99.7
8552719	1792.01	88.407	176.28	P	3.8	0.08	5288	4.6	0.77	0.23	P	3.16	0.95	3.2
8559863		22.470	143.28	R	32.5	0.13	5375	4.6	0.76	0.23	P	27.01	8.10	19.8
8560940	3450.01	31.971	133.88	P	1.0	0.08	5852	4.5	0.89	0.27	P	0.97	0.30	21.4
8564587	1270.01	5.729	132.82	P	2.7	0.13	5289	4.6	0.74	0.22	P	2.14	0.65	110.4
8564674	2022.01	5.930	135.50	P	1.8	0.04	5936	4.5	0.91	0.27	P	1.83	0.55	224.8
8565266	578.01	6.412	137.80	P	3.1	0.05	5990	4.4	1.10	0.33	P	3.75	1.13	309.1
8572936		27.796	146.73	R	84.1	0.89	6003	4.4	1.01	0.30	P	92.45	27.75	36.6
8573193	4337.01	8.185	134.56	P	1.0	0.11	5981	4.5	0.93	0.28	P	1.02	0.33	154.3
8580438		6.496	135.48	R	29.8	0.02	5504	4.4	0.96	0.29	P	31.31	9.39	187.0
8583696	1275.01	50.285	167.66	P	3.4	0.16	5907	4.3	1.20	0.12	SM	4.49	0.50	21.0
8591693	2123.01	29.455	154.19	P	2.2	0.18	6030	4.5	0.95	0.28	P	2.24	0.70	29.9
8611257	2931.01	99.250	148.55	P	2.1	0.32	4995	4.6	0.72	0.07	SM	1.65	0.30	2.0
8611781	2185.01	76.964	192.28	P	1.9	0.21	5887	4.4	1.08	0.32	P	2.23	0.71	10.4
8611832	2414.01	22.597	140.44	P	1.3	0.08	5587	4.4	0.98	0.10	SM	1.37	0.16	39.0
8618226		5.882	131.76	R	66.4	3.00	6044	4.3	1.12	0.34	P	81.07	24.59	366.2
8621348	461.01	11.344	138.83	VD	2.1	0.07	5643	4.6	0.83	0.25	P	1.91	0.58	67.4
8625732	4701.01	31.971	133.92	P	0.9	0.07	5597	4.6	0.82	0.25	P	0.84	0.26	16.1
8625925	580.01	6.521	136.58	P	2.6	0.19	5795	4.5	0.87	0.26	P	2.47	0.76	167.7
8628758	1279.01	14.374	138.21	P	1.7	0.04	5771	4.4	1.06	0.11	SM	1.94	0.20	85.4
8644288	137.02	14.859	143.02	P	5.2	0.07	5424	4.5	0.91	0.09	SM	5.17	0.52	47.3
8644365	3384.02	19.916	139.36	P	1.1	0.07	6049	4.4	1.12	0.11	SM	1.34	0.16	67.7
8644545		295.963	138.91	P	1.9	0.28	5507	4.4	0.95	0.10	SM	2.03	0.36	1.1
8652999	1953.01	15.161	136.54	VD	1.7	0.20	5892	4.3	1.17	0.35	P	2.22	0.71	105.9
8681734	2340.01	7.685	137.64	P	1.6	0.10	5621	4.4	0.97	0.29	P	1.73	0.53	161.2
8686097	374.01	172.699	236.95	P	2.6	0.17	5706	4.3	1.04	0.10	SM	2.96	0.36	3.1
8692861	172.01	13.722	137.85	P	2.2	0.06	5603	4.4	0.98	0.10	SM	2.38	0.25	75.0
8733497	3527.01	76.818	188.13	R	56.7	7.31	5692	4.6	0.84	0.25	P	52.08	17.00	5.6
8742590	1281.01	49.478	141.83	P	2.2	0.15	5773	4.5	0.86	0.26	P	2.03	0.63	11.0
8746295	2475.01	6.856	136.03	P	1.4	0.27	5691	4.5	0.85	0.26	P	1.35	0.47	144.3
8751933	1257.01	86.648	173.79	P	7.8	0.22	5472	4.4	0.99	0.10	SM	8.40	0.87	5.5
8802165	694.01	17.421	131.98	P	2.8	0.02	5702	4.4	1.05	0.11	SM	3.16	0.32	59.5
8804283	1276.01	22.790	138.68	P	2.4	0.19	5594	4.6	0.82	0.24	P	2.14	0.66	25.1
8804455	2159.01	7.597	131.96	P	1.0	0.04	5714	4.4	1.07	0.11	SM	1.14	0.13	191.9
8804845	2039.01	5.426	135.86	P	1.6	0.17	5597	4.6	0.82	0.25	P	1.38	0.44	171.1
8806072	1273.01	40.058	169.93	P	3.3	0.11	5633	4.6	0.83	0.25	P	2.95	0.89	12.4
8822216	581.01	6.997	133.94	P	3.3	0.07	5653	4.6	0.83	0.25	P	2.97	0.89	129.6
8826168	1850.01	11.551	134.90	P	1.9	0.09	5905	4.4	1.08	0.11	SM	2.24	0.25	124.8
8827575	3052.02	15.611	144.85	P	1.0	0.05	5386	4.5	0.82	0.08	SM	0.89	0.10	38.5
8832512	1821.01	9.977	131.76	P	2.9	0.13	5487	4.4	0.94	0.28	P	2.95	0.90	100.1
8848271	1256.01	9.992	137.44	SE	10.1	0.08	5855	4.3	1.11	0.33	P	12.21	3.67	164.8
8869680	696.01	7.034	131.96	C	1.2	0.06	5964	4.4	1.09	0.33	P	1.49	0.45	266.4
8879427		16.313	136.87	R	27.3	0.19	5995	4.5	0.99	0.30	P	29.48	8.85	71.6
8890783	464.01	58.363	138.19	P	6.7	0.13	5490	4.5	0.90	0.27	P	6.56	1.97	8.5
8939211		27.078	137.15	SE	1.3	0.02	5984	4.5	0.99	0.30	P	1.36	0.41	35.9
8949247	1387.01	23.800	152.56	R	24.7	0.17	5918	4.5	0.96	0.29	P	26.04	7.81	39.7
8950568	2038.01	8.306	139.73	P	1.8	0.06	5438	4.5	0.89	0.09	SM	1.78	0.19	105.1
8962094	700.01	30.864	142.08	P	2.2	0.11	5785	4.3	1.05	0.11	SM	2.53	0.28	32.3
8972058	159.01	8.991	136.74	P	2.1	0.15	5964	4.4	1.09	0.11	SM	2.46	0.30	187.7
8973000		28.028	148.78	R	40.7	0.09	5407	4.6	0.80	0.24	P	35.68	10.70	17.0
8984706		10.135	137.50	R	71.6	0.76	5914	4.1	1.50	0.45	P	117.22	35.19	289.6

KIC	KOI	P days	t_0 days	Disp.	p %	$\sigma(p)$	T_{eff} K	$\log g$ cgs	$R_\star$ $R_\odot$	$\sigma(R_\star)$	Prov.	R_P $R_\oplus$	$\sigma(R_P)$	F_P $F_\oplus$
9002278	701.01	18.164	144.47	P	2.8	0.06	4968	4.6	0.70	0.07	SM	2.14	0.22	18.5
9006186	2169.01	5.453	134.15	P	0.9	0.06	5395	4.5	0.87	0.09	SM	0.85	0.10	163.2
9006449	1413.01	12.646	138.60	P	1.3	0.03	5630	4.4	0.94	0.28	P	1.33	0.40	76.4
9020160	582.01	5.945	134.80	P	2.7	0.13	5236	4.6	0.73	0.22	P	2.16	0.66	99.2
9025971	3680.01	141.243	256.20	P	10.3	0.10	5710	4.4	1.07	0.11	SM	12.10	1.22	3.8
9031703	4520.01	9.334	137.62	P	0.9	0.05	5490	4.1	1.47	0.44	P	1.38	0.42	253.2
9042357	1993.01	16.004	146.39	P	2.3	0.22	5367	4.6	0.78	0.23	P	1.98	0.62	32.7
9086154	4060.01	225.257	225.00	P	1.9	0.19	5795	4.3	1.27	0.13	SM	2.69	0.37	3.0
9101496	1915.01	6.562	132.61	P	1.5	0.08	5873	4.1	1.74	0.17	SM	2.87	0.33	580.6
9116075		24.498	154.70	P	1.3	0.21	4570	4.7	0.60	0.18	P	0.82	0.28	6.9
9119458	525.01	11.531	139.11	P	2.8	0.15	5738	4.3	1.14	0.34	P	3.50	1.07	134.1
9119568	3087.01	5.548	133.96	C	0.8	0.05	5257	4.5	0.87	0.09	SM	0.75	0.09	148.0
9139084	323.01	5.836	134.86	P	2.1	0.05	5403	4.5	0.85	0.08	SM	1.95	0.20	149.1
9146018	584.01	9.927	135.97	P	2.8	0.10	5464	4.5	0.93	0.09	SM	2.88	0.30	86.2
9150827	1408.01	14.534	145.43	P	2.1	0.10	4252	4.7	0.48	0.05	SM	1.08	0.12	8.4
9164836	213.01	48.119	170.85	R	38.9	0.87	6031	4.5	0.95	0.28	P	40.21	12.10	15.5
9177629	2522.01	5.604	133.84	P	1.2	0.12	4849	4.6	0.75	0.08	SM	0.99	0.14	86.6
9226339	3477.01	21.461	132.25	P	1.0	0.06	5995	4.3	1.24	0.37	P	1.36	0.41	77.4
9266285		5.614	132.57	R	36.8	0.04	4452	4.7	0.59	0.18	P	23.67	7.10	44.4
9266431	704.01	18.396	148.35	P	2.8	0.15	5313	4.6	0.80	0.08	SM	2.43	0.27	27.2
9283156	2657.01	5.224	132.84	P	0.6	0.04	5422	4.5	0.84	0.08	SM	0.58	0.07	178.3
9284741		20.729	141.24	R	79.2	1.63	5265	4.5	0.83	0.25	P	71.55	21.52	25.6
9334893	2298.01	16.667	141.77	P	1.2	0.07	4922	4.6	0.70	0.21	P	0.90	0.28	20.1
9353182		10.476	136.54	R	31.6	0.01	6100	4.3	1.24	0.37	P	42.72	12.82	210.7
9353314	1900.01	5.185	131.88	P	2.0	0.16	4451	4.7	0.59	0.18	P	1.29	0.40	49.4
9364290	2374.01	5.262	136.35	P	1.3	0.09	5622	4.4	1.00	0.30	P	1.44	0.44	279.8
9364609	2137.01	14.974	141.50	P	1.6	0.11	5332	4.5	0.83	0.08	SM	1.43	0.17	40.1
9394762		77.136	166.60	P	2.2	0.30	5688	4.6	0.84	0.25	P	2.01	0.66	5.5
9412445	3970.01	10.186	132.55	C	1.5	0.03	4168	4.7	0.54	0.16	P	0.86	0.26	13.7
9412462		10.187	132.53	R	77.7	0.77	5540	4.5	0.91	0.27	P	77.02	23.12	91.9
9412760	1977.01	9.387	137.40	P	2.0	0.18	4346	4.7	0.60	0.06	SM	1.34	0.18	19.3
9425139		305.071	294.06	P	5.9	0.33	5642	4.4	1.12	0.11	SM	7.22	0.83	1.4
9447166	3296.01	62.868	166.04	P	1.9	0.26	4838	4.6	0.68	0.20	P	1.41	0.46	3.0
9455325	1813.01	9.768	139.46	P	2.2	0.06	5369	4.5	0.85	0.09	SM	2.03	0.21	74.5
9458343	2246.01	11.895	132.90	P	1.3	0.12	5650	4.4	0.97	0.10	SM	1.39	0.19	90.9
9471974	119.01	49.184	141.91	P	3.8	0.06	5642	4.2	1.44	0.14	SM	5.93	0.60	25.0
9472000	2082.01	31.589	155.62	P	1.7	0.10	5875	4.2	1.50	0.15	SM	2.79	0.32	54.7
9489953	3238.01	58.345	169.84	P	3.4	1.36	5861	4.2	1.33	0.40	P	4.93	2.48	22.2
9491832	4226.01	49.565	170.68	P	1.0	0.05	5641	4.1	1.53	0.46	P	1.73	0.53	31.5
9509343	4346.01	6.392	135.64	P	1.3	0.12	5390	4.4	0.89	0.27	P	1.27	0.40	153.6
9514372	4242.01	145.787	215.04	P	2.1	0.29	5574	4.4	0.93	0.09	SM	2.08	0.36	2.8
9520838	1866.01	105.304	207.18	P	3.4	0.26	5530	4.5	0.87	0.09	SM	3.26	0.41	3.6
9527915	165.01	13.222	139.56	P	2.7	0.06	5214	4.6	0.78	0.08	SM	2.28	0.23	39.2
9549471		15.714	132.08	SE	8.9	0.79	5818	4.4	0.97	0.29	P	9.41	2.95	67.2
9549472		15.714	132.10	R	28.9	0.40	5842	4.4	1.01	0.30	P	31.93	9.59	73.8
9570741	586.01	15.780	144.41	P	2.3	0.12	5934	4.5	0.91	0.27	P	2.24	0.68	60.8
9571186	3313.01	34.953	163.53	P	2.2	0.17	4805	4.6	0.67	0.20	P	1.63	0.50	6.4
9573539	180.01	10.046	139.13	P	2.4	0.16	5561	4.5	0.94	0.09	SM	2.49	0.29	95.9
9576197		7.964	136.19	R	23.8	0.02	5311	4.5	0.79	0.24	P	20.57	6.17	85.1
9578686	709.01	21.385	136.01	P	2.4	0.10	5343	4.5	0.86	0.09	SM	2.26	0.25	27.3
9583881	467.01	18.009	146.43	P	5.2	0.14	5803	4.5	0.88	0.26	P	4.96	1.49	44.7
9589524	468.01	22.185	152.39	P	4.4	0.11	5132	4.5	0.77	0.23	P	3.72	1.12	18.8

KIC	KOI	P days	t_0 days	Disp.	p %	$\sigma(p)$	$T_{\rm eff}$ K	$\log g$ cgs	$R_\star$ $R_\odot$	$\sigma(R_\star)$	Prov.	R_P $R_\oplus$	$\sigma(R_P)$	F_P $F_\oplus$
9597058	1819.01	12.057	135.43	P	2.1	0.06	5368	4.5	0.84	0.08	SM	1.91	0.20	54.5
9597345	711.01	44.700	174.81	P	2.6	0.04	5556	4.4	1.08	0.11	SM	3.06	0.31	16.1
9607164	587.01	14.035	143.53	P	2.6	0.10	5290	4.5	0.84	0.25	P	2.42	0.73	45.3
9631762	588.01	10.356	134.25	P	2.5	0.16	4678	4.6	0.64	0.19	P	1.72	0.53	26.9
9631995	22.01	7.892	137.79	P	9.1	0.01	5789	4.3	1.26	0.13	SM	12.60	1.26	255.2
9632895	1451.01	27.322	132.43	R	25.3	0.01	5662	4.6	0.83	0.25	P	22.97	6.89	21.3
9635606	2535.01	48.889	153.83	P	2.0	0.11	4930	4.6	0.71	0.21	P	1.54	0.47	4.9
9636569	527.01	10.636	139.79	VD	1.5	0.09	5897	4.5	0.90	0.27	P	1.46	0.45	98.7
9651234	1938.01	96.914	187.11	P	2.8	0.22	5170	4.6	0.77	0.08	SM	2.34	0.30	2.6
9661979	2132.01	69.895	160.67	P	2.2	0.23	5584	4.5	0.84	0.25	P	2.05	0.65	6.0
9662811	1854.01	43.034	137.70	P	2.1	0.09	5548	4.5	0.91	0.09	SM	2.14	0.23	13.1
9663113	179.01	20.740	142.79	P	2.9	0.03	6230	4.3	1.38	0.14	SM	4.38	0.44	100.6
9673173		21.294	147.10	R	50.4	0.32	6024	4.2	1.27	0.38	P	69.92	20.98	83.0
9704384	1913.01	5.509	132.31	P	1.3	0.07	5448	4.5	0.92	0.09	SM	1.34	0.15	185.0
9714358		6.474	134.39	R	44.9	0.37	5057	4.6	0.75	0.22	P	36.56	10.97	86.7
9718066	2287.01	16.092	142.52	P	1.0	0.09	4470	4.7	0.62	0.06	SM	0.69	0.09	11.6
9729691	1751.01	8.689	133.66	P	3.2	0.14	5165	4.5	0.79	0.24	P	2.73	0.83	69.3
9735426	1849.01	8.088	138.74	P	2.8	0.06	5170	4.6	0.71	0.21	P	2.16	0.65	60.4
9758089	1871.01	92.728	177.47	C	3.0	0.15	4569	4.7	0.66	0.07	SM	2.15	0.24	1.3
9762519		7.515	138.09	R	43.4	4.33	5709	4.5	0.89	0.27	P	42.11	13.31	141.2
9765975	1520.01	18.458	138.17	P	2.1	0.06	5372	4.5	0.83	0.25	P	1.92	0.58	31.6
9783760	3487.01	89.738	205.28	R	29.3	5.05	5859	4.5	0.89	0.27	P	28.43	9.83	5.5
9815053	2923.01	5.839	136.89	P	1.5	0.08	5262	4.6	0.76	0.23	P	1.22	0.37	112.7
9818462	1521.01	25.943	156.18	P	2.2	0.07	5136	4.5	0.77	0.23	P	1.89	0.57	15.4
9821078		8.429	132.29	R	65.1	0.11	4246	4.7	0.55	0.17	P	39.20	11.76	19.5
9838468	2943.01	54.411	175.40	P	1.3	0.11	5750	4.3	1.23	0.12	SM	1.73	0.23	17.4
9846086	617.01	37.864	160.75	P	13.2	0.48	5781	4.5	0.88	0.26	P	12.70	3.84	16.5
9849884	4516.01	5.357	131.63	P	0.8	0.09	6093	4.5	0.99	0.30	P	0.84	0.27	326.5
9850893	1523.01	8.481	135.82	VD	1.6	0.05	5263	4.5	0.83	0.25	P	1.44	0.44	84.0
9851271	2003.01	8.480	135.86	P	1.8	0.04	5881	4.4	1.07	0.32	P	2.10	0.63	193.4
9851662	2483.01	15.054	135.54	P	1.4	0.15	5520	4.4	0.96	0.29	P	1.42	0.45	60.6
9873254	717.01	14.707	131.68	P	1.5	0.06	5641	4.4	1.08	0.11	SM	1.77	0.19	75.0
9886661	1606.01	5.083	133.23	P	1.5	0.05	5403	4.5	0.89	0.09	SM	1.50	0.16	194.3
9895006	1717.01	10.561	133.76	P	1.5	0.19	5440	4.4	0.93	0.28	P	1.56	0.50	87.6
9910828		8.480	135.88	P	1.4	0.09	5504	4.5	0.82	0.25	P	1.28	0.39	92.5
9941387		27.660	141.26	R	76.3	2.62	5298	4.6	0.75	0.22	P	62.16	18.77	13.9
9941859	528.01	9.577	138.38	P	2.7	0.26	5675	4.3	1.05	0.32	P	3.12	0.98	143.5
9957627	592.01	39.753	135.72	P	2.1	0.08	6090	4.4	1.06	0.32	P	2.43	0.74	26.3
9958962	593.01	9.998	131.80	P	2.3	0.10	5964	4.5	0.92	0.28	P	2.32	0.70	116.1
9962455	2748.01	23.198	142.65	P	1.5	0.11	5426	4.0	1.88	0.19	SM	3.04	0.38	98.7
9962595		11.375	142.44	P	15.3	0.21	5264	4.5	0.79	0.24	P	13.12	3.94	50.8
9963009		40.070	153.01	R	21.4	0.02	5795	4.3	1.11	0.33	P	25.89	7.77	24.9
9963524	720.01	5.691	134.21	P	3.3	0.04	5246	4.6	0.80	0.08	SM	2.90	0.29	125.0
9964801	721.01	13.724	139.48	P	1.8	0.19	5819	4.3	1.22	0.12	SM	2.33	0.34	115.9
9967884	425.01	5.428	131.76	P	13.6	0.83	5866	4.5	0.90	0.27	P	13.31	4.08	237.7
9973109	2018.01	27.496	133.27	P	2.2	0.16	5707	4.4	1.03	0.31	P	2.50	0.77	34.6
9991621	3382.01	18.925	145.55	VD	1.1	0.05	5456	4.4	0.93	0.28	P	1.14	0.35	41.0
9993683		29.940	145.08	P	1.5	0.12	5241	4.5	0.82	0.25	P	1.34	0.41	15.1
10004738	1598.01	56.477	143.81	P	3.2	0.34	5816	4.5	0.90	0.27	P	3.13	1.00	10.2
10006581	1595.01	40.110	142.08	P	2.6	0.16	5965	4.5	0.93	0.28	P	2.58	0.79	18.4
10016874	426.01	16.302	139.54	P	2.7	0.10	6059	4.3	1.14	0.34	P	3.36	1.02	97.9
10019643	471.01	21.347	150.39	P	2.4	0.15	5732	4.6	0.85	0.26	P	2.27	0.69	32.1

KIC	KOI	P days	t_0 days	Disp.	p %	$\sigma(p)$	T_{eff} K	$\log g$ cgs	$R_\star$ $R_\odot$	$\sigma(R_\star)$	Prov.	R_P $R_\oplus$	$\sigma(R_P)$	F_P $F_\oplus$
10022908	1586.01	6.991	135.48	P	2.2	0.13	4735	4.7	0.63	0.19	P	1.50	0.46	44.0
10024701	2002.01	14.375	139.05	P	1.5	0.10	5935	4.4	1.06	0.11	SM	1.72	0.21	91.8
10028792	1574.01	114.737	165.14	P	6.6	0.16	5802	4.3	1.30	0.13	SM	9.39	0.97	7.5
10031885	329.01	8.590	132.02	SE	1.4	0.02	6035	4.5	0.95	0.28	P	1.44	0.43	154.6
10031907	3828.01	8.590	132.02	SE	2.8	0.02	5632	4.6	0.83	0.25	P	2.50	0.75	97.7
10031918	4894.01	8.590	131.96	P	1.0	0.08	4944	4.6	0.71	0.21	P	0.78	0.24	50.3
10033279	1604.01	72.492	139.77	P	3.1	0.17	5812	4.4	1.04	0.31	P	3.56	1.09	10.0
10053138		11.773	138.79	P	0.9	0.07	5703	4.6	0.85	0.26	P	0.83	0.26	70.0
10063208	4292.01	9.328	132.90	P	0.6	0.04	5780	4.5	0.87	0.26	P	0.53	0.16	102.5
10064256	2849.01	5.960	135.01	P	1.0	0.08	5301	4.6	0.78	0.23	P	0.88	0.27	118.7
10098844	2964.01	47.449	173.46	P	1.8	0.06	6008	4.3	1.11	0.11	SM	2.17	0.23	22.0
10122255	1086.01	27.665	144.88	P	2.1	0.10	6057	4.4	1.05	0.32	P	2.38	0.72	41.1
10134152	2056.01	39.314	154.93	P	2.2	0.14	6060	4.5	0.96	0.29	P	2.33	0.71	21.0
10136549	1929.01	9.693	132.80	P	1.2	0.08	5681	4.1	1.60	0.16	SM	2.01	0.24	259.7
10154388	991.01	12.062	138.23	P	1.8	0.11	5541	4.4	0.91	0.09	SM	1.80	0.21	74.1
10155434	473.01	12.706	142.50	P	2.6	0.13	5541	4.6	0.80	0.24	P	2.30	0.70	51.6
10158418	1784.01	5.007	135.03	P	5.6	0.20	5956	4.4	1.04	0.10	SM	6.32	0.67	366.5
10187159	1870.01	7.964	136.82	P	2.6	0.16	5101	4.6	0.76	0.23	P	2.15	0.66	70.3
10189542		24.615	142.53	P	1.6	0.24	5645	4.5	0.85	0.26	P	1.48	0.49	25.8
10189546	427.01	24.615	142.51	C	3.6	0.12	5462	4.5	0.85	0.26	P	3.35	1.01	23.9
10190075	3007.01	11.192	138.03	P	1.3	0.15	5879	4.5	0.89	0.27	P	1.28	0.41	89.7
10198109		17.919	146.39	R	31.5	0.01	5971	4.0	1.66	0.50	P	57.15	17.15	166.4
10215422		24.847	154.11	R	75.0	1.44	5615	4.6	0.84	0.25	P	68.60	20.62	24.1
10252275	3130.01	14.863	143.00	P	1.3	0.11	5141	4.5	0.78	0.23	P	1.14	0.35	32.6
10266615	530.01	10.940	137.48	P	2.2	0.16	5720	4.6	0.85	0.25	P	2.08	0.64	77.1
10268809		24.709	138.99	R	25.0	0.81	6058	4.4	1.03	0.31	P	27.97	8.44	45.4
10274244		13.684	135.21	R	43.4	0.10	5453	4.5	0.83	0.25	P	39.18	11.75	48.3
10285631	331.01	18.684	133.47	P	1.9	0.11	5689	4.4	1.04	0.10	SM	2.12	0.25	53.0
10289119	2390.01	16.104	135.05	P	1.0	0.04	6077	4.2	1.42	0.14	SM	1.58	0.17	135.1
10290666	332.01	5.458	133.88	P	1.5	0.09	5720	4.2	1.34	0.13	SM	2.15	0.25	426.3
10292238	3526.01	143.116	245.53	R	59.4	7.13	5687	4.6	0.84	0.25	P	54.43	17.59	2.4
10319590		21.321	132.74	SE	0.2	0.15	5738	4.4	1.04	0.31	P	0.22	0.18	49.9
10328393	1905.01	7.626	136.03	P	1.7	0.09	4954	4.6	0.72	0.07	SM	1.30	0.15	58.8
10330495		18.060	138.60	R	22.4	0.04	5333	4.5	0.86	0.26	P	21.10	6.33	35.0
10336951	2401.01	38.229	166.02	P	2.3	0.41	4625	4.7	0.63	0.19	P	1.59	0.56	4.4
10337517	1165.01	7.054	136.37	P	2.1	0.16	5357	4.5	0.86	0.09	SM	1.96	0.24	117.7
10345862		58.289	152.46	R	22.3	0.05	5374	4.4	0.89	0.27	P	21.59	6.48	7.9
10353968	618.01	9.071	132.98	P	2.8	0.04	5591	4.5	0.86	0.26	P	2.65	0.79	97.7
10384798	1997.01	38.506	158.30	P	2.4	0.11	6019	4.5	0.94	0.28	P	2.43	0.74	20.6
10404582	2147.01	37.865	134.37	P	2.0	0.21	5867	4.5	0.89	0.27	P	1.97	0.63	17.5
10420279		45.434	172.95	R	86.1	1.56	5665	4.4	1.03	0.31	P	96.75	29.08	17.2
10426656	1161.01	6.057	135.92	P	1.9	0.07	5294	4.5	0.84	0.25	P	1.72	0.52	139.7
10453588	2484.01	68.887	160.30	P	1.1	0.10	5739	4.3	1.07	0.11	SM	1.31	0.18	11.2
10480915	2040.01	19.586	132.37	P	2.2	0.27	5623	4.4	1.01	0.10	SM	2.42	0.38	47.3
10482160	1170.01	7.344	137.31	P	2.3	0.26	5805	4.5	0.87	0.26	P	2.22	0.71	145.1
10483644		5.111	133.31	R	24.5	0.52	6056	4.5	0.96	0.29	P	25.60	7.70	319.1
10490960		5.682	133.64	R	67.0	0.16	5871	4.3	1.17	0.35	P	85.36	25.61	386.4
10513530	533.01	16.550	138.58	P	2.6	0.16	5335	4.5	0.87	0.26	P	2.45	0.75	39.6
10514429	1614.01	20.720	143.28	P	1.1	0.09	5899	4.3	1.13	0.34	P	1.39	0.43	65.1
10514430	263.01	20.720	143.28	P	1.2	0.08	5855	4.3	1.13	0.11	SM	1.44	0.17	61.9
10545066	337.01	19.783	138.15	P	1.9	0.13	5751	4.3	1.13	0.11	SM	2.30	0.28	60.9
10554999	534.01	6.400	135.64	P	2.6	0.15	5283	4.6	0.74	0.22	P	2.07	0.63	94.4

KIC	KOI	P days	t_0 days	Disp.	p %	$\sigma(p)$	T_{eff} K	$\log g$ cgs	$R_\star$ $R_\odot$	$\sigma(R_\star)$	Prov.	R_P $R_\oplus$	$\sigma(R_P)$	F_P $F_\oplus$
10577994	475.01	8.181	135.78	P	2.5	0.04	5236	4.5	0.79	0.24	P	2.14	0.64	78.1
10586208	1308.01	23.585	145.94	P	1.9	0.04	5647	4.2	1.56	0.16	SM	3.29	0.34	73.4
10586744	4892.01	21.376	143.63	P	1.0	0.06	6035	4.3	1.17	0.35	P	1.23	0.38	71.5
10593626	87.01	289.862	133.70	P	2.2	0.16	5567	4.4	0.93	0.09	SM	2.25	0.28	1.1
10599206	476.01	18.428	141.59	P	2.4	0.11	5139	4.5	0.78	0.23	P	2.05	0.62	24.4
10600955	2227.01	65.650	173.30	P	2.2	0.26	5819	4.4	1.01	0.30	P	2.44	0.79	10.8
10616679	429.01	8.600	138.13	P	5.3	0.09	5254	4.5	0.82	0.25	P	4.78	1.44	81.1
10656823	598.01	8.308	137.93	P	2.4	0.11	5292	4.6	0.74	0.22	P	1.96	0.59	67.8
10657406	1837.01	34.174	137.78	P	2.2	0.08	5166	4.6	0.80	0.08	SM	1.94	0.21	10.8
10666242	198.01	87.242	153.35	V	17.7	2.25	5731	4.6	0.85	0.26	P	16.47	5.36	4.9
10674871	2068.01	41.889	171.99	P	3.0	0.30	5939	4.5	0.92	0.27	P	3.00	0.95	16.7
10676014	1797.01	16.782	139.79	P	2.8	0.13	4925	4.6	0.74	0.07	SM	2.26	0.25	20.9
10709622	2108.01	51.329	177.67	P	2.5	0.17	6096	4.4	1.13	0.34	P	3.13	0.96	21.1
10717241	430.01	12.376	142.28	P	4.1	0.57	4286	4.7	0.56	0.17	P	2.50	0.83	12.4
10724369	1302.01	55.638	131.94	P	2.8	0.33	5906	4.5	0.90	0.27	P	2.80	0.90	11.0
10753734		19.407	149.80	R	66.4	0.32	5655	4.6	0.83	0.25	P	60.25	18.08	33.4
10779233	1989.01	201.111	187.60	P	2.5	0.22	5647	4.4	0.98	0.10	SM	2.68	0.36	2.0
10793172	2871.01	12.100	143.04	P	1.4	0.16	5678	4.6	0.84	0.25	P	1.25	0.40	65.2
10794242		7.144	137.80	R	41.6	0.02	5645	4.4	0.99	0.30	P	44.73	13.42	184.2
10798331	2373.01	147.281	148.80	P	2.1	0.18	5712	4.4	1.13	0.11	SM	2.57	0.34	3.9
10798605	3390.01	56.049	159.16	R	33.5	0.95	5243	4.5	0.82	0.25	P	29.90	9.01	6.6
10798838	3449.01	62.127	172.07	R	27.7	1.52	5381	4.4	0.89	0.27	P	26.89	8.20	7.3
10810838	174.01	56.355	144.83	P	2.9	0.19	4752	4.6	0.68	0.07	SM	2.19	0.26	3.2
10843590	431.01	18.870	140.97	P	3.1	0.11	5417	4.4	0.91	0.27	P	3.03	0.92	38.4
10845188	3602.01	249.357	279.64	R	26.0	2.36	5982	4.4	1.10	0.33	P	31.09	9.75	2.3
10858832	432.01	5.263	132.25	P	3.1	0.21	6045	4.5	1.00	0.30	P	3.32	1.02	334.2
10867062	1303.01	34.302	143.53	P	2.4	0.07	5506	4.1	1.46	0.44	P	3.82	1.15	44.0
10873260	535.01	5.853	136.07	P	3.1	0.09	6021	4.4	1.00	0.30	P	3.42	1.03	291.7
10875245	117.01	14.749	138.79	P	2.2	0.17	5807	4.3	1.28	0.13	SM	3.03	0.39	111.2
10878263		7.171	133.64	P	2.6	0.06	5450	4.5	0.89	0.09	SM	2.52	0.26	125.2
10880507	2936.01	6.480	132.86	P	1.2	0.15	5690	4.6	0.84	0.25	P	1.06	0.35	150.6
10908248	3146.01	39.855	154.85	P	1.2	0.08	5902	4.4	1.08	0.33	P	1.36	0.42	25.3
10917433	3248.01	6.912	132.19	P	0.5	0.06	5767	4.4	1.05	0.11	SM	0.62	0.09	223.1
10917681	1963.01	12.896	136.84	P	1.9	0.17	6074	4.5	0.97	0.29	P	2.03	0.64	95.3
10925104	156.03	11.776	142.71	P	3.3	0.04	4587	4.7	0.66	0.07	SM	2.35	0.24	21.3
10933561	291.01	31.518	153.64	P	1.7	0.03	5727	4.3	1.24	0.12	SM	2.33	0.24	36.5
10934674	477.01	16.543	136.56	P	2.5	0.07	5088	4.6	0.75	0.23	P	2.01	0.61	25.8
10936427		14.361	131.67	R	62.4	0.50	5333	4.6	0.76	0.23	P	51.48	15.45	34.9
10964440	1310.01	19.130	139.42	P	2.0	0.13	6045	4.5	0.96	0.29	P	2.13	0.65	54.6
10965008		81.170	178.59	P	3.2	0.19	5808	4.5	0.87	0.26	P	3.08	0.94	5.9
10965963		6.640	132.76	R	66.5	1.47	6056	4.3	1.20	0.36	P	87.02	26.18	357.2
10973814	1307.01	44.852	172.48	P	2.6	0.12	5783	4.4	1.00	0.30	P	2.89	0.88	17.5
10977671		199.038	180.22	P	1.4	0.24	5161	3.5	3.38	0.34	SM	5.30	1.02	12.9
10990917	1643.01	11.046	136.41	P	1.8	0.13	6072	4.4	1.03	0.31	P	2.02	0.62	135.9
11015108	344.01	39.309	132.02	P	3.2	0.14	5581	4.4	0.92	0.09	SM	3.25	0.35	16.2
11015323	479.01	34.189	159.20	P	3.0	0.08	5516	4.5	0.91	0.09	SM	3.03	0.31	18.1
11017901	1800.01	7.794	137.27	P	6.0	0.35	5540	4.5	0.88	0.09	SM	5.77	0.67	118.2
11037335	1435.01	40.716	146.55	P	2.2	0.03	5993	4.5	0.93	0.28	P	2.21	0.66	18.4
11045383	1645.01	41.166	158.93	P	10.3	1.24	5199	4.5	0.79	0.24	P	8.96	2.89	9.1
11069176	2007.01	15.379	143.38	P	1.3	0.12	6063	4.4	1.05	0.32	P	1.43	0.45	89.8
11075279	1431.01	345.158	318.30	P	7.8	0.16	5495	4.4	0.99	0.10	SM	8.44	0.86	0.9
11100383	346.01	12.925	132.00	P	2.9	0.15	5104	4.6	0.76	0.08	SM	2.39	0.27	35.2

KIC	KOI	P days	t_0 days	Disp.	p %	$\sigma(p)$	$T_{\rm eff}$ K	$\log g$ cgs	$R_\star$ $R_\odot$	$\sigma(R_\star)$	Prov.	R_P $R_\oplus$	$\sigma(R_P)$	F_P $F_\oplus$
11124436	4442.01	13.948	132.76	P	1.1	0.08	5964	4.4	1.03	0.31	P	1.22	0.38	93.9
11125797		12.254	143.69	P	1.2	0.11	5444	4.6	0.79	0.24	P	1.00	0.31	49.3
11147814	3334.01	95.177	224.61	R	42.5	5.07	4538	4.7	0.61	0.18	P	28.18	9.10	1.1
11153121	1647.01	14.971	134.49	P	1.6	0.07	5741	4.4	1.13	0.11	SM	1.92	0.21	84.8
11177543	1648.01	38.326	142.10	P	1.8	0.11	5333	4.6	0.75	0.23	P	1.50	0.46	9.2
11177676		47.032	175.44	P	2.0	0.07	5586	4.6	0.81	0.24	P	1.80	0.54	9.5
11192998	481.01	7.650	133.72	P	2.8	0.06	5429	4.6	0.78	0.23	P	2.39	0.72	89.4
11193263	1438.01	6.911	136.64	P	1.3	0.06	5767	4.2	1.32	0.13	SM	1.94	0.21	329.8
11194032	348.01	28.511	158.87	P	3.8	0.04	4686	4.6	0.68	0.07	SM	2.86	0.29	7.5
11250587	107.01	7.257	134.02	P	2.0	0.07	5883	4.3	1.29	0.13	SM	2.82	0.30	303.0
11253711	1972.01	17.791	149.25	P	1.9	0.18	6074	4.5	0.97	0.29	P	2.03	0.64	62.4
11253827	2672.01	88.516	182.66	P	5.6	0.26	5569	4.5	0.93	0.09	SM	5.66	0.62	5.1
11255231	3003.01	13.655	137.52	C	1.2	0.08	6058	4.5	0.97	0.29	P	1.29	0.40	87.7
11288051	241.01	13.821	131.80	P	2.5	0.09	4987	4.6	0.70	0.07	SM	1.93	0.21	26.9
11297236	1857.01	88.642	145.49	P	2.4	0.15	5657	4.5	0.92	0.09	SM	2.39	0.28	5.5
11305996	3256.01	55.699	152.72	C	2.0	0.31	4238	4.7	0.55	0.17	P	1.17	0.40	1.6
11337833	1651.01	51.300	153.54	P	2.3	0.28	6026	4.5	0.94	0.28	P	2.40	0.78	14.1
11358389	2163.01	10.665	132.00	P	1.5	0.06	5983	4.4	1.01	0.30	P	1.71	0.52	132.1
11360805	2422.01	26.784	140.75	P	1.9	0.13	5412	4.4	0.91	0.27	P	1.86	0.57	24.0
11361646	330.01	7.974	134.68	P	1.9	0.06	5969	4.4	1.10	0.11	SM	2.30	0.24	216.9
11391018	189.01	30.361	148.08	P	13.1	0.01	4905	4.6	0.70	0.21	P	9.96	2.99	8.8
11392618	1623.01	110.919	174.24	P	2.0	0.10	5606	4.2	1.39	0.14	SM	3.04	0.34	8.4
11394027	349.01	14.387	141.69	P	2.3	0.13	5725	4.4	1.14	0.11	SM	2.87	0.33	89.0
11395587	350.01	12.990	138.28	P	1.9	0.11	5786	4.4	1.04	0.10	SM	2.12	0.25	93.0
11402995	173.01	10.061	138.97	P	2.0	0.03	5707	4.3	1.19	0.12	SM	2.55	0.26	160.2
11403389	2482.01	45.090	133.58	P	1.9	0.13	5753	4.6	0.86	0.26	P	1.83	0.56	12.2
11413812	1885.01	5.654	131.72	P	1.9	0.13	5973	4.5	0.93	0.28	P	1.92	0.59	250.1
11415243	4036.01	168.814	211.45	P	2.3	0.23	4794	4.6	0.70	0.07	SM	1.74	0.25	0.8
11449844	125.01	38.479	151.86	P	13.9	0.01	5486	4.5	0.85	0.26	P	12.89	3.87	13.3
11450414	1992.01	12.798	133.66	P	1.7	0.07	6069	4.5	0.96	0.29	P	1.79	0.54	94.8
11461844	2356.01	13.681	139.23	P	1.2	0.07	6055	4.5	0.96	0.29	P	1.23	0.37	85.9
11462341	2124.01	42.337	158.28	P	1.8	0.08	4252	4.7	0.55	0.17	P	1.06	0.32	2.3
11495458	2318.01	10.459	137.64	P	1.7	0.13	4702	4.6	0.65	0.19	P	1.18	0.37	27.4
11498128	2296.01	106.252	135.72	P	1.8	0.14	5673	4.4	0.95	0.10	SM	1.89	0.24	4.7
11502172		25.432	135.62	R	32.6	0.11	5787	4.4	0.96	0.29	P	34.11	10.23	33.8
11506235		20.413	140.01	R	30.2	0.10	5908	4.5	0.94	0.28	P	30.94	9.28	45.5
11519226		22.161	148.47	SE	10.4	2.41	5938	4.5	0.91	0.27	P	10.39	3.93	38.8
11521048	540.01	25.703	143.40	VD	11.4	0.50	5569	4.5	0.88	0.26	P	10.89	3.30	24.9
11521793	352.01	27.083	137.64	P	1.8	0.06	5855	4.3	1.21	0.12	SM	2.42	0.26	47.6
11554435	63.01	9.434	140.11	P	5.9	0.18	5551	4.5	0.91	0.09	SM	5.86	0.61	94.0
11601584	1831.01	51.810	182.96	P	2.9	0.11	5192	4.5	0.84	0.08	SM	2.68	0.29	6.8
11614617	1990.01	24.757	142.08	P	2.0	0.07	6088	4.5	0.97	0.29	P	2.09	0.63	40.3
11619964		10.369	132.72	R	46.4	1.41	5899	4.4	1.00	0.30	P	50.45	15.21	127.7
11623629	365.01	81.737	211.69	P	2.3	0.09	5465	4.5	0.85	0.09	SM	2.16	0.23	4.8
11651712	3363.01	14.532	140.48	P	1.7	0.12	5996	4.5	0.94	0.28	P	1.70	0.52	73.6
11656302	434.01	22.265	150.82	SE	13.5	0.05	5700	4.6	0.85	0.26	P	12.57	3.77	29.9
11656721	541.01	13.646	139.40	P	2.4	0.10	5536	4.6	0.80	0.24	P	2.07	0.63	46.6
11656918	1945.01	62.139	161.14	P	2.9	0.21	5434	4.6	0.81	0.24	P	2.52	0.78	6.1
11657614	3370.02	5.942	133.80	P	1.5	0.11	4870	4.6	0.69	0.21	P	1.11	0.34	73.9
11662184	2791.01	27.572	145.41	P	1.7	0.08	6046	4.5	0.95	0.29	P	1.72	0.52	33.2
11669239	542.01	41.886	136.80	P	2.5	0.10	5731	4.4	1.04	0.31	P	2.77	0.84	20.0
11671579	4510.01	5.176	133.78	P	0.9	0.08	5557	4.6	0.81	0.24	P	0.78	0.24	173.6

Table S2 (cont'd)

KIC	KOI	P days	t_0 days	Disp.	p %	$\sigma(p)$	$T_{\rm eff}$ K	$\log g$ cgs	$R_\star$ $R_\odot$	$\sigma(R_\star)$	Prov.	R_P $R_\oplus$	$\sigma(R_P)$	F_P $F_\oplus$
11702948	1465.01	9.771	135.60	P	7.2	0.05	5811	4.5	0.88	0.26	P	6.86	2.06	99.9
11709124	435.01	20.550	137.85	P	3.4	0.07	5706	4.4	0.99	0.10	SM	3.71	0.38	44.9
11718144	2310.01	16.458	134.04	P	2.0	0.12	5808	4.5	0.87	0.26	P	1.92	0.59	49.5
11724210		5.746	132.04	R	19.3	0.20	5971	4.4	1.02	0.31	P	21.50	6.45	303.2
11754430	3403.01	39.817	166.68	P	1.5	0.11	5715	4.1	1.80	0.18	SM	2.98	0.36	47.8
11760231	1841.01	49.608	138.42	P	2.3	0.09	5151	4.6	0.79	0.08	SM	1.98	0.21	6.5
11764462	1531.01	5.699	136.58	P	1.2	0.04	5738	4.4	0.99	0.10	SM	1.27	0.13	259.2
11769146		282.962	350.44	R	67.9	5.69	5966	4.5	0.93	0.28	P	68.67	21.39	1.4
11769689	4551.01	14.719	135.62	P	1.1	0.07	6078	4.5	1.00	0.30	P	1.18	0.36	86.7
11769890	1980.01	122.884	165.45	P	2.6	0.35	5413	4.5	0.89	0.09	SM	2.57	0.43	2.8
11773022	620.01	45.156	159.12	P	7.1	0.01	6023	4.5	0.94	0.28	P	7.33	2.20	16.7
11773328	1906.01	8.710	134.64	P	2.8	0.15	5380	4.6	0.77	0.23	P	2.37	0.72	71.1
11774991	2173.01	37.815	141.11	P	1.5	0.05	4705	4.6	0.69	0.07	SM	1.14	0.12	5.4
11802615	296.01	28.863	149.62	P	2.2	0.10	5754	4.4	1.01	0.10	SM	2.43	0.27	31.3
11812199		37.321	135.41	SE	10.7	0.28	5878	4.5	0.91	0.27	P	10.53	3.17	18.6
11818607	2467.01	5.057	134.39	P	1.3	0.14	5885	4.5	0.90	0.27	P	1.28	0.41	261.2
11818872	2581.01	12.737	136.01	P	1.0	0.09	5424	4.5	0.91	0.09	SM	1.01	0.13	58.4
11824222	437.01	15.841	145.47	R	20.7	2.53	5189	4.6	0.76	0.23	P	17.17	5.56	29.1
11858541		5.674	135.74	R	29.1	0.22	5585	4.3	1.07	0.32	P	33.96	10.19	287.2
11869052	120.01	20.546	137.91	TTV	1.5	0.17	5619	4.2	1.20	0.36	P	1.94	0.63	65.7
11875734	1828.01	99.747	208.40	P	3.4	0.23	5638	4.2	1.18	0.35	P	4.36	1.34	7.8
11906217		37.910	162.47	R	45.7	1.72	4772	4.6	0.66	0.20	P	33.02	9.98	5.4
11909686	1483.01	185.937	288.87	P	10.0	2.65	5861	4.5	0.89	0.27	P	9.71	3.89	2.1
11922778	3408.01	65.427	176.32	P	1.7	0.17	6010	4.5	0.94	0.28	P	1.78	0.56	10.0
11955499	1512.01	9.042	137.87	C	2.4	0.07	5118	4.6	0.70	0.21	P	1.86	0.56	49.0
12055539	3261.01	12.271	137.58	P	1.4	0.10	6066	4.5	0.96	0.29	P	1.48	0.46	100.1
12058204	2218.01	5.535	132.76	P	1.5	0.05	5803	4.5	0.87	0.26	P	1.43	0.43	211.2
12061222	484.01	17.205	140.65	P	3.0	0.05	5254	4.6	0.73	0.22	P	2.40	0.72	24.4
12071037	2388.01	6.096	135.11	C	1.0	0.03	5901	4.4	0.99	0.30	P	1.06	0.32	257.4
12105785		31.953	142.69	SE	15.9	0.21	5508	4.6	0.80	0.24	P	13.81	4.15	14.5
12106929	359.01	5.937	135.97	P	1.8	0.04	5954	4.5	0.92	0.28	P	1.79	0.54	229.3
12107008	4297.01	5.937	135.93	P	1.0	0.05	5480	4.5	0.86	0.26	P	0.93	0.28	162.4
12116489	547.01	25.303	137.44	P	4.4	0.20	5170	4.6	0.72	0.22	P	3.45	1.05	13.7
12121570	2290.01	91.500	165.68	P	2.5	0.19	4977	4.6	0.70	0.07	SM	1.95	0.25	2.2
12154526	2004.01	56.188	146.39	P	1.9	0.20	5663	4.3	1.21	0.12	SM	2.54	0.37	15.4
12251650	621.01	17.762	138.68	P	20.2	2.61	5166	4.6	0.73	0.22	P	16.11	5.26	22.4
12253474	1947.01	6.423	135.56	P	1.3	0.06	6085	4.5	1.01	0.30	P	1.47	0.44	265.7
12253769	3310.01	20.551	141.07	C	1.3	0.09	5450	4.5	0.92	0.09	SM	1.29	0.16	31.7
12254792	1506.01	40.429	139.52	P	2.8	0.06	5831	4.5	0.88	0.26	P	2.71	0.82	15.3
12256520	2264.01	33.243	143.44	P	1.7	0.11	5559	4.4	1.00	0.30	P	1.89	0.58	23.2
12266636	1522.01	33.386	148.92	P	2.2	0.12	5801	4.4	0.99	0.30	P	2.41	0.73	25.7
12301181	2059.01	6.147	134.88	P	1.0	0.05	4999	4.6	0.74	0.07	SM	0.84	0.09	84.0
12302530	438.01	5.931	133.29	P	3.2	0.27	4478	4.7	0.63	0.06	SM	2.18	0.29	44.9
12306808		37.879	138.13	R	65.9	0.42	6055	4.5	0.96	0.29	P	68.73	20.62	22.0
12400538	1503.01	150.244	138.27	P	5.1	0.36	5598	4.5	0.96	0.10	SM	5.33	0.65	2.8
12403119	1478.01	76.135	199.49	P	5.5	0.11	5551	4.5	0.94	0.09	SM	5.58	0.57	6.4
12404305	486.01	22.183	147.31	P	2.7	0.16	5566	4.4	1.01	0.10	SM	2.96	0.34	41.1
12417486	622.01	155.042	213.51	P	7.1	0.13	5005	3.5	3.28	0.33	SM	25.33	2.58	16.3
12454461	2463.01	7.467	136.39	P	0.8	0.05	6027	4.3	1.26	0.13	SM	1.11	0.13	300.3
12505654	2353.01	5.187	135.01	P	2.1	0.20	5182	4.6	0.73	0.22	P	1.71	0.54	118.3
12508335	215.01	42.944	155.21	P	15.3	0.44	5802	4.4	1.02	0.31	P	17.10	5.15	19.4
12557713		7.215	132.51	R	29.1	2.62	4873	4.6	0.69	0.21	P	21.86	6.85	57.3

Table S2 (cont'd)

KIC	KOI	P days	t_0 days	Disp.	p %	$\sigma(p)$	$T_{\rm eff}$ K	$\log g$ cgs	$R_\star$ $R_\odot$	$\sigma(R_\star)$	Prov.	R_P $R_\oplus$	$\sigma(R_P)$	F_P $F_\oplus$
12644769	1611.01	41.078	132.66	VD	33.6	0.16	4198	4.7	0.54	0.16	P	19.94	5.98	2.2
12735740	3663.01	282.521	363.06	P	8.9	0.10	5576	4.4	0.93	0.09	SM	9.03	0.91	1.2
12735830	3311.01	31.829	134.58	P	1.9	0.28	4712	4.6	0.65	0.19	P	1.33	0.45	6.3
12834874	487.01	7.659	134.74	P	2.4	0.06	5666	4.5	0.88	0.26	P	2.26	0.68	131.5

Note. — For each of the 836 eKOIs, we list the target star identifier, ephemeris, false positive status, transit fit parameters, host star properties, and planet radius. KIC — *Kepler* Input Catalog (*22*) identifier. KOI — *Kepler* team identifier, if eKOI appears in 13 September 2013 cumulative list of candidates from the NASA Exoplanet Archive (*1*). Disp. — disposition according to the false positive vetting described in S5. eKOIs may be designated as a false positives for any of the following reasons: 'SE' — secondary eclipse, 'VD' — variable depth transits, 'TTV' — large transit timing variations, 'V' — V-shaped transit, 'C' — centroid offset. If an eKOI passes all the vetting steps, it is considered a planet, 'P.' p — planet to star radius ratio, $R_P/R_\star$. Prov. — provenience of stellar parameters: SpecMatch 'SM' or photometric 'P'.

Table S3.   Spectroscopic properties of 13 eKOIs (added in proof)

KIC	KOI	P days	t_0 days	Disp.	p %	$\sigma(p)$	$T_{\rm eff}$ K	$\log g$ cgs	$R_\star$ $R_\odot$	$\sigma(R_\star)$	Prov.	R_P $R_\oplus$	$\sigma(R_P)$	F_P $F_\oplus$
4478142		219.909	329.43	P	2.5	0.34	5648	4.3	1.06	0.11	SM	2.92	0.49	2.3
4820550	3823.01	202.121	292.04	P	5.7	0.65	5594	4.5	0.94	0.09	SM	5.79	0.88	1.8
6225454		89.338	218.54	P	2.4	0.58	4652	4.6	0.68	0.07	SM	1.73	0.46	1.6
6307083	2050.01	75.378	167.11	SE	1.7	0.09	5109	4.6	0.77	0.08	SM	1.43	0.16	3.4
7101828	455.01	47.878	145.35	VD	2.2	0.10	4328	4.7	0.55	0.05	SM	1.33	0.15	2.0
7866914	3971.01	366.020	182.66	SE	4.0	1.15	5713	4.3	1.06	0.11	SM	4.67	1.40	1.2
7877978	2760.01	56.573	146.59	P	2.5	0.35	4675	4.6	0.68	0.07	SM	1.87	0.32	3.0
8044608	3523.01	106.176	234.62	R	55.2	2.76	6056	4.4	1.12	0.11	SM	67.58	7.56	7.7
9447166	3296.01	62.868	166.04	P	1.9	0.26	4739	4.6	0.72	0.07	SM	1.48	0.25	2.9
10292238	3526.01	143.116	245.53	R	59.4	7.13	5957	4.4	1.09	0.11	SM	70.56	11.03	4.7
11305996	3256.01	55.699	152.72	C	2.0	0.31	4241	4.7	0.48	0.05	SM	1.03	0.19	1.4
11462341	2124.01	42.337	158.28	P	1.8	0.08	4282	4.7	0.54	0.05	SM	1.04	0.11	2.3
11769146		282.962	350.44	R	67.9	5.69	5787	4.5	0.95	0.10	SM	70.64	9.21	1.3

Note. — We obtained 13 additional spectra of long period eKOIs during peer-review. In this work, we used photometric properties for these 13 eKOIs, but we include them here for completeness. Column descriptions are the same as Table S2.